A Characterization of Bromine and Chlorine Stable Isotopes in the Sand Hills Region of Nebraska, USA

by

Corinne Hanlon

A thesis

presented to the University of Waterloo

in fulfillment of the

thesis requirement for the degree of

Master of Science

in

Earth Sciences

Waterloo, Ontario, Canada, 2015

I hereby declare that I am the sole author of this thesis. This is a true copy of the thesis, including any required final revisions, as accepted by my examiners.

I understand that my thesis may be made electronically available to the public.

Abstract

Saline lakes and salt flats are capable of releasing a significant flux of reactive bromine into the atmosphere, a compound which is 45-70 times more efficient at ozone destruction than chlorine (Eggenkamp, 2014; Risacher et al., 2006). Currently, very little information is available regarding the extent to which evaporitic environments contribute bromine to the atmosphere. Isotopic analyses using $\delta^{81}Br$ and $\delta^{37}Cl$ can help in distinguishing between natural and anthropogenic sources of atmospheric bromine. However, for this to be a possibility, a more thorough understanding of the environmental cycling of $\delta^{81}Br$ and $\delta^{37}Cl$ is required.

Lake and salt samples were collected in 1992 and 1993 from previous studies in the region. The same lakes and salts were sampled again in 2012, 2013, and 2014 for this study, and were analyzed for $\delta^{81}Br$, $\delta^{37}Cl$, $\delta^{18}O$, and $\delta^{2}H$ isotopic ratios, and geochemical properties. Several end-members within the region were analysed for isotopic and chemical parameters, as the interactions between these end-members may control the cycling of the isotopes throughout the region. The end-members which were considered in this study include the lake surface waters, the release of halide volatile gas, the precipitation of salts along the shorelines of the alkaline lakes, and the regional and local fresh groundwater systems.

On the surficial salts and soils of the alkaline lakes, it was determined that two main processes, or end-members, are responsible for $\delta^{81}Br$ and $\delta^{37}Cl$ fractionation in this environment: salt precipitation, and microbial or photochemical reduction. It was demonstrated through the isotopic comparison of bulk salt samples and corresponding lake water samples that salt precipitation in this environment preferentially sequesters the lighter ^{79}Br and the heavier ^{37}Cl isotopes from solution. Captured gas samples from the shorelines of three different lake sites also showed depleted values in $\delta^{81}Br$ isotopic signatures, which ranged between -1.02‰ to -0.72‰. This demonstrated that some process, photochemical or microbial, may lead to an enrichment of $\delta^{81}Br$ in the soils as gas is released. Over time, regional changes in $\delta^{81}Br$ and $\delta^{37}Cl$ may be noted as these processes continue, causing lake waters to eventually enrich in $\delta^{81}Br$ and deplete in

$\delta^{37}Cl$. The ephemeral lakes in the region (Group 3 Lakes) may be particularly susceptible to these changes as they have high concentrations of TDS, and therefore salt precipitation is more common.

In the subsurface of this environment, the behaviour of $\delta^{81}Br$ and $\delta^{37}Cl$ isotopes is controlled by the interaction between the saline lake waters and the fresh groundwater systems. It was determined that there are two isotopically distinct groundwater systems in this region. The regional system is highly depleted in both $\delta^{81}Br$ and $\delta^{37}Cl$ isotopic values relative to the surface waters ($\delta^{81}Br$ = -1.16‰ – 1.48‰, $\delta^{37}Cl$ = -1.1‰ – 0.72‰), whereas the isotopic values of the meteoric system is comparable to that of the lakes. The $\delta^{81}Br$ isotopic signatures of the regional groundwater component range between -1.55‰ to -0.90‰, and the $\delta^{37}Cl$ isotopic signatures range between -2.50‰ to -0.21‰. In comparison, the $\delta^{81}Br$ isotopic signatures of the meteoric groundwater system range between 0.77‰ to 1.30‰, and the $\delta^{37}Cl$ isotopic signatures range between -0.13‰ to 0.28‰.

Four sediment cores were collected at three different lake sites in 2014 in order to observe the effects of the groundwater systems on the $\delta^{81}Br$ isotopic signatures of the sediments with depth. It is possible that diffusional, and/or salt wash-down processes are present, as evidence of these exist in the cores from Wilkinson Lake and UNNJ Lake. The $\delta^{37}Cl$ isotopic signature of the bottom of the Wilkinson Core is depleted to -1.79‰, which is similar to the $\delta^{37}Cl$ isotopic signatures of the regional groundwater system, suggesting that there may be a slow upwards diffusion of the underlying regional groundwater into the subsurface of this area. The $\delta^{81}Br$ isotopic signatures of the UNNJ core show regions of depletion which correspond to regions of higher TDS concentrations, indicating the possible presence of a salt wash-down effect.

Acknowledgements

First and foremost, I would like to thank my supervisor, Professor Shaun K. Frape, for his immense guidance and valued expertise throughout the entirety of this project. This would not have been possible without his critical input and support. His continued encouragement and new ideas allowed me to complete this project to the best of my ability.

Secondly, I would like to thank my committee members, Professor Brian Kendall, and Professor Ling Ling Wu, for taking the time to provide me with valuable feedback and criticism. Their advice was a great help in the development of this thesis, especially in its final stages.

I would also like to extend appreciation to Professor Randy Stotler, from Kansas University, for his help during field sampling, organizing the sample chemical analyses which was completed in Kansas University, as well as his valued perspective regarding the direction of this thesis.

Lastly, I would like to express my gratitude to Rhys Gwynne, for his hard work, flexibility, patience, and dedication, in helping me to prepare my samples in the Environmental Isotope Laboratory (EIL) at the University of Waterloo. Rhys was always more than willing to lend a hand, even on very short notice, and for that I cannot thank him enough.

Table of Contents

List of Figures

List of Tables

Introduction

The unique and dynamic hydrology of the alkaline lakes in the Nebraska Sand Hills provides a rare opportunity to study the behaviour of bromine and chlorine in a highly evaporitic environment. Isotopic analyses of these regions can provide key insight in determining the extent to which salt lakes contribute reactive bromine to the atmosphere. In order to do this, a more thorough understanding of the environmental cycling of bromine and chlorine in evaporitic environments is required.

This thesis expands on previous work by Gosselin et al. (1994), and Gosselin et al. (1997), in order to better understand the cycling of bromine and chlorine isotopes in a salt environment. Gosselin sampled the alkaline lakes in 1992 because the region experienced very low amounts of precipitation prior to and during this time. The water samples were analyzed for geochemistry, $\delta^{18}O$, and $\delta^{2}H$. Then in 1993, he sampled the same lakes and repeated the same chemical analyses because the annual precipitation showed a drastic increase from the previous year. This data was used to determine the primary geochemical controls on the lakes, as well as the relative influences of lake hydrology on lake geochemistry. A summary of these publications is provided in an upcoming section, titled "Previous Geochemical Studies".

Similar to 1992, in 2012 low precipitation rates allowed many of the lakes in the region to return to highly evaporitic conditions. This prompted further sampling of the same alkaline lakes which were sampled by Gosselin, as well as adjacent surface salts, and subsurface soils for geochemistry, and $\delta^{18}O$, $\delta^{2}H$, $\delta^{81}Br$, and $\delta^{37}Cl$ isotopic signatures. Following this, wet and rainy conditions occurred in 2013 and 2014 that were comparable to 1993, and therefore lakes and sediments in the region were sampled again during these years. The comparable climatic conditions between 1992 and 2012, and between 1993, 2013, and 2014, provided an ideal opportunity to observe any ensuing geochemical and isotopic changes in the lakes and surrounding sediments in response to different climatic conditions. An overview of precipitation and air temperature data from 1992, 1993, and 2012 to 2014 is provided in Table 1. This data was summarized from daily

NOAA Climate Data that was collected at the Alliance 19.2 ENE Nebraska US Station. The data provided are annual averages of daily recordings of maximum and minimum temperature values, and annual totals of precipitation. Data collected for each year begins at the start of the month of January of that year and finishes at the end of December. Percentages of the data that is available are also listed, as not all the daily data during the sampling years exists.

Table 1. Summary of NOAA Climate Data Global Historical Climatology Network at the Alliance 19.2 ENE Nebraska US Station during sampling years. NA indicates no data available that year.

Year	Average Max. Temperature (^{0}C)	Average Min. Temperature (^{0}C)	Annual Precipitation (mm)	Percentage of Data Available
1992	17.4	1.4	270.8	89%
1993	11.4	-2.8	279.7	67%
2012	19.0	2.1	178.5	97.5%
2013	15.7	1.5	394.0	98.1%
2014	NA	NA	423.6	53.4%

Objectives

The aim of this thesis is to provide a suggestive identification of mechanisms which control the fractionation of bromine and chlorine stable isotopes in an evaporitic environment, such as precipitation and dissolution events, salt deflation, and reduction processes including microbial activity and photochemical oxidation. To accomplish this, the lake water chemical composition and isotopic data from Gosselin et al. (1994), and Gosselin et al. (1997) are combined with lake water chemical data from 2012, 2013, and 2014. In addition to the water samples, surficial salt samples were also collected in 2012, and five sediment cores were taken from the shorelines of several lakes in 2014. The depths of these cores ranged from 0.5 m to 1.5 m in length. Core material was analyzed for several physical parameters including water content, loss on ignition (volatile loss), and bulk salts (electrical conductivity converted to TDS). This information was used to select regions of the cores to extract salts and analyze them for δ^{81}Br and δ^{37}Cl isotopic data. As well, soil gas

bromine was also captured in 2014 from three sample locations adjacent to saline lakes and analyzed for $\delta^{81}Br$. Collectively, the results describe the evolution of the saline lakes and adjacent areas under dynamic climatic conditions.

Alkaline Lakes Review

Alkaline lakes are water bodies with excessively high alkalinity (usually ranging from 2 – 400 g/L), and thus are characterized by high pH values (7.5 – 11) (Brauner et al., 2013). These lakes are known to exist in arid to semiarid areas across North and South America, Australia, China, India, Africa, and the middle and southeast Asia (Salama et al., 1999). There is also evidence of alkaline lakes existing throughout the geologic record, such as the Green River formation in Utah, which has been estimated to be between 36 and 55 million years old (Grant, 2006). More recently it was postulated that the 2.7 billion year old Tumbiana Formation in Australia was part of an alkaline lake system (Newton, 2015).

Alkaline lakes are characterized by high evaporation rates that result in the accumulation of carbonates as a result of low Ca^{2+} and Mg^{2+} in solution and the surrounding geological environment (Brauner et al., 2013). Geochemically the presence of these ions in combination with CO_3^{2-} will preferentially precipitate calcite ($CaCO_3$), magnesite ($MgCO_3$), and dolomite ($MgCa(CO_3)_2$), thus removing carbonate from solution (Grant, 2006). The absence of Ca^{2+} and Mg^{2+} will therefore favour the development of high alkalinity, assuming CO_3^{2-} is in excess over Ca^{2+} and Mg^{2+}, as a result of a shift in the bicarbonate equilibrium (Grant, 2006). Additionally, these water bodies are often situated in a geological environment containing high concentrations of Na^{+} that in combination with abundant CO_3^{2-}, results in carbonate rich solutions (Grant, 2006). This process is visually represented on the right side of Figure 1 (Deocampo and Jones, 2014).

Alkaline lakes generally exist in naturally occurring closed basins. In these regions, the groundwater outflow or discharge is minimal to none, while water influx (from groundwater or surface water) remains steady (Hardie and Eugster, 1970). High evaporation rates concentrate the salts resulting in very high total

dissolved solids (TDS) values that can exceed 250,000 mg/L (Gosselin, 1997). Contrarily, more dilute alkaline lakes have a higher inflow/outflow ratio and therefore are less affected by the evaporitic concentration of salts.

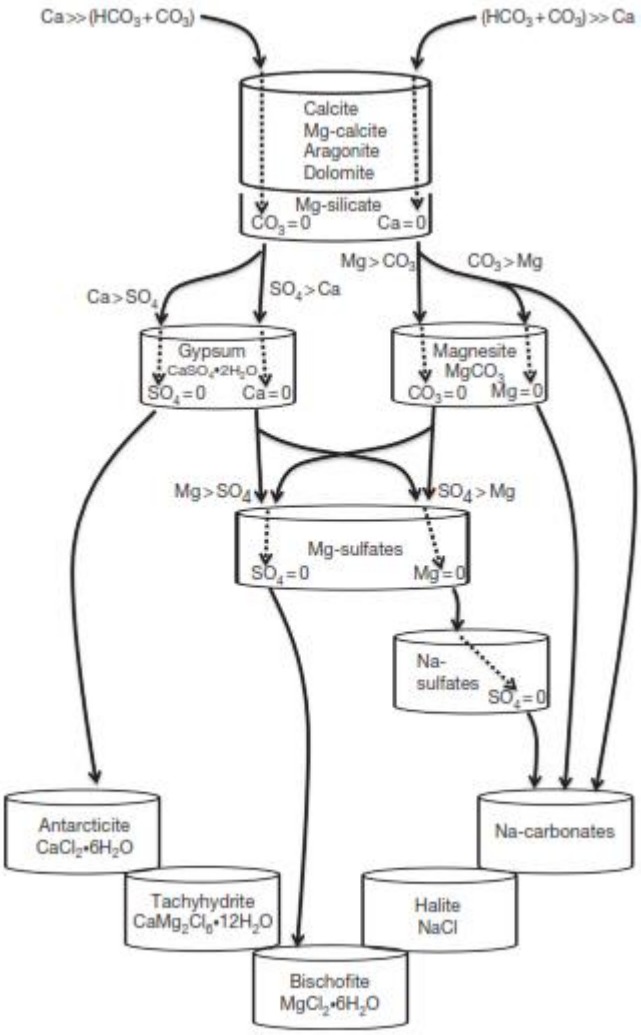

Figure 1. Brine Evolution showing the effects of the dominance of one chemical constituent over another in brines on the resulting mineral precipitates. In high alkaline lakes, brine evolution follows the right-most pathway, precipitating calcium and magnesium carbonate minerals initially, followed by sodium carbonates, then halite, and finally bischofite. (Deocampo and Jones, 2014).

Salt Lakes around the World

Saline lakes are found in a variety of locations across the globe, and can become acidic, neutral, or alkaline under certain conditions. Geochemically, the water compositions range from dominantly Na-Cl, which is

very near standard seawater, to dominantly Na-CO_3 (Hardie and Eugster, 1980). On rare occasions alkaline and acidic salt lakes are found adjacent to one another, separated by a clay layer, as seen in the salt lake region in Australia (Bowen and Benison, 2009). For the most part, the processes responsible for the formation of alkaline lakes and their resulting geochemical compositions are variable, as they are dependent on surrounding geology, climate, and the geological history of the region.

The formation of alkaline lakes commonly results from tectonic activity, such as the alkaline lakes found in East Africa, China, and Egypt (Damm and Edmond, 1984; Lowenstein and Risacher, 2009; Taher, 1999). In East Africa, the downfaulting and thinning of the Ethiopian Plateau crust resulted in high regional heat flow (Gizaw, 1996). The hydrothermal activity resulted in solute accumulation due to evaporation, which over time caused the terminal lakes in the region to become alkaline (Damm and Edmond, 1984). An example is the ephemeral Lake Magadi, which is said to be the most saline lake in this area (Eugster, 1970). In China, the Qaidam Basin was also created as a result of tectonic uplift. Succeeding periods of erosion and depositional activity lead to the development of numerous inland alkaline lakes (Kong et al., 2014). One of the more studied lakes in this region is the Qaidam Lake, whose high salinity is due to higher rates of evaporation than precipitation (Dong et al., 2006), and a low permeable bedrock resulting in little or no groundwater flux to the lake (Henderson, 2003). In Egypt, the formation of the Wadi El Natrun depression was also a result of tectonic activity and was also later modified by erosion (El-Baz, 1984). Low rates of precipitation combined with an arid climate and low humidity have caused the basin to fill with numerous inland alkaline lakes, both perennial and ephemeral (Taher, 1999).

In addition to tectonic activity, it is also not unusual for alkaline lakes to form as remnants of ancient large extensive lakes, as seen in California, Nevada, and Utah (Galat et al., 1981; Jones et al., 2009; Mono Basin Research Group, 1977; Reddy, 1995). Pyramid Lake in Nevada, and Mono Lake in California have been distinguished as remnants of Pleistocene lakes: Lake Lahontan and Russell lake, respectively (Reddy, 1995), and the Great Salt Lake in Utah results from the recession of the ancient Pleistocene lake known as Lake Bonneville (Jones et al., 2009). All three of these lakes are terminal basins, and therefore are highly

saline due to the accumulation of salts from precipitation, groundwater inflow, and incoming drainage from connecting river systems (Spencer et al., 1985).

The chemical composition of these lakes varies slightly depending on location. Lake Magadi and Great Salt Lake are both dominantly Na-CO_3. In Lake Magadi, this composition is believed to be a result of the influx of water from surrounding streams, runoff, the repeated precipitation and dissolution of trona (Na_2CO_3•$NaHCO_3$•$2H_2O$) found in thick layers on the shorelines, and the presence of a volcanic bedrock (Eugster, 1970). In Great Salt Lake, however, the geochemistry of the brine is thought to be caused by incoming $CaCO_3$ rich rivers and NaCl groundwater, as well as factors such as weathering, evaporation, and biotic activity (Spencer et al., 1985). In contrast to this, Pyramid Lake and Mono Lake are both dominantly Na-Cl-CO_3 in composition (Benson, 1984; Jellison and Melack, 1993), and the alkaline lakes in the Wadi El Natrun depression in Egypt are primarily Na-SO_4-Cl (Taher, 1999). In these cases, and similarly to Lake Magadi and Great Salt Lake, the resulting lake geochemistry is strongly influenced by surrounding geology, and incoming surface water and groundwater chemistries.

Sand Hills, Nebraska

Overview

The remainder of this thesis will focus solely on the alkaline lakes situated in the Sand Hills region of Nebraska, USA, shown in Figure 2. The area is a large dune field covering approximately 58,000 km^2 of the mid-northern United States. It is the largest grass-stabilized dune field in the Western Hemisphere (Sridhar and Hubbard, 2010), bordered to the north by the Niobrara River, and to the south by the North Platte River (Ziegler, 1915). The western Sand Hills Region lacks surface drainage, although a few smaller rivers flow in the eastern part of the area. The region directly overlies the High Plains aquifer. Subsequent groundwater discharge from this aquifer, combined with meteoric precipitation, has resulted in the generation of hundreds of shallow lakes in close proximity (Sridhar and Hubbard, 2010). In addition, the

interdunal area encompasses 450 km^2 of open water, 260 km^2 marsh land, and 4,000 km^2 of wet meadows where hay crops are cultivated (Rundquist, 1983).

The dunes themselves can reach 122 m in height and occasionally 32 km in length, and trend west to east in direction (Bleed and Flowerday, 1991; Gosselin et al., 2006). They are composed of highly permeable sand superimposing a thick layer of sand and gravel. This results in a high recharge capacity in the soils (Bleed and Flowerday, 1991). Consequently, the portion of the High Plains aquifer directly beneath the Sand Hills Region holds roughly 65% of the total water in the aquifer (Loope and Swinehart, 2000). Observationally, this characteristic is evident when comparing the dry, white sandy dune tops, and the wet, peaty interdunes (Loope and Swinehart, 2000).

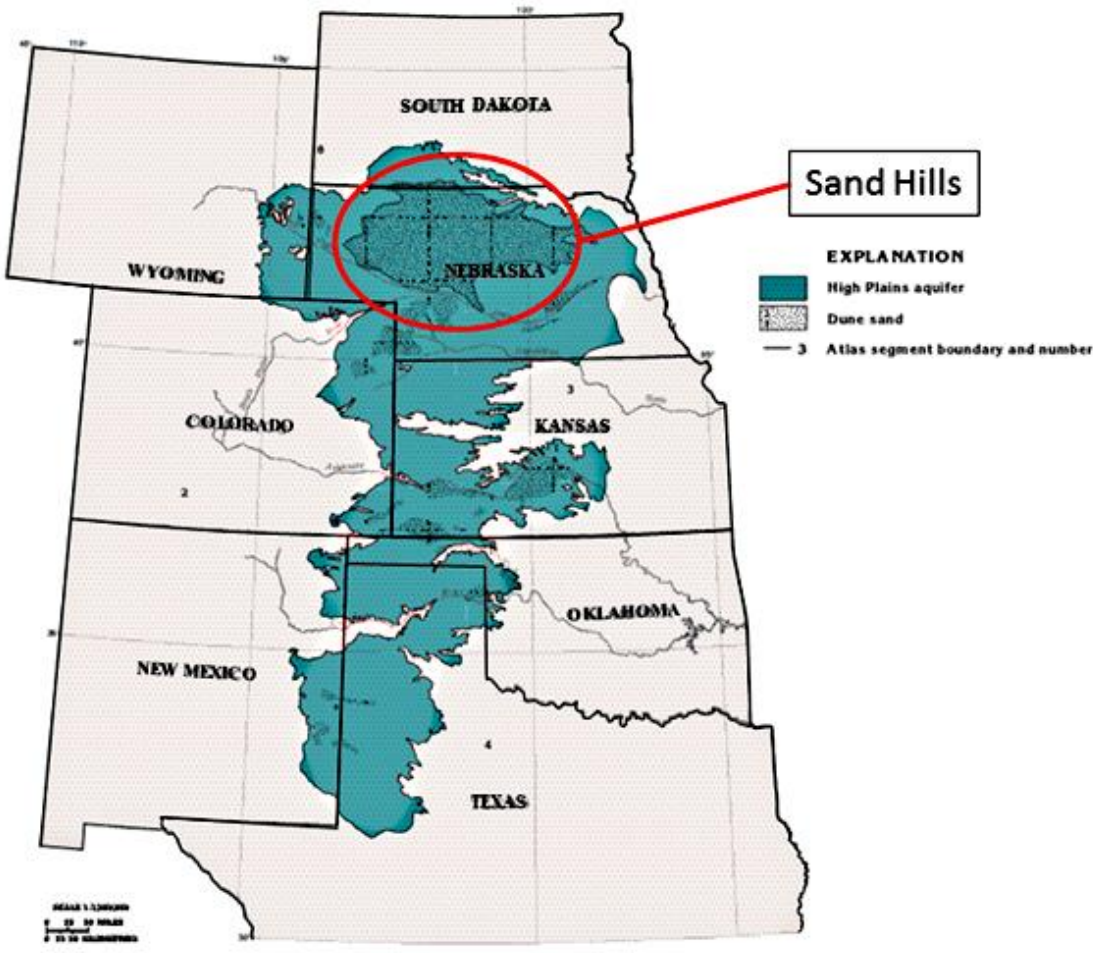

Figure 2. Location of the Nebraska Sand Hills. Modified from USGS, Groundwater Atlas of the United States, 1997 (USGS, 1997).

Climate

The Nebraska Sand Hills' climate is variable, but categorized as sub-humid in the east and semi-arid in the west (Bleed and Flowerday, 1991). It is known for its hot summers, cold winters, high wind speeds, and intermittent snow storms and severe thunderstorms (Bleed and Flowerday, 1991). The mean annual temperature is 10^{o}C (Szilagyi et al., 2011). Regional rainfall is well known for being sparse and highly variable (Loope and Swinehart, 2000). The annual precipitation is roughly 533 mm, however a significant precipitation gradient exists from the east (700 mm/year) to the west (400 mm/year) (Szilagyi et al., 2011). Most precipitation events are triggered by east moving storms that mix with moist air from the Gulf of Mexico (Loope and Swinehart, 2000). As such, approximately half of the annual precipitation is received during the growing season (May through July) (Whitcomb, 1989). Annual evaporation from the lakes is approximately 1,150 mm, which greatly exceeds the rates of precipitation in the area (Winter, 1986). Furthermore, persistent winds exist primarily from the west, but occasionally shift to the north or south directions (Whitcomb, 1989).

Geological Review

The formation of the modern day Sand Hills Region began an estimated 98 million years ago, during which time the district was fully submerged by large inland Cretaceous seas (Whitcomb, 1989). Sediments in the water settled and accumulated over the span of 33 million years, at which time the sea level began to retreat. This left an array of deposits, ranging from fine grained volcanic sediments to alluvial deposits (Whitcomb, 1989).

Cenozoic clastic deposits compose 150 m – 300 m of sediment underlying the dunes (Loope et al, 1995), and consist of several formations. A stratigraphic column of Nebraska is shown in Figure 3. The oldest Tertiary deposits are composed of the Chadron and Brule Formations, together known as the White River Group (Weeks and Gutentag, 1988). These formations outcrop to the north and west of the Sand Hills area,

and they are primarily composed of uncemented clay, sand, gravel, and volcanic ash (Ziegler, 1915). Both formations have low permeability (Weeks and Gutentag, 1988). The overlying Arikaree Formation is mainly cemented sandstone, and outcrops to the north, west, and southwest of the Sand Hills (Ziegler, 1915). This formation is very susceptible to weathering and erosion, and is therefore a major source of sand to the dunes in the area (Weeks and Gutentag, 1988). Overlying these units is the principle geological unit in the region, the Ogallala Formation. The exact depositional history of the aquifer is debated, however it is generally agreed upon that it is likely the result of a vast fluvial deposition from streams followed by periods of erosion (Kromm and White, 1992), and it is composed primarily of gravel, sand, silt, and clay (Weeks & Gutentag, 1988). Superimposing the High Plains aquifer are Quaternary alluvial deposits, and dune sand (Whitcomb, 1989). A simplistic cross section of the Sand Hills is given in Figure 4 for reference (Ahlbrandt and Fryberger, 1980).

<table>
<tr><th>System</th><th>Series</th><th colspan="2">Geologic Unit</th><th>Lithology</th><th>Hydrogeologic Unit</th></tr>
<tr><td rowspan="2">Quaternary</td><td>Holocene and Pleistocene</td><td colspan="2">Valley-till deposits and dune sand</td><td>Gravel, sand, silt, and clay. Dune sands prominent in Nebraska</td><td rowspan="5">High Plains Aquifer</td></tr>
<tr><td>Pleistocene</td><td colspan="2">Alluvial deposits</td><td>Gravel, sand, silt, and clay. Locally cemented</td></tr>
<tr><td rowspan="4">Tertiary</td><td rowspan="2">Miocene</td><td colspan="2">Ogallala Formation</td><td>Unconsolidated poorly sorted gravel, sand, silt, and clay</td></tr>
<tr><td colspan="2">Arikaree Group</td><td>Sandstone, fine- to very fine-grained. Local beds of volcanic ash siltstone, claystone, and mud</td></tr>
<tr><td rowspan="2">Oligocene</td><td rowspan="2">White River Group</td><td>Brule Formation</td><td>Siltstone with sandstone beds and channel deposits</td></tr>
<tr><td>Chadron Formation</td><td>Clay and silt</td><td>Confining Unit</td></tr>
</table>

Figure 3. Stratigraphic column of the Nebraska Sand Hills (USGS, 2009).

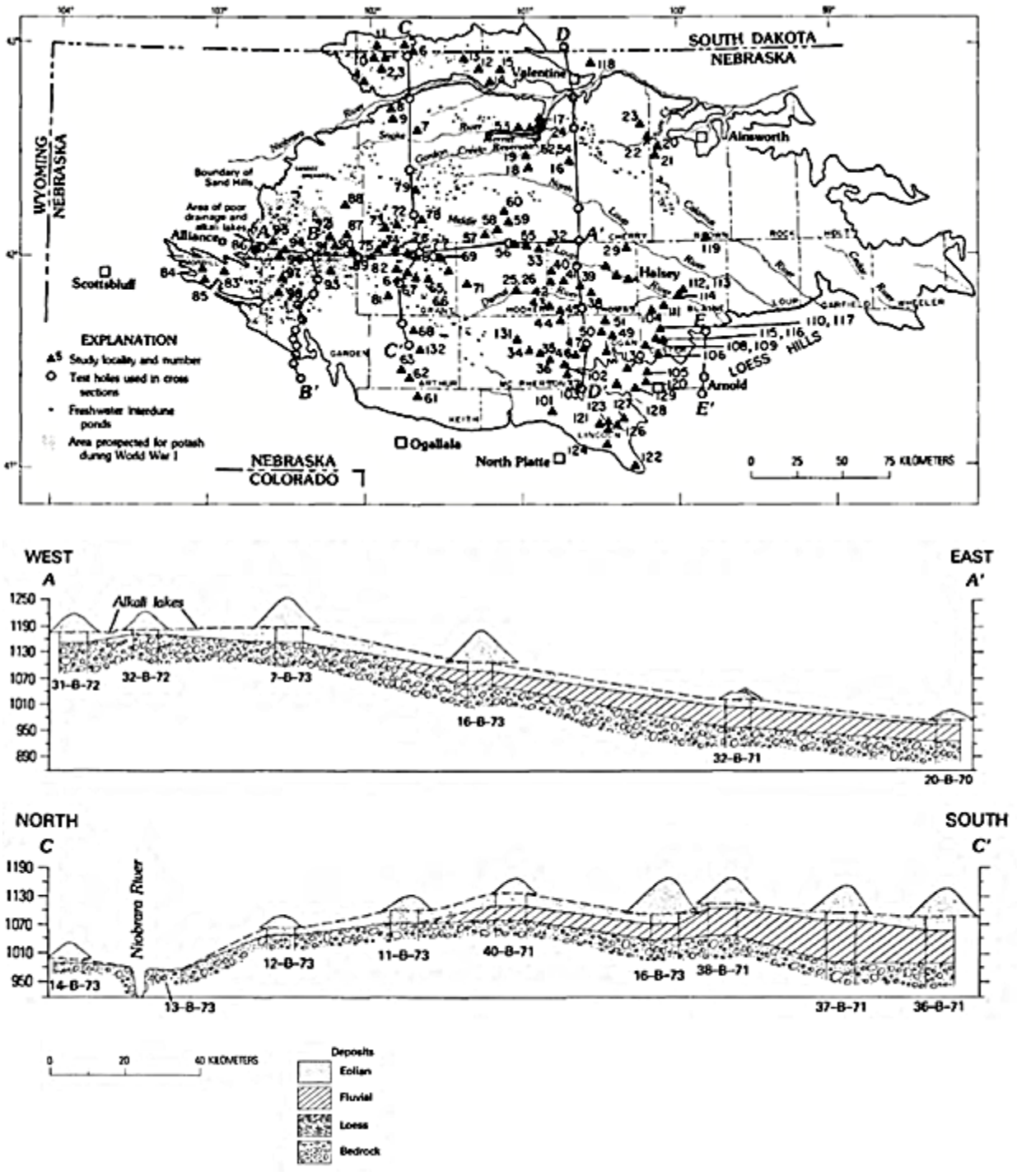

Figure 4. Cross Section showing major geological units beneath the Sand Hills through Grant County, Nebraska USA. Highly permeable eolian sand overlies fluvial deposits, if present, which overlies the bedrock. Modified from Ahlbrandt and Fryberger, (1980).

The Sand Hills' eolian sand is the region's most dominant geological feature (Whitcomb, 1989). The layer of eolian sand can reach 9 m – 18 m thick in the southern and western portions of the Sand Hills (Whitcomb, 1989) and is therefore highly susceptible to dune activation from prevailing winds. It is estimated that dune remobilization occurred approximately 12,000 years before present (ybp), 6,000 ybp, 3,000 ybp, and 1,000 ybp (Loope and Swinehart, 2000). A graphical representation of the duration and magnitude of the events is presented in Figure 5. More recently, optical aging techniques have allowed for more precise estimations of 13,110 ybp, 8,430 ybp, 6,180 ybp, 3,560 ybp, 2,300 ybp, 840 ybp, and 115 ybp (Goble et al., 2004). The environmental conditions allowing for dune reactivation during these time periods have been debated, especially following the observation showing that prolonged drought alone may not be sufficient to remobilize the dunes. For example, the Sand Hills dunes remained relatively stable following the occurrence of the 6 year drought from 1934 to 1940. Mangan et al. (2004) attributed this to the prevalence of the underground biomass root system. Modelling results estimated that the combination of a drought period lasting more than ten years, increased erosional activity, and the domination of one plant functional type, would adequately reduce above and below ground vegetation coverage, resulting in dune remobilization (Mangan et al., 2004). This effect is exaggerated by human activity (Yizhaq et al., 2009).

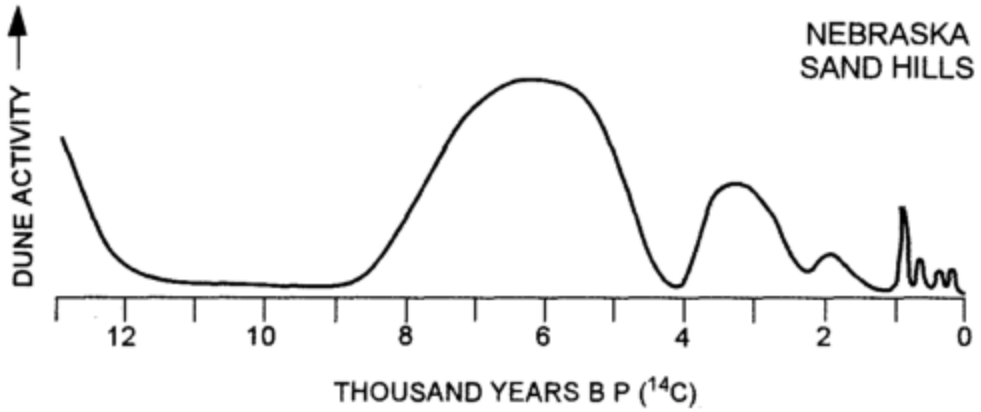

Figure 5. Magnitude and duration of eolian activity, or movement, in the past 13,000 years (Loope & Swinehart, 2000).

Scarce rainfall, high evaporation rates, highly permeable dune material, and no historical evidence of glaciation make the presence of lakes in this area unusual (Loope and Swinehart, 2000). Dune dams provide the only reasonable explanation for their existence. It is speculated that dune dams formed when mobile dunes shifted to block ancestral drainage basins, presently known as Snake Creek and Blue Creek drainages (Loope and Swinehart, 2000). The surface drainage was forced to reroute, resulting in a rise in the water table, by as much as 25 m in some places (Loope et al., 1995). It is estimated these blockage events occurred 12,000 ybp and 6,000 ybp (Loope et al., 1995).

The subsequent lake formation in response to dune dams raising the water table demonstrates that the underlying groundwater aquifer system is an integral part of the modern lake watershed. The surface water configuration is therefore reliant on the topographies of the ground surface and water table, as well as the hydraulic conductivity of the subsurface (Winter, 1976). A conceptual diagram based on the Sand Hills area showing the effects of the landscape topography and water table configuration on lake dynamics is shown in Figure 6 (Winter, 1976).

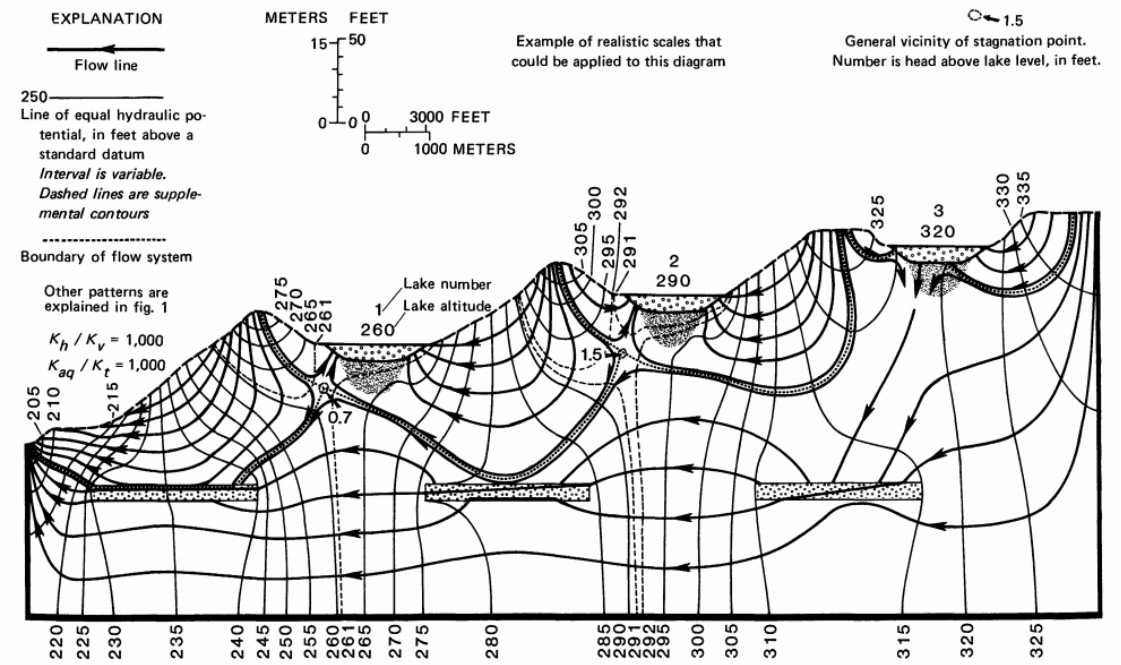

Figure 6. Two-dimensional flow net diagram of groundwater near multiple lakes, showing the connectiveness of the lake watershed to the underlying aquifer, and the effect of the ground surface and water table topographies on surrounding lakes (Winter, 1976).

Measured alkalinity ranges from across the region are shown in Figure 7 (Zlotnik, 2012). Overall, the majority of the lakes found in the west are of moderate to high alkalinity, whereas the majority of the lakes in the east are of slight to medium alkalinity. This is due to the configuration of the local and regional water table, which is variable depending on the duration and magnitude of local precipitation and evapotranspiration events, vegetation cover, and surface topography (Gosselin et al., 2006; Zlotnik et al., 2009). The regional water table flows from the west to the east, as shown in Figure 7 (Zlotnik, 2012). The local groundwater table configuration changes with the formation of mounds and troughs. These features are known to form beneath dunes as a result of a change in hydrologic parameters, such as an increase in precipitation or evaporation (Winter, 1986). The ratio of the regional water table to the local water table (G) determines the flow regime of the lakes, and is illustrated in Figure 8. If $G > 1$, the lake is a flow-through regime, whereas if $G < 1$, the lake is in a region of discharge (Zlotnik et al., 2009).

Repeated cycles of groundwater discharge, meteoric precipitation, and evaporation over the past 12,000 years have concentrated fine grained silt and organic sediments in the lakebeds, making them nearly impermeable (Loope et al., 1995; Ziegler, 1915). In flow-through lakes ($G > 1$), groundwater flushing dominates which prevents the lakes from reaching high levels of alkalinity. In discharge lakes ($G < 1$), minimal to no groundwater outflow results in the accumulation of solutes under evaporative conditions, and consequently lakes with this flow regime can become significantly alkaline (Zlotnik et al., 2009). Both lake types are illustrated in Figure 7 using blue and red symbols, respectively. In addition to the individual lake flow regime, alkalinity levels of these lakes are affected by climatic conditions. In this region, climate changes slightly from the eastern to the western Sand Hills. The eastern Sand Hills receive 700 mm of precipitation per year, whereas the western Sand Hills receives only 400 mm (Szilagyi et al., 2011). Lakes in the western portion are therefore more susceptible to solute accumulation and higher alkalinity.

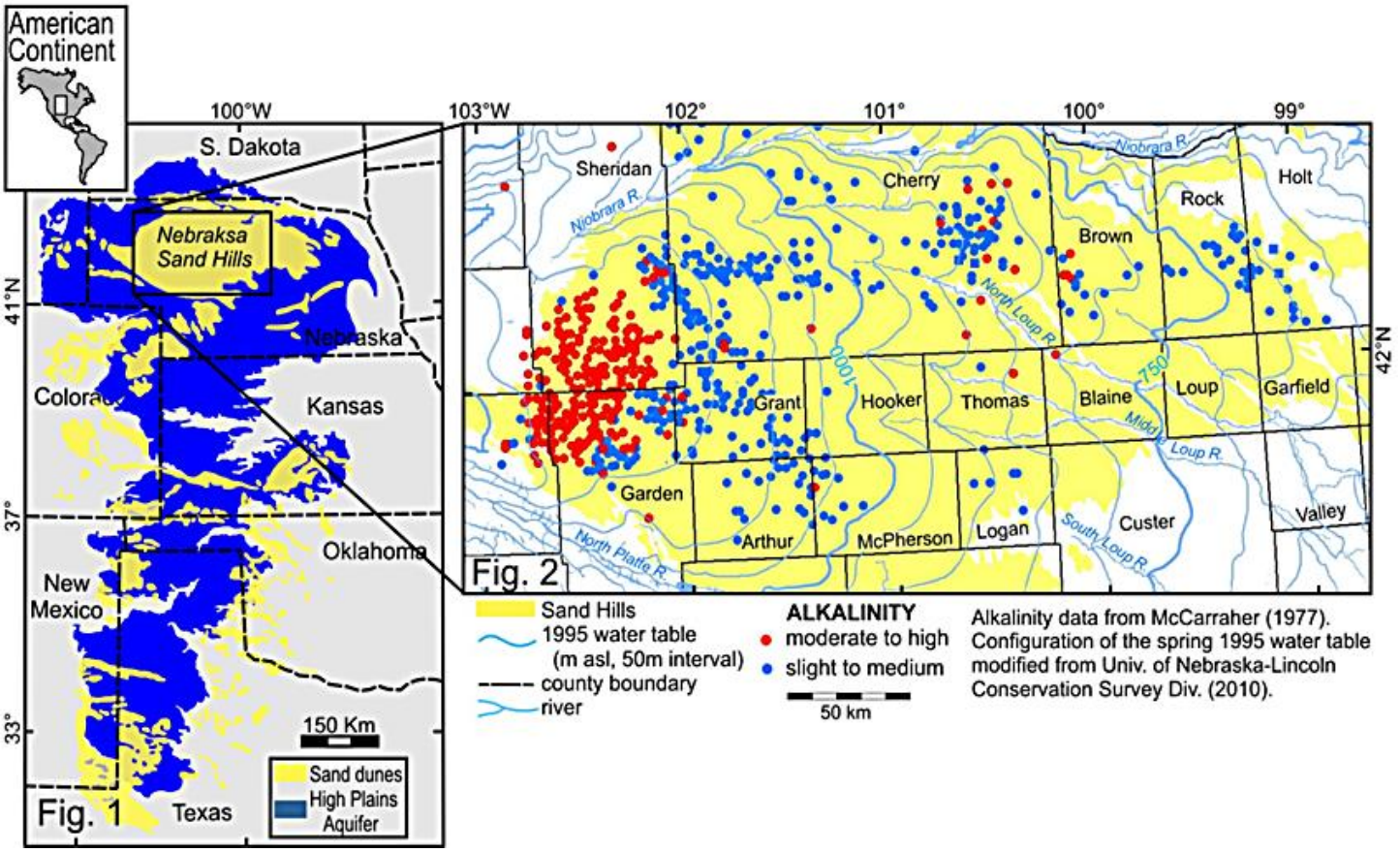

Figure 7. Alkalinity data identifying lakes of moderate to high alkalinity and lakes of slight to medium alkalinity. Modified after McCarraher, (1977), and Zlotnik, (2012).

Flow-through Regime

Discharge Regime

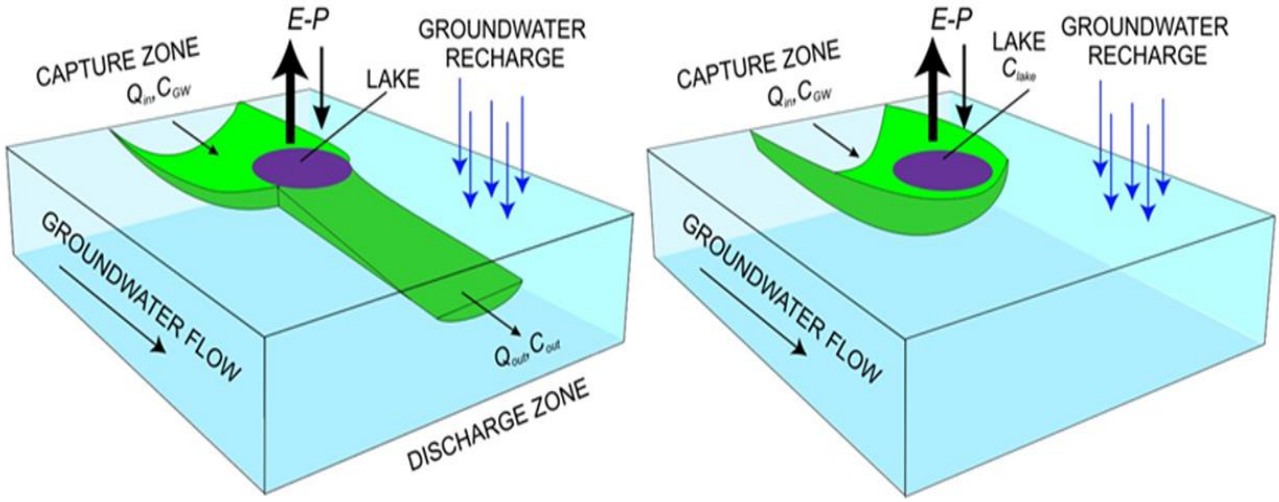

$$C_{lake} = C_{GW}\frac{Q_{in}}{Q_{out}}$$

$$C_{lake} \approx \frac{C_{GW}Q_{in}}{Q_{out}}t$$

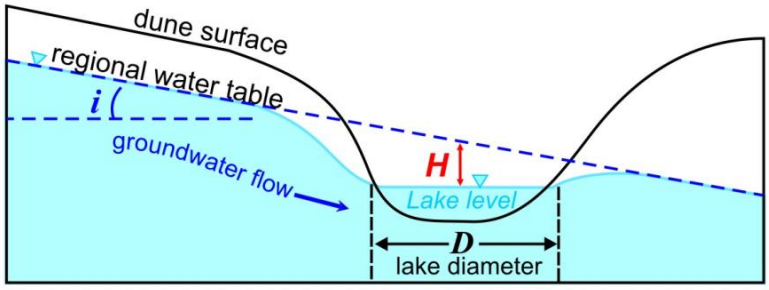

Gradient ratio, $G = \frac{regional\ water\ table\ slope}{local\ water\ table\ gradient} = \frac{i}{H/D}$

G > 1 → Flow Through
G < 1 → Solute Accumulation

Figure 8. Input and output fluxes contributing to flow-through and discharge lake systems, where Q is flux, and C is concentration. Modified from Zlotnik et al. (2009).

In addition to hydrologic parameters, the geochemical characteristics of the lakes in the Sand Hills Region are also not consistent. Historically, the lakes have been classified as Na-CO_3-(SO_4)-(Cl) or Na-SO_4-(CO_3)-(Cl), in compliance with the Eugster and Hardie classification scheme developed in 1978 (Gosselin, 1997). The higher concentration lakes, whose TDS can reach over 250,000 mg/L, have anion compositions closer to Cl-SO_4, and cation compositions of the Na-K type (Gosselin et al., 1994). In comparison, the groundwater is freshwater in composition with greater amounts of bicarbonate, calcium, and magnesium than the accompanying lake water, and a TDS concentration that is close to 200 mg/L. Using the same classification scheme, groundwater chemical composition varies between Na-Ca-(Mg)-CO_3-(SO_4)-(Cl) and Na-(Ca)-(Mg)-CO_3-(SO_4) (Gosselin, 1997). The geochemical composition of the groundwater is essential because the high hydraulic conductivity of the interdunal areas means that the primary source of water to the saline lakes in most years is groundwater (Szilagyi et al., 2011; Wang et al., 2008). Lakes which are more closely connected with the groundwater system tend to have a lower concentration of TDS, and their chemical composition more closely resembles the chemical composition of the groundwater. In contrast, the geochemical compositions of the higher TDS lakes are much more variable.

Over time, repeated wetting and drying cycles in the region have resulted in a slight alteration in the chemical compositions of the lakes. Previous research has noted a minor depletion in the concentrations of K^+, SO_4^{2-}, and inorganic carbon with the 1:1 evaporation line (Gosselin, 1997). This pattern indicates that re-dissolution of salt minerals containing K^+, SO_4^{2-}, and CO_3^{2-}, such as aphthitalite ($K_3Na(SO_4)_2$), mirabilite ($Na_2SO_4 \cdot 10H_2O$), thenardite (Na_2SO_4), thermonatrite ($Na_2CO_3 \cdot H_2O$), and trona ($Na_3H(CO_3)_2 \cdot 2H_2O$) (Gosselin, 1997) occurs at less than 100% efficiency. It also implies that removal processes of these salts, such as eolian activity, may be occurring (Gosselin, 1997). The dominant minerals present in surficial salts include thenardite (Na_2SO_4) and mirabilite ($Na_2SO_4 \cdot 10H_2O$), whereas minor mineral precipitates include bloedite ($Na_2Mg(SO_4)_2 \cdot 4H_2O$), halite (NaCl), burkeite ($Na_6CO_3(SO_4)_2$), and calcite ($CaCO_3$) (Joeckel et al., 2005). The composition of mineral precipitates within individual lakes in combination with the balance of

precipitation and dissolution events for various mineral phases most likely exerts major controls on the highly variable composition seen in the more saline lakes.

Historical Potash Mining

The major economic boom of the Nebraska Sand Hills Region was the potash exploitation in the early 1900s. Germany was originally the leading distributor of the mineral and had ceased all production and export to the United States during World War I. This caused the cost of potash in the United States to increase considerably. The pressure of the rising costs lead to the construction of the first potash plant in Nebraska in 1915 (Ziegler, 1915). In an effort to increase efficiency and reduce costs, the methods used for salt extraction were consistently changing (Anderson, 2003). Initially, it involved pumping brines through pipelines from high concentration lakes into storage tanks. Solar evaporation was then used to concentrate the brines until they were ready for distribution (Ziegler, 1915). Eventually, coal or oil fired dryers replaced solar evaporation (Anderson, 2003). Companies also began to focus extractions from the lakes which contained the highest brine concentrations, such as Jesse Lake (Ziegler, 1915). Currently, remnants of the pipes used for salt extraction are seen at Homestead Lake, and are shown in Figure 9.

By 1917, five main companies were in production: Potash Products Co, Nebraska Potash Works Co, American Potash Co, Hord Alkali Products Co, and Palmer Alkali Co (Crawford, 1917), along with a number of smaller reduction companies (Anderson, 2003). Salt extraction was concentrated on the western side of the Sand Hills region, encompassing southern Sheridan County, northwest Garden County, and northeast Morrill County, outlined on Figure 10 (Anderson, 2003).

The lakes which were sampled in this project and were also major sites for salt extraction include Homestead, Jesse, Krause, Long, Johnston, Shriner, Wilkinson, Cravath, and Diamond lakes (Hicks, 1921). The average composition of extractable brines consisted of 17.72% potassium, 24.72% sodium, 4.9%

chlorine, 9.64% sulphate, 28.56% carbonate, 14.41% bicarbonate, and 0.05% silica (Hicks, 1921). Over half of the potash extracted originated from lake brines with 5-10% solids (Hicks, 1921).

Figure 9. Field evidence of pipes used for potash extraction at Homestead Lake, 2014.

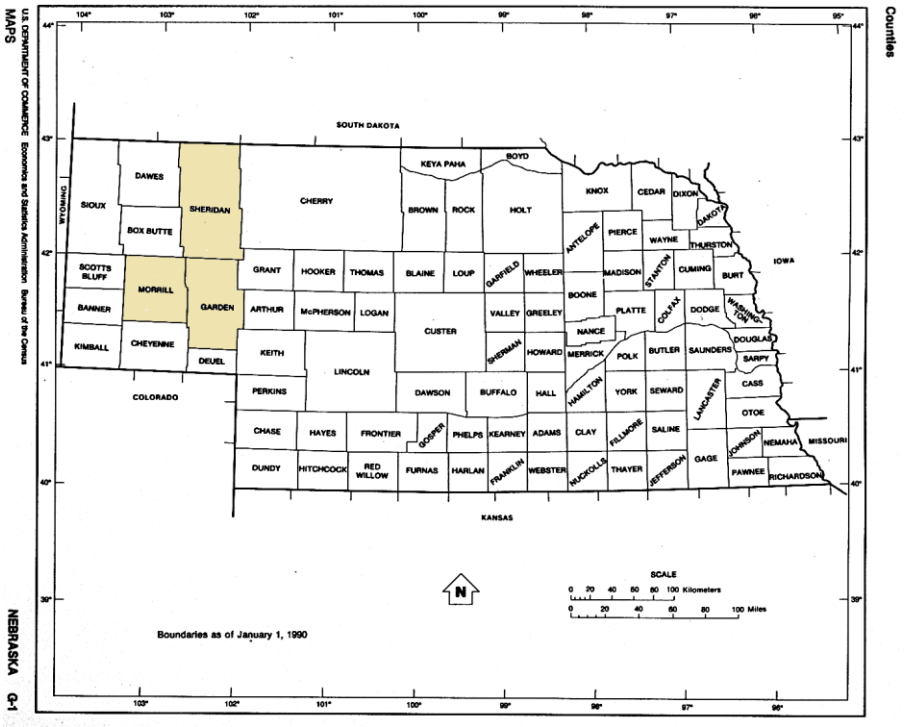

Figure 10. Nebraska County Map. Sheridan, Morrill, and Garden Counties are indicated in light yellow. (U.S. Bureau of the Census, 1990).

The potash economic boom was short-lived, as the fertilizer industry could not afford to continue to purchase potash following World War I, as acquisition resumed from Germany (Anderson, 2003). By 1922, the Nebraska potash plants were completely bankrupt, and the last plant was shut down (Anderson, 2003). The alkaline lakes of the Sand Hills Region remained of very little industrial or scientific interest until the mid-1900s, during which time the research focused on fishery management. It was not until the late 1970s that geochemistry became a new topic of interest, and the early 1990s that it was more thoroughly studied.

Previous Geochemical Studies

In 1992 and 1993, geochemical sampling and field research was conducted on a large number of different lakes in the Sand Hills Region (Gosselin et al., 1994; Gosselin, 1997; Gosselin et al., 1997). The field data collected included temperature, pH, specific conductance, total alkalinity, and specific gravity. Performed laboratory analyses included a quantification of total dissolved solids, and cation and anion concentrations. For a complete description of the methodology, the reader is referred to Gosselin et al. (1994). Prior to 1992, prolonged drought and low precipitation rates had concentrated many of the more saline lakes in the region. Regional precipitation in 1993 greatly exceeded precipitation in 1992, and Gosselin noted that lake depth nearly doubled in 1993.

Gosselin et al. (1994) aimed to determine the primary geochemical controls on these lakes, as well as the relative influence of lake hydrology on lake geochemistry. The apparent conservative behaviour of Cl^-, Na^+, K^+, and SO_4^{2-} was of interest, as this characterization is unusual for saline lakes of this nature. Gosselin recognized the high variability among ephemeral lakes, and attributed this behaviour to the repeated drying and wetting cycles, and subsequent mineral crystallization and re-dissolution events. Gosselin also noted the recurrence of several mineral assemblages in efflorescent salt crusts on UNNJ Lake, Homestead Lake, and Jesse Lake. These mineral assemblages consisted of aphthitalite ($K_3Na(SO_4)_2$), mirabilite ($Na_2SO_4 \cdot 10H_2O$), thenardite (Na_2SO_4), trona ($Na_3Ca(CO_3)_2 \cdot 2H_2O$), and thermonatrite ($Na_2CO_3 \cdot H_2O$).

Using a combination of PHRQPITZ (Plummer et al., 1988) and NETPATH (Plummer et al., 1991) models, Gosselin demonstrated that in 1992 and 1993 groundwater discharge followed by evaporation was almost exclusively responsible for the current concentration of solutes in the lakes, and that the extent of salt precipitation is highly dependent on the groundwater inflow/outflow ratio at any single lake. This in turn is reliant on the lake flow regime, which is determined by the relative configurations of the regional and local water tables, shown in Figures 6, 7, and 8 (Winter, 1976; Winter, 1986; Zlotnik et al., 2009).

Gosselin et al. (1997) expanded on the lake geochemistry descriptions by analyzing for isotopic parameters such as $\delta^{18}O$, $\delta^{2}H$, and ^{87}Sr composition of both groundwater and surface waters. He performed field tests on a seasonal basis in order to understand the geochemical and isotopic evolution of the lake systems. From this he was able to classify the lakes into three groups according to their $\delta^{18}O$ and $\delta^{2}H$ isotopic seasonal variability, illustrated in Figure 11. Group 1 lakes experienced an isotopic enrichment from the spring to fall sampling periods. This enrichment reflects the increase in evaporation, which occurs over the summer as the light isotopic inflows from groundwater are not sufficient enough to balance the enrichment from evaporation. Conversely, Group 2 lakes experienced an isotopic depletion between spring and fall sampling periods. Gosselin attributed this trend to an earlier seasonal transition to higher groundwater inflows compared with Group 1 lakes. It is also possible that varying atmospheric humidity may play a role, as upwind lakes may alter the humidity of other lakes. Gosselin also noted the slight relative enrichment of Group 2 lakes in relation to Group 1. He suggested this is due to reduced groundwater inflow, or higher evaporative conditions in these areas. Finally, Group 3 lakes are ephemeral. The seasonal isotopic trends in $\delta^{18}O$ and $\delta^{2}H$ in these lakes are thus not consistent, as they are affected by numerous cycles of mineral precipitation and dissolution. Furthermore, the complicated behaviour of $\delta^{18}O$ and $\delta^{2}H$ isotopic signatures in these lakes are further convoluted by the mineral precipitation and dissolution of hydrous salt minerals, such as mirabilite, trona, and thermonatrite. For example, the formation or precipitation of one molecule of mirabilite will remove ten molecules of water from solution. The precipitation and dissolution of the many different hydrous mineral phases identified in and around these lakes could change the isotopic signatures

significantly, particularly in periods of low water content. Additionally the inconsistencies in the $\delta^{18}O$ and $\delta^{2}H$ isotopic values in the Group 3 lakes may arise as a consequence of periods of higher meteoric precipitation and of these lakes taking on hydrological characteristics of the other two lake groups as they contain greater volumes of water.

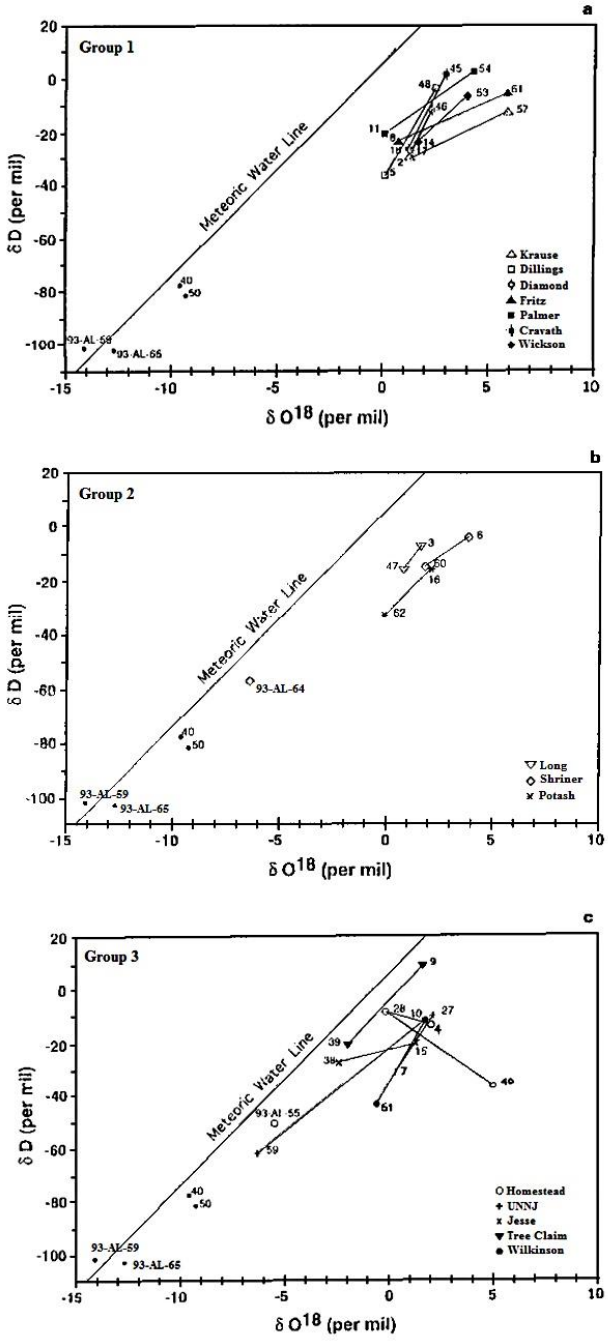

Figure 11. Seasonal data of a) Group 1, b) Group 2, and c) Group 3 lakes collected in May and October of 1992 (Gosselin et al., 1997).

Methodology

The geochemical and isotopic results from samples collected between 2012 and 2014 were used in combination with results gathered in 1992 and 1993 from Gosselin et al. (1994) and Gosselin et al. (1997). In 1992, water samples were taken three times during the year; once in late May, once in mid-August, and once in mid-October. The lakes sampled included Cravath, Diamond, Dillings, Fritz, Homestead, Jesse, Krause, Long, Palmer, Potash, Shriner, Tree Claim, UNNJ, Wickson, and Wilkinson lakes. Groundwater was also sampled from the Homestead Spring and the Krause Well. Similarly, in 1993 the lakes were sampled in mid-May, mid-August, and mid-October. The water samples were collected from Dillings, Gallagher, Homestead, Johnston, Krause, Potash, Shriner, Tree Claim, UNNJ, and Wilkinson lakes. Groundwater was sampled from the Homestead Spring, and Shriner groundwater. More recently, the lakes in the Nebraska Sand Hills were visited once a year from 2012 to 2014. Each sampling period occurred during late July to mid-August. The sample sites were focused in the Sheridan County. Figure 12 indicates the location of all the sampled lakes (names shown) and can be used as reference.

In 2012, water samples were taken from Dillings, Fritz, Homestead, Joe, Shriner, UNNJ Area, and Wilkinson lakes. The water samples were analyzed for geochemistry, as well as $\delta^{81}Br$ and $\delta^{37}Cl$ isotopic signatures. The procedure used for the geochemical and isotopic analyses is outlined in the upcoming sections, “Water Chemical Analysis”, “Chlorine Stable Isotopic Analysis”, and “Bromine Stable Isotopic Analysis”. The results are listed in the Results section under the headings “Geochemistry” and “$\delta^{81}Br$ and $\delta^{37}Cl$”. Thick surficial salt crusts were noted and collected from Fritz Lake, Homestead Lake, and UNNJ Lakes. The salts collected from UNNJ Lake and Fritz Lake had visible salt layers, which ranged in thickness from 0.5 mm to 5 mm. The layers were analyzed for $\delta^{37}Cl$ isotopic signatures following the procedure summarized in the Methodology section titled “Chlorine Stable Isotope Analysis”, and in Appendix A. The results of this analysis are outlined in the results section under the heading “$\delta^{81}Br$ and $\delta^{37}Cl$”.

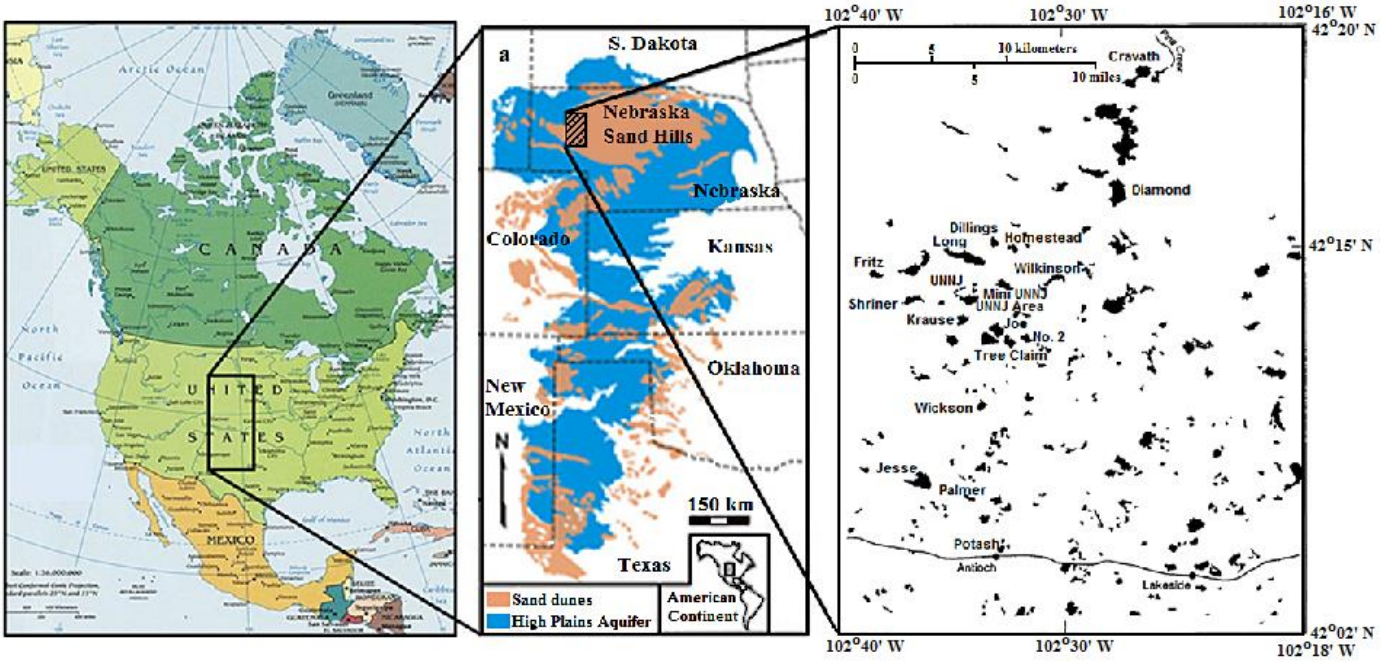

Figure 12. Location of the study site. The map showing the relative location of High Plains Aquifer and the Nebraska Sand Dunes is modified from Zlotnik et al. (2012), and the map showing the locations of the alkaline lakes used in this thesis is modified from Gosselin et al. (1994).

In 2013, the lakes sampled for water included Homestead Lake, Joe Lake, Mini UNNJ Lake, UNNJ Lake, and Wilkinson Lake. Groundwater was also sampled from the spring at Homestead Lake (called Homestead Spring), from a mini-piezometer installed on the small island created by the flowing spring at Homestead Lake (called Homestead Island Piezo), from the water trough near UNNJ Lake which is hydraulically connected to the underlying aquifer (UNNJ Windmill), and from a series of mini-piezometers installed on the southwestern shoreline at Wilkinson Lake. A total of five mini-piezometers were installed at Wilkinson Lake: at the grass-line at 1.2 m (4 feet) deep, at the water-line at 0.6 m (2 feet) and 1.2 m (4 feet) deep, and in the lake itself at 0.6 m (2 feet) and 1.2 m (4 feet) deep. Water sampled from the mini-piezometers represented shallow meteoric groundwater, whereas water sampled from the Homestead Spring and the UNNJ Windmill represented groundwater from the deeper High Plains Aquifer. Both surface water and groundwater samples were analyzed for water chemistry and $\delta^{81}Br$ and $\delta^{37}Cl$ isotopic signatures. The results of this analysis can be found in the Results section under the headings "Geochemistry" and "$\delta^{81}Br$ and $\delta^{37}Cl$".

In 2014, as part of this thesis, water samples were collected at Dillings Lake, Fritz Lake, Big Harvey Lake, Homestead Lake, Joe Lake, Mini UNNJ Lake, No. 2 Lake, Shriner Lake, UNNJ Lake, UNNJ Area Lake, and Wilkinson Lake. Wilkinson Lake was sampled at both the southwest and northeast corners of the lake. From each lake, 1 L of filtered water and 500 mL of unfiltered water was taken. Prior to 2014, the 2012 and 2013 lake water samples were not filtered in the field due to the difficulty of dealing with the high TDS values and the persistent microbial or colloidal clogging of filters. Again, deeper groundwater from the High Plains Aquifer was sampled from Homestead Spring, and UNNJ Windmill, and the shallower groundwater from the mini-piezometers at Wilkinson Lake. One mini-piezometer was positioned at the water-line at 0.6 m (2 feet) deep and one at 1.2 m (4 feet) deep, and one at the mid-beach section at 0.6 m (2 feet) deep. The surface water and groundwater samples were analyzed for geochemistry, as well as $\delta^{81}Br$ and $\delta^{37}Cl$ isotopic signatures. The procedure used for the geochemical and isotopic analyses is outlined in the upcoming sections, "Water Chemical Analysis", "Chlorine Stable Isotopic Analysis", and "Bromine Stable Isotopic Analysis". The results are listed in the Results section under the headings "Geochemistry" and "$\delta^{81}Br$ and $\delta^{37}Cl$". Finally, five cores were taken using 3" and 2" aluminum core tubes driven in place using a jack hammer. The deepest core (1.58 m) was from Wilkinson Lake, the next deepest core (1.22 m) was from UNNJ Lake, and the last three cores were from Homestead Lake. Homestead 1 Core was sampled the closest to the shoreline and was 0.88 m in depth, Homestead MB Core lay mid-beach and was 0.40 m in depth, and Homestead 3 Core was closest to the grass line and was 0.74 m in depth. Sections of the cores were logged for sediment description, and analyzed for total dissolved solids, loss on ignition (volatile loss), and water content. A description of the methodologies used for these analyses is provided in "Core Sampling Methodology". Results of the core analyses are given in the Results section titled "$\delta^{81}Br$ and $\delta^{37}Cl$". Further description of the core, water, and gas sampling methodologies is given in the following sections.

Water Sampling Methodology

Figure 13. Water sampling during the 2014 sampling year, showing a) drawing water from the lake with a peristaltic pump, and b) conducting field measurements.

Water samples were gathered from each lake using a peristaltic pump that drained water from a location a few meters from shore, shown in Figure 13a. Approximately 1 L of lake water was drawn before sampling began, at which point several field measurements were collected, including electrical conductivity (EC), Eh, pH, temperature, and dissolved oxygen content, shown in Figure 13b.

In 2012 and 2013, water samples were filtered for the water chemical analysis and the $\delta^{18}O$ and $\delta^{2}H$ isotopic analyses. However, there was difficulty in filtering large volumes of the lake water in the field, and therefore unfiltered samples were collected for the $\delta^{81}Br$ and $\delta^{37}Cl$ isotopic analyses. Portions of each halide isotopic sample were filtered in the laboratory prior to analyses. In 2014, large volumes of filtered water samples were made possible by the use of a 0.45 µm Porpack filtering system. A comparison of filtered and unfiltered water samples showed minor differences for the isotopic values of $\delta^{81}Br$ and $\delta^{37}Cl$ for some samples, and is shown on Figure 25 in the "$\delta^{81}Br$ and $\delta^{37}Cl$" section of the Results. It is apparent that a component of Br is included in the material trapped on the filters, and that this needs further study to identify the bromide hosted substrate captured on the filters.

Water Chemical Analysis

Water samples were tested for their chemical composition, total dissolved solids, laboratory specific conductivity, and charge balance was calculated at the University of Kansas. The concentrations of Ca^{2+}, Mg^{2+}, Na^{+}, K^{+}, Sr^{2+}, B^{3+}, and silica were determined using an inductively coupled plasma optical emission spectrometer. Concentrations of Cl^{-}, SO_4^{2-}, NO_3^{-}, F^{-}, and Br^{-} were analyzed using an ion chromatograph. The analytical error for each constituent was approximately 2%, and the charge balance errors were below 3.5%. The major and minor dissolved constituents were summed to calculate the total dissolved solids. The total carbonate concentrations and total bicarbonate concentrations were summed together and expressed as the total bicarbonate. The bicarbonate concentration was also multiplied by a factor of 0.4917 to more accurately represent precipitable carbonate, as some of it will be released into the atmosphere as $CO_{2(g)}$. A representation of the total concentration of HCO_3^{-} and CO_3^{2-} in an open system at various pH values is shown in Figure 14. At pH 11, the concentration of CO_3^{2-} becomes nearly equivalent to the concentration of HCO_3^{-}. The pH values of the alkaline lakes in the Sand Hills typically range between 7.9 and 10.4.

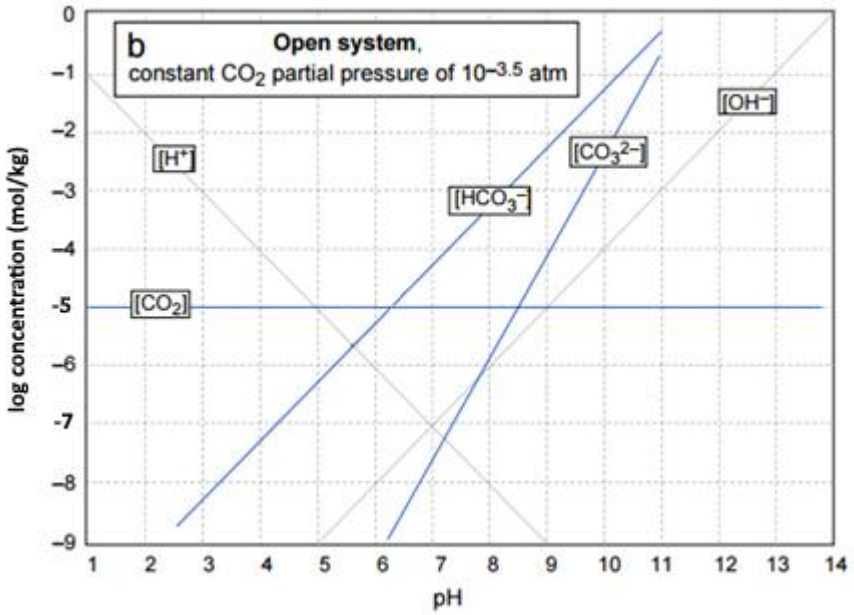

Figure 14. Carbonate Equilibria in an open system at various pH values. HCO_3^{-} is the dominant carbonate phase between pH 6.3 and 10.3 (Lower, 1996).

Oxygen and Hydrogen Isotope Analysis

The stable hydrogen and oxygen isotopic compositions were analyzed at the Keck Paleoenvironmental Stable Isotope Laboratory at the University of Kansas. The analysis was done using an L2120-i Picarro Cavity Ring-Down Spectrometer with High-Precision Vaporizer A0211. Salt clogging was dealt with by washing the needle on the nebulizer machine with deionized water (DI) following each sample analysis, in addition to the standard cleaning procedures. Isotopic measurements were reported in the standard δ (‰) notation, relative to Vienna Standard Mean Ocean Water (VSMOW), according to Equation 1 in the "Isotope Data Notation" section. The precision for $\delta^{2}H$ was <0.5‰, and for $\delta^{18}O$ was <0.1‰.

Chlorine Stable Isotope Analysis

Chlorine stable isotopic signatures were determined at the University of Waterloo Environmental Isotope Laboratory. Isotopic measurements were performed by the conversion of silver chloride salts to methyl chloride followed by an injection into an Agilent 6890 gas chromatograph (GC) via a CombiPAL autosampler and measured on a Micromass Isoprime Continuous Flow Isotope Ratio Mass Spectrometer (CF-IRMS), with an internal precision of ±0.03‰. The standard used to calibrate the data were Standard Mean Ocean Chloride (SMOC), as well as at least two internal inter-lab calibrated standards to test the linearity of the equipment at extreme values. A simple protocol was followed in order to isolate the chlorine from each sample and prepare it for isotopic analysis. This protocol is fully explained in Shouakar-Stash et al. (2005a), and is summarized in Appendix A.

Bromine Stable Isotope Analysis

Similar to chlorine, bromine stable isotopic signatures were analysed at the University of Waterloo Environmental Isotope Lab. Bromine was isolated from each sample, using the methodology outlined in Appendix A, then isotopes were measured by injecting methyl bromide into an Agilent 7890 GC via a

CombiPAL autosampler and measured on a Thermo Scientific MAT 253 CF-IRMS, with an internal precision of ±0.03‰. The standard used to calibrate the data were Standard Mean Ocean Bromide (SMOB), as well as at least two internal inter-lab calibrated standards to test the linearity of the equipment at extreme values. A full methodology is described in Shouakar-Stash et al. (2005b), and is summarized in Appendix A.

Isotope Data Notation

All oxygen, hydrogen, bromine, and chlorine stable isotopes are reported in parts per thousand, or per mil (‰) notation, relating the sample isotope ratio to an international standard (SMOB or SMOC). Internal standards had been cross correlated with laboratories at the University of New Mexico, and the University of Illinois at Chicago. The stable bromine isotope data is reported according to Equation 1:

$$\delta^{81}Br = [\frac{(^{81}Br/^{79}Br)_{sample} - (^{81}Br/^{79}Br)_{standard}}{(^{81}Br/^{79}Br)_{standard}}] \times 10^3 \quad (1)$$

The stable chlorine, oxygen, and hydrogen isotope data is calculated using $^{37}Cl/^{35}Cl$, $^{18}O/^{16}O$, and $^{2}H/^{1}H$, respectively, in the same equation.

Salt and Soil Sampling Methodology

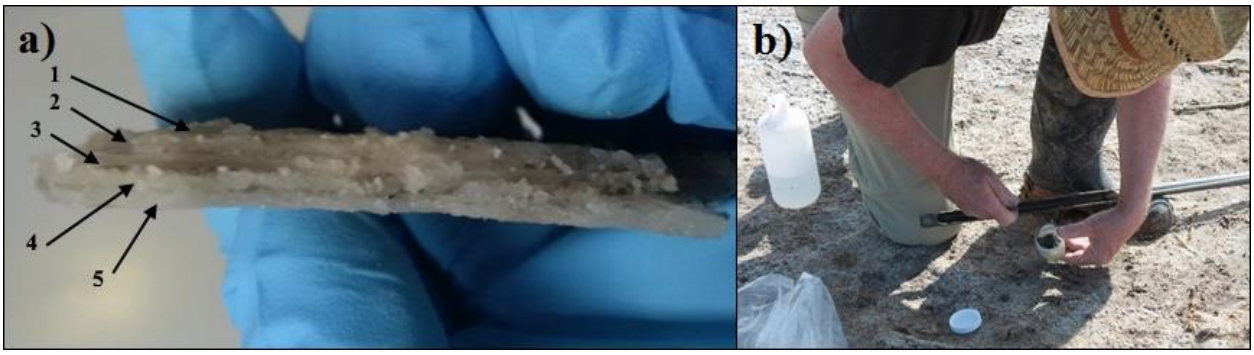

Figure 15. Salt sampling during the 2013 and 2014 sampling years, showing a) visible salt layers from a salt sample collected in 2012, and b) the collection process of surficial salt samples.

In 2012, several layered salt crusts were collected from the lake shorelines. If the sample was small or wet it was stored in double plastic bags. Alternatively if sufficient dry salt was removed it was stored in plastic bottles. The salts were divided into layers if visible, such as the salt sample shown in Figure 15a, and were analyzed for $\delta^{37}Cl$ isotopic signatures following the procedure summarized in the Methodology section titled "Chlorine Stable Isotope Analysis", and in Appendix A. The results of this analysis are outlined in the results section under the heading "$\delta^{81}Br$ and $\delta^{37}Cl$". In 2013 and 2014, both surficial salts and subsurface soils were sampled. These were gathered in a combination of 60 mL and 250 mL wide mouth plastic sampling containers, shown in Figure 15b. These salts were analyzed for $\delta^{81}Br$ and $\delta^{37}Cl$ isotopic signatures following the procedures summarized in the sections "Chlorine Stable Isotope Analysis", "Bromine Stable Isotope Analysis", and in Appendix A. One salt sample was additionally analyzed for geochemistry, following the procedure in the "Water Chemical Analysis" section. The results of these analyses are outlined in the Results under "$\delta^{81}Br$ and $\delta^{37}Cl$", and in the Discussion under "Geochemistry".

Core Sampling Methodology

Figure 16. Sediment core sampling in the 2014 sampling year, showing a) inserting core into ground using a jack hammer, and b) the removal of the core using a vacuum suction pump and a railway jack.

In the 2014 field program, sediment cores were collected using either a 2" or 3" ID aluminum core tube with a core sediment catcher on the lower end. This device was driven into the ground using a jackhammer, shown in Figure 16a, and then pulled back out using a railway jack, shown in Figure 16b. As much core as possible was recovered from each location, however the wet, sticky nature of the salty, saturated sand meant that at times not more than a few feet was recoverable. Once collected, each core tube was capped at both ends, securely taped and labelled, and stored in coolers.

At the University of Waterloo, each core was divided into 2 cm intervals. The sediment composition of each segment of core was described and logged before placed in sealed 60 mL plastic cups, similar to Figure 15b. These cups were then stored in refrigerators until ready for analysis. Each interval was tested for water content (WC), loss on ignition (LOI), and electric conductivity (EC) according to the methodologies outlined in the following section. Based on these values, select intervals were then chosen for $\delta^{81}Br$ and $\delta^{37}Cl$ isotopic analyses. Sediment intervals with higher concentrations of TDS were preferentially selected to ensure the best possible results for the $\delta^{81}Br$ and $\delta^{37}Cl$ isotopic analyses; however, regions with sudden variations in any of the parameters were also explored. The procedure for the bromine and chlorine stable

isotopic analysis is outlined in "Water Sampling Methodology", with the exception that during preparation the soil samples were mixed in a 1:10 solute:solvent ratio and placed on a shaker for 24 hours to ensure all salts were leached out for the isotopic analysis. The data of these analyses can be found in the Results under "$\delta^{81}Br$ and $\delta^{37}Cl$".

Water Content, Loss on Ignition, and Total Dissolved Solids

The procedure for water content is outlined in McLeod, (1980). Approximately 5 g of wet sample was weighed and put in an oven at 40°C for 4 hours. The initial cup weight (X) and the initial cup plus sample weight (Y) was recorded, as well as the final cup plus sample weight (Z). The weight percent of water was then calculated using Formula 2.

$$Wt\ (\%) = \frac{(Y - X) - (Z - X)}{(Y - X)} * 100\% \quad (2)$$

LOI was also calculated using the procedure outlined in McLeod, (1980). This process is similar to the water content methodology, however during the drying process the sample is combusted for one hour at 200°C, then two hours at 280°C, and lastly for 4 hours at 450°C. Samples are put in crucibles, which can withstand very high temperatures. The crucibles were each weighed with (Y) and without the initial sample weight (X), and once again following the completion of the combusting process (Z). LOI was then calculated using the Formula 2, above.

EC was measured using a CDM 83 Conductivity Meter. Each sample was dissolved in ultra-pure water in a solute:solvent ratio of 1:10, such that 5 g of sample was mixed with 50 g of ultra-pure water. This mixture was then placed on a shaker set at 160 rpm for a period of 24 hours to allow the sample to reach a state of complete homogeneity. Once mixed, the samples were allowed to settle for a short time before

measurements were made from the residual solution. Formula 3, shown below, was used to get an estimation of the total dissolved salt in each sample (Williams, 1986). Here, EC is expressed in mS/cm.

$$TDS\ \left(\frac{mg}{L}\right) = 466 * EC^{1.0878} \quad (3)$$

This equation was derived using 109 water samples from 89 different saline lakes in Australia. Linear regression was used to formulate a relationship between EC and TDS. A graphical representation from the study is shown in Figure 17a. The measured lake water TDS concentration and specific conductivity values from this study were graphed along with the derived linear relationship from Williams, (1986) in Figure 17b. Aside from five outlying samples, which belong to 2013 Homestead Lake, 2013 UNNJ Lake, 2013 Mini UNNJ Lake, 2013 Wilkinson Lake, and 2014 Mini UNNJ Lake, there is a reasonable linear relationship between the two (r^2 = 0.92107). This continues even at high values of specific conductivity.

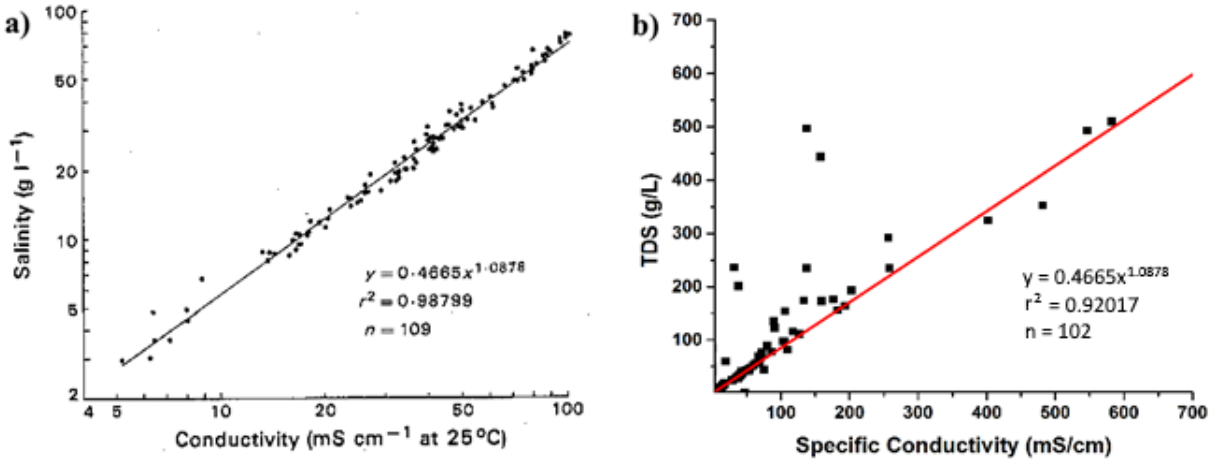

Figure 17. Relationship of TDS and EC measurements from a) 89 different Australian saline lakes, from Williams, (1986), and b) measured values from this study. The red line is the graphical representation of the same equation derived from Williams, (1986). Aside from five outlying measurements, the Williams, (1986) equation gives a good relationship between TDS and Specific Conductivity in the Nebraska alkaline lakes.

Gas Sampling Methodology

Figure 18. Gas sampling during the 2014 sampling year, a) positioning the capture device over the disturbed sediment along the Wilkinson shoreline, b) the final capture device setup.

After choosing a section of shoreline at Homestead Lake, Mini UNNJ Lake, and Wilkinson Lake, the sediment was manually disturbed to allow maximum surface and shallow subsurface exchange of gases. The disturbed site was covered using thick plastic sheeting, approximately 2m x 2m in size (Figure 18a). The edges of the plastic were buried using saturated soils to prevent released gas from escaping (Figure 18b). A diaphragm pump was used to pump gas from underneath the sheeting. The gases were then bubbled through an ultrapure 10 g/L solution of KOH intended to capture and convert all gaseous forms of bromine as bromide. The mechanism was left running for approximately 3 – 4 hours to ensure a suitable yield of bromine was collected.

Once captured, gas sample bottles were immediately put into coolers for storage. At the University of Waterloo, samples were stored in refrigerators until ready for bromine separation. The captured solutions were carefully concentrated under reducing conditions to the appropriate volume required for the typical bromine separation technique. The steps followed for bromine separation are outlined in Appendix A.

Results

$\delta^{18}O$ and $\delta^{2}H$

The study by Gosselin et al. (1994), and Gosselin et al. (1997) sampled the alkaline lakes in the Sand Hills Region of Nebraska, USA, during a year that experienced very low amounts of precipitation and high temperatures (1992), followed by a year with increased precipitation and lower temperatures (1993). The water samples were analyzed for geochemistry, and $\delta^{18}O$ and $\delta^{2}H$ isotopic signatures. Dry conditions similar to those seen in 1992 occurred in 2012, prompting further sampling and chemical analyses of the same lakes during this time. Following this year, increasingly wet and rainy conditions occurred in 2013 and 2014, comparable to the setting observed in 1993. The water samples that were collected in 2012, 2013, and 2014 were analyzed both geochemically and isotopically.

In continuation of the research by Gosselin et al. (1994), and Gosselin et al. (1997), lake water samples that were collected in 2014 were analyzed for the $\delta^{18}O$ and $\delta^{2}H$ isotopic signatures, similar to the water samples from 1992 and 1993. These analyses were done for the reason that the $\delta^{18}O$ and $\delta^{2}H$ signatures of surface waters can be used to indicate the extent to which the water body has been evolved through evaporation, and/or mixed with subsurface waters (Clark and Fritz, 1997). Furthermore, $\delta^{18}O$ and $\delta^{2}H$ isotopic information coupled with geochemical data from 1992, 1993, and the 2012 to 2014 sampling years could be used to analyze how the lake water composition has changed with time. The lake water and groundwater results for $\delta^{18}O$ and $\delta^{2}H$ isotopic signatures are given in Table 2, and Table 3, respectively. In 1992 and 1993, water samples were collected multiple times throughout the year to demonstrate seasonal changes in the $\delta^{18}O$ and $\delta^{2}H$ signatures (Gosselin et al., 1997). Generally, sampling occurred once in May and once in October, however, occasionally the water sampling occurred in August of that year as opposed to May. The lakes sampled in the 2012 to 2014 field seasons were sampled only once per year, in the month of August.

Table 2. $\delta^{18}O$ and $\delta^{2}H$ of sampled lakes in 1992, 1993, and 2014 from the Sand Hills Region of Nebraska, USA. [T] Notates data that was published in Gosselin et al. (1997).

Lake Name	Sampling Date	$\delta^{18}O$ (‰) (VSMOW)	St. Dev.	$\delta^{2}H$ (‰) (VSMOW)	St. Dev.
Big Harvey	14-Aug-21	5.0	0.2	3.2	0.3
Cravath	92-May-29 [T]	1.2		-26.0	
	92-Oct-13 [T]	3.0		2.0	
Diamond	92-May-29 [T]	1.3		-27.0	
	92-Oct-13 [T]	2.3		-11.0	
Dillings	92-May-27 [T]	0.1		-36.0	
	92-Oct-14 [T]	2.5		3.0	
Fritz	92-May-28 [T]	0.8		-23.3	
	92-Oct-15 [T]	5.9		-5.0	
	14-Aug-21	0.9	0.04	-17.3	0.2
Homestead	92-May-27 [T]	2.0		-13.0	
	92-Aug-12 [T]	-0.2		-8.0	
	92-Oct-14 [T]	5.0		-36.0	
	93-Oct-14 [T]	-5.5		-50.0	
	14-Aug-19	4.9	0.1	1.4	0.3
Jesse	92-May-29 [T]	1.3		-20.0	
	92-Aug-13 [T]	-2.4		-27.0	
Joe	14-Aug-21	-1.5	0.1	-33.0	1.0
Krause	92-May-27 [T]	1.3		-30.0	
	92-Oct-15 [T]	5.9		-12.0	
Long	92-May-27 [T]	1.6		-7.0	
	92-Oct-15 [T]	0.8		-15.0	
Mini UNNJ	14-Aug-20	5.7	0.3	5.4	0.3
No. 2	14-Aug-21	5.0	0.1	0.2	0.1
Palmer	92-May-28 [T]	0.1		-20.0	
	92-Oct-14 [T]	4.3		3.0	
Potash	92-May-29 [T]	2.1		-15.0	
	92-Oct-15 [T]	-0.1		-32.0	
Shriner	92-May-27 [T]	3.8		-4.0	
	92-Oct-15 [T]	1.8		-14.0	
	93-Oct-15 [T]	-6.4		-56.0	
	14-Aug-21	0.6	0.03	-18.0	0.1
Tree Claim	92-May-28 [T]	-2.0		-20.0	
	92-Aug-13 [T]	1.6		10.0	
UNNJ	92-May-28 [T]	2.1		-9.0	
	92-Aug-12 [T]	0.3		-30.0	
	14-Aug-20	5.0	0.4	-1.8	0.7
UNNJ Area	14-Aug-20	2.6	0.6	-6.7	1.5
Wickson	92-May-28 [T]	1.7		-23.0	
	92-Oct-14 [T]	4.0		-6.0	
Wilkinson	92-May-28 [T]	1.7		-11.0	
	92-Oct-14 [T]	-0.6		-46.0	
	14-Aug-18	3.6	0.3	-5.4	0.6

Table 3. $\delta^{18}O$ and $\delta^{2}H$ of sampled groundwater in 1992, 1993, and 2014 from the Sand Hills Region of Nebraska, USA. [T] Notates data that was published in Gosselin et al. (1997).

Groundwater Name	Sampling Date	$\delta^{18}O$ (‰) (VSMOW)	St. Dev.	$\delta^{2}H$ (‰) (VSMOW)	St. Dev.
Homestead	92-Oct-15 [T]	-9.3		-81.0	
	93-Oct-14 [T]	-14.1		-101.0	
	14-Aug-19	-12.8	0.1	-95.6	0.6
Krause	92-Aug-14 [T]	-5.6		-77.0	
Shriner	93-Oct-15 [T]	-12.7		-102.0	
UNNJ	14-Aug-20	-12.4	0.1	-93.6	0.3
Wilk. MB2'	14-Aug-18	-2.8	0.2	-41.2	0.6
Wilk. WL2'	14-Aug-18	-5.8	0.5	-61.3	0.8
Wilk. WL 4'	14-Aug-18	-7.2	0.4	-65.2	1.2

Figure 19 displays a graph of the $\delta^{18}O$ and $\delta^{2}H$ data collected in this study, as well as the published data from Gosselin et al. (1997), plotted against the Global Meteoric Water Line (GMWL). The figure is divided into plots according to the Group classification scheme outlined by Gosselin et al. (1997), which was discussed earlier, as well as the collected groundwater samples. The $\delta^{18}O$ and $\delta^{2}H$ isotopic data gathered from the 2014 lake and groundwater samples have similar values and behave in a similar way to the 1992 and 1993 dataset from the Gosselin study. For instance, all 2014 samples are displaced to the right of the GMWL; and the Group 3 lake samples from 2014 are more isotopically enriched than the 2014 Group 2 lakes, which are in turn are more enriched than the 2014 Group 1 lakes. This is also in agreement with David Gosselin's observation that Group 2 lakes are slightly more enriched than Group 1 lakes.

In addition to the similarities, there are also slight differences when comparing the datasets. The 2014 data for $\delta^{18}O$ and $\delta^{2}H$ signatures in Group 1 and Group 2 are slightly depleted or near equal to the isotopic data from the same lakes in 1992 and 1993. However, all sampled Group 3 lakes are more enriched in 2014 than in 1992 and 1993. The trend in Group 1 and 2 lakes is to be expected, since 2014 was a wetter year than 1992 and 1993 (refer to Table 1). The isotopic enrichment of $\delta^{18}O$ and $\delta^{2}H$ isotopic signatures in the 2014 Group 3 lake samples, however, was not expected. These brines could not have reached a higher degree of evaporation in 2014 than in 1992, since the added precipitation in 2014 resulted in lower measurements of field specific conductivity at Wilkinson Lake, UNNJ Lake, and Homestead Lake compared to 1992, shown in Table 4.

Table 4. Comparison of field specific conductivity measurements at Homestead, Wilkinson, and UNNJ lakes in 1992 and 2014.

Lake Name	Year	Specific Conductivity (µS/cm)
Homestead	1992	256,600
	2014	89,670
Wilkinson	1992	193,500
	2014	71,810
UNNJ	1992	582,400
	2014	105,900

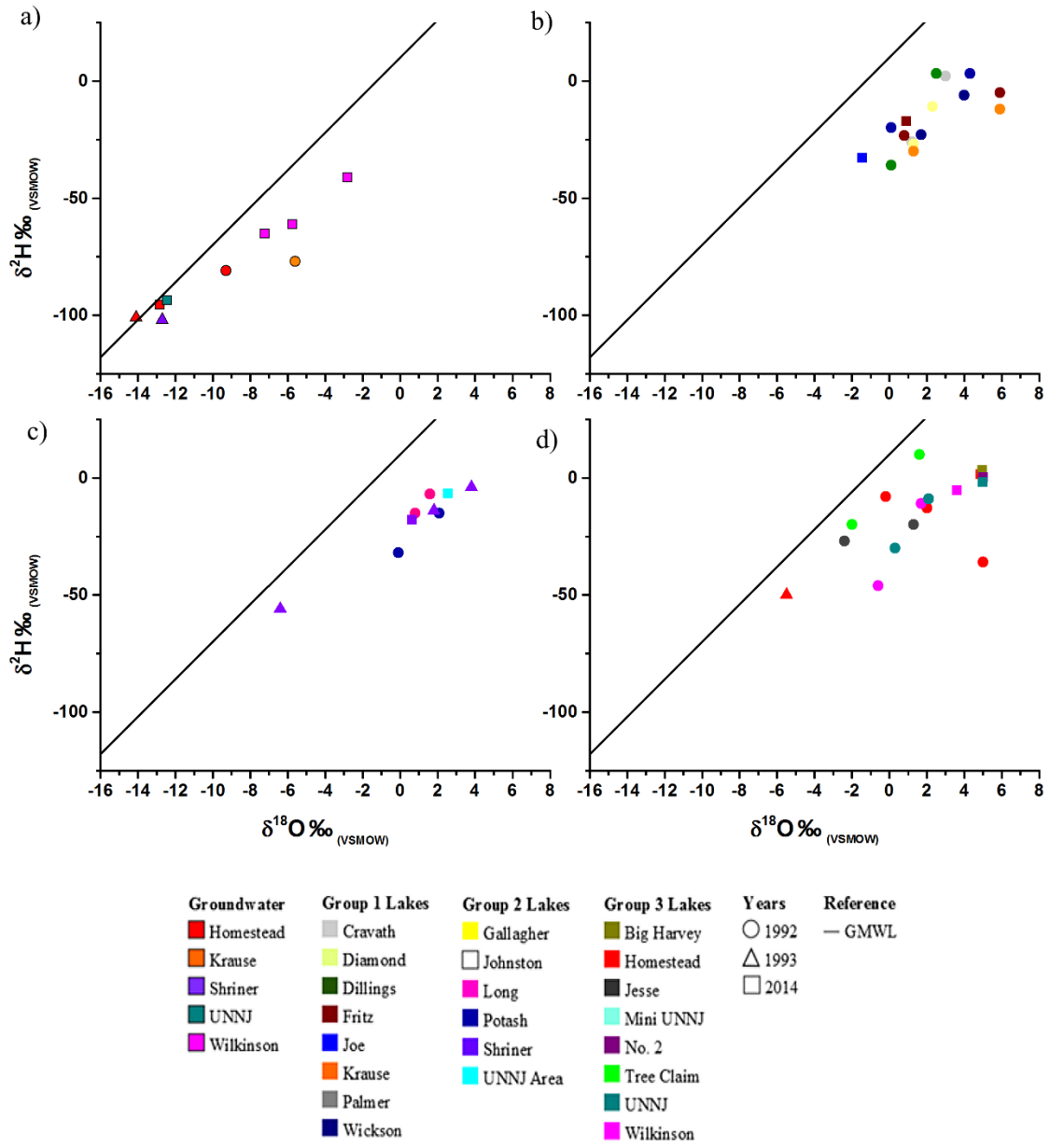

Figure 19. Combined $\delta^{18}O$ and $\delta^{2}H$ from present study and Gosselin et al. (1997). Divided into a) Groundwater, b) Group 1 Lakes, c) Group 2 Lakes, and d) Group 3 Lakes.

A comparison of all the $\delta^{18}O$ and $\delta^{2}H$ isotopic signatures of the lake water and groundwater samples shows that each water type falls in a discrete isotopic region (Figure 20). These three regions represent three different "end-members" of the Sand Hills Region. The first end-member is the lake surface water, and is represented by the lake water samples. Overall, excessive evaporation of the lake water has resulted in the $\delta^{18}O$ and $\delta^{2}H$ isotopic signatures of the lake water samples to be displaced further to the right of the GMWL than the groundwater samples. The second end-member is the local groundwater system, and is represented by the 2014 Wilkinson piezometers (Local Groundwater on Figure 20). The piezometers were set at a depth of either 0.6 m (2 feet) or 1.2 m (4 feet), thus drawing on the local shallow groundwater. The $\delta^{18}O$ and $\delta^{2}H$ isotopic signatures of these samples are slightly displaced from the GMWL, and the specific conductivity measurements of the piezometer groundwater samples (38,900 µS/cm – 79,560 µS/cm) are very similar in comparison to the lake water samples (71,810 µS/cm). This is also supported by the evaporation line of the Wilkinson piezometers and the Wilkinson Lake waters, which is shown in Figure 21. The third end-member is the regional High Plains Aquifer groundwater system, and is represented by the UNNJ Windmill and Homestead Spring groundwater samples, all of which lie almost directly on the GMWL (Regional Groundwater on Figure 20). These samples are all isotopically consistent over the years they were sampled.

A diagram showing all the possible end-members in the Sand Hills Region is given in Figure 22. In addition to lake surface water, local groundwater, and regional groundwater, other end-members include surficial salts on the shorelines adjacent to the lakes, volatile loss from the lake shorelines, and precipitation events. These end-members are critical to understanding the cycling of bromine and chlorine stable isotopes in the region, and will be referred to in the future sections of this thesis.

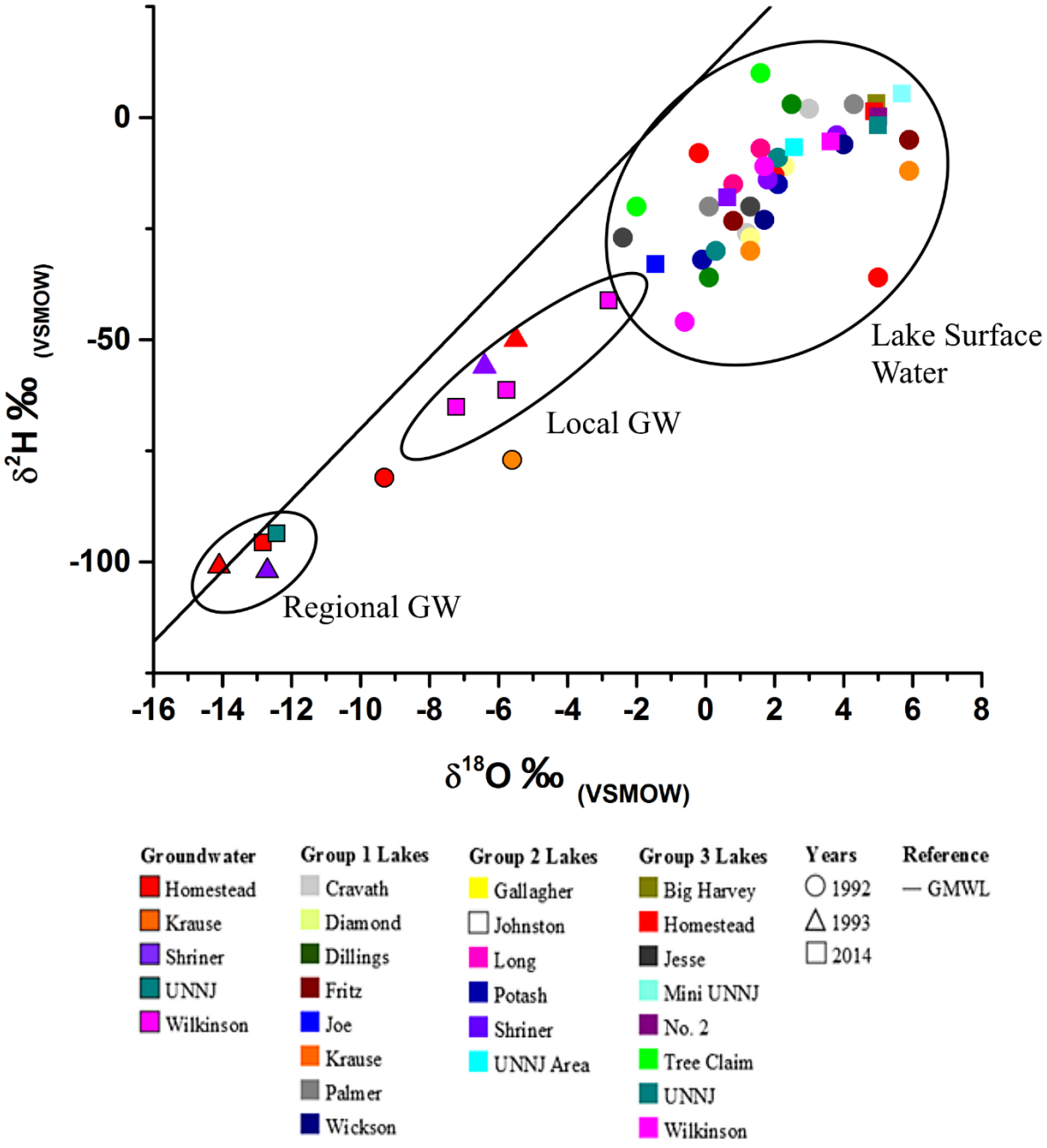

Figure 20. $\delta^{18}O$ and $\delta^{2}H$ of all sampled lakes in 1992, 1993, and 2014 showing the Regional Groundwater, Local Groundwater, and Lake Surface Water end member regions.

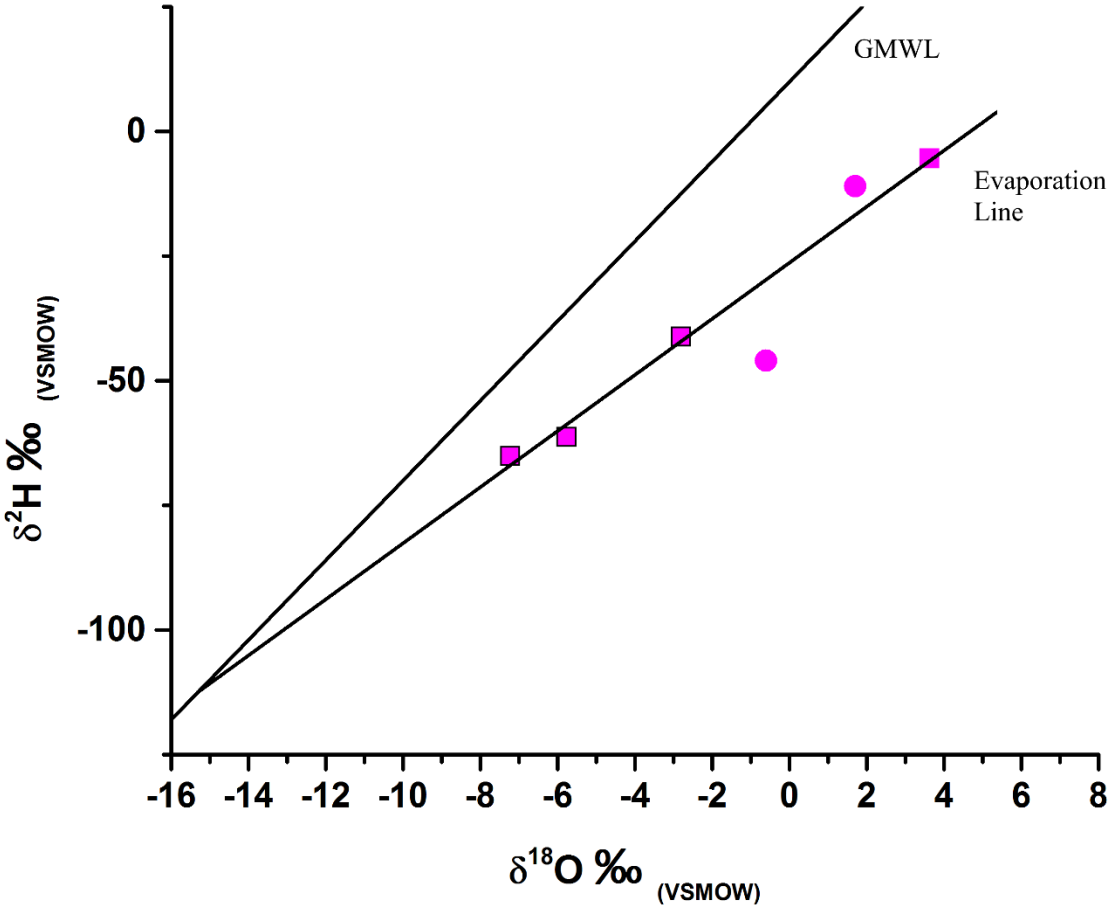

Figure 21. $\delta^{18}O$ and $\delta^{2}H$ (‰) mixing line of 2014 Wilkinson Piezometers (squares with black outline), 2014 Wilkinson lake (squares without outline), and 1992 Wilkinson lake samples (circles) compared to the Global Meteoric Water Line (GMWL).

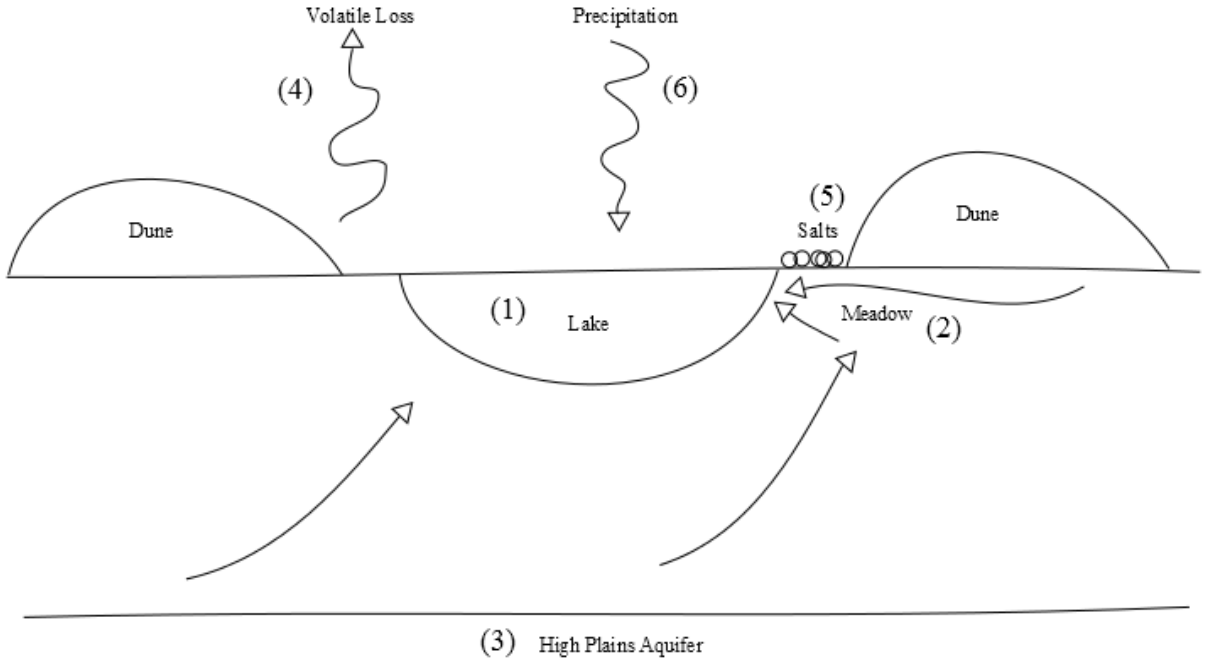

Figure 22. Various end-members in the Sand Hills Region of Nebraska, USA, that are discussed in this thesis; including (1) lake surface water, (2) local groundwater, (3) regional groundwater, (4) volatile loss, (5) salt precipitation and dissolution, (6) precipitation events.

Geochemistry

In previous research, David Gosselin classified the composition of most of the lakes in the Sand Hills Region as either Na-K-CO_3-(SO_4)-(Cl), or Na-K-SO_4-CO_3-(Cl), and the highest TDS lakes as Cl-SO_4 (Gosselin, 1997). Slight geochemical variations exist between the lakes, owing to deviations in the local hydrological conditions, and varying degrees of brine evaporation (Deocampo and Jones, 2014). A geochemical analysis can help to differentiate between the hydrological flow regimes of each lake. This is because a lake dominated by flow-through will contain a lower concentration of TDS, and display a chemical composition that is impacted by the regional groundwater system; whereas a lake dominated by groundwater discharge and evaporative concentration will contain a higher amount of TDS, and may display geochemical trends towards a chloride or sulphate dominant chemistry. A summary of the lake

water and groundwater chemistry can be found in Table 5. This table provides only a selection of the total data used, and is intended for reference purposes in the body of the manuscript.

Ternary diagrams of the major cations and anions of Group 1, Group 2, and Group 3 lakes, using data from this study and Gosselin et al. (1994, 1997), are shown in Figure 23. Due to the low concentrations of Ca^{2+} and Mg^{2+} in each lake, the axes of the cation diagrams are divided into Na^{+}, K^{+}, and $100x(Ca^{2+} + Mg^{2+})$, as opposed to Ca^{2+}, Mg^{2+}, and $(Na^{+} + K^{+})$. When analyzing the diagrams, it is important to consider the climate differences between sampling years. The earlier chemical and isotopic sampling and research from 1992 carried out by Gosselin et al. (1994) was after a prolonged dry period in the region, and was followed by a wet year in 1993. Similarly, sampling in 2012 was conducted to examine the chemistry and isotopic signatures after a prolonged dry period. However, the 2012 data is currently being reanalyzed to ascertain that year's chemical variability. Therefore, in a few cases the 1992 geochemical dataset is substituted for the 2012 dataset. Comparably to 1993, 2013 and 2014 experienced increasingly large amounts of precipitation. Refer to Table 1 for a summary of precipitation for the region of Alliance from 1992 to 1993, and 2012 to 2014.

The geochemical compositions of four separate end-members are displayed on the ternary diagrams in Figure 23: lake surface water, local groundwater, regional groundwater, and surficial salts. The lake water geochemical compositions are variable. The anion chemistry of Group 1 and Group 2 lakes, shown in Figure 23a and 23b, are dominantly composed of $HCO_3^{-}+CO_3^{2-}$, with minor amounts of Cl^{-} and SO_4^{2-}. In contrast, the anion chemistry of Group 3 lakes, shown in Figure 23c, ranges between dominantly carbonate rich, to dominantly Cl-SO_4 rich. The geochemical composition of the local groundwater samples, represented by the Wilkinson Piezometers, range between sulphate rich to Cl-SO_4 rich, and are similar in composition to the Wilkinson Lake water samples. The regional groundwater, which is represented by the Homestead Spring and UNNJ Windmill groundwater samples, is dominantly composed of carbonate.

Table 5. Geochemistry of selected lakes from the Sand Hills Region of Nebraska, USA. [T] Notates published data by David Gosselin (Gosselin et al., 1994).

Lake Name	Sample Number	Sample Date	pH	Temp (ºC)	Spec. Cond. (umhos/cm)	Alkalinity (HCO_3) (mg/L)	TDS (mg/L)	Na (mg/L)	K (mg/L)	Mg (mg/L)	Ca (mg/L)	Cl (mg/L)	SO_4 (mg/L)	PO_4 (mg/L)	NO_3 (mg/L)	Br (mg/L)	F (mg/L)
Lake Samples																	
Dillings	92-AL-29[T]	92-Aug-12	9.77	23.0	7,900	4,184	7,744	1,307	1,491	16	5	238	488	3	1	6	6
	93-AL-29[T]	93-Aug-11	9.41	23.9	5,680	5,680	7,974	812	911	10	4.5	174	334	1	0	4	3
	14066	14-Aug-21	9.80	30.3	6,833	3,401	6,299	1,078	1,134	11	8	183	472	0	0	4	4
Fritz	92-AL-25[T]	92-Aug-12	10.04	17.9	11,970	4,571	10,991	1,296	2,682	1	5	265	2,154	0	3	2	12
	14068	14-Aug-21	8.72	18.3	3.4	2,578	6,662	789	1,649	1	7	145	1,378	0	0	1	1
Homestead	92-AL-28[T]	92-Aug-12	10.33	27.4	256,600	175,828	291,910	47,264	37,659	1	4	18,179	12,103	337	0	314	221
	93-AL-28[T]	93-Aug-11	10.07	21.5	54,800	27,109	47,307	8,841	6,427	0.2	1	2,844	1,583	16	0.5	82	10
	13082	13-Jul-30	10.34	34.8	31,700	136,152	236,184	46,311	33,121	0	77	10,717	7,505	243	0	337	75
	14059	14-Aug-19	10.22	22.1	89,670	78,934	134,919	25,804	19,374	0	9	5,562	4,099	134	0	204	48
Joe	13085	13-Jul-31	7.90	31.0	5,120	2,031	4,691	655	783	73	15	107	913	0	0.3	1	3
	14061	14-Aug-21	9.70	25.0	3,645	1,347	3,160	468	555	43	10	65	658	0	1	1	1
Krause	92-AL-26[T]	92-Aug-12	8.76	25.2	2,100	1,203	2,123	215	362	81	17	1	190	0	1	0.4	2
	93-AL-32[T]	93-Aug-12	8.67	17.8	2,130	1,298	2,228	227	329	92	28	44	140	0	0.1	1	3
Mini UNNJ	13087	13-Jul-31	9.13	35.8	158,000	64,782	443,678	118,559	36,863	12	521	1,630	153,546	0	0	760	12
	14057	14-Aug-20	9.50	33.3	137,000	20,606	234,601	61,614	18,440	26	185	23,365	110,066	0	0	295	4
Shriner	92-AL-24[T]	92-Aug-12	10.04	15.9	40,200	13,167	33,243	204	6,811	1	3	784	7,720	0	30	16	28
	93-AL-31[T]	93-Aug-11	9.69	26.8	15,730	6,203	15,892	105	93	0.06	0.09	420	3.095	0	0	9	4
	14067	14-Aug-21	9.95	24.2	16,130	6,795	15,667	2,093	3,445	0.5	11	315	2,912	0	0	2	4
Tree Claim	92-AL-39[T]	92-Aug-13	9.99	25.6	258,000	87,230	234,791	44,666	32,349	1	2	21,087	1,009	0	30	282	179
	93-AL-36[T]	93-Aug-12	9.70	18.4	51,300	14,838	42,648	8,907	5,708	0.2	0.02	4,276	8,550	7	0	68	5
UNNJ	92-AL-27[T]	92-Aug-12	10.13	33.8	582,400	205,202	510,404	131,649	50,050	7	5	35,085	86,791	656	22	481	456
	93-AL-30[T]	93-Aug-12	9.89	17.9	68,400	20,113	58,192	12,002	7,126	5	1	5,085	13,734	0	0	85	4
	13088	13-Jul-31	9.35	35.4	138,000	224,724	497,279	120,213	41,642	0	103	31,339	73,970	122	0	437	41
	14056	14-Aug-20	10.04	24.7	105,900	53,436	154,327	31,369	20,873	0	187	9,442	38,798	0	0	118	10
UNNJ Area	14058	14-Aug-20	9.72	30.1	90,540	26,474	122,951	30,317	11,072	10	188	8,093	46,365	0	0	82	324
Wilkinson	92-AL-32[T]	92-Aug-13	9.74	17.7	193,500	30,396	164,057	43,392	14,628	28	5	31,507	43,512	44	20	431	94
	93-AL-30[T]	93-Aug-11	10.13	28.1	53,400	6,815	42,988	10,197	3,145	29	3	10,633	12,032	0	0	126	2
	13088	13-Jul-29	8.94	26.3	38,100	33,379	200,976	57,141	16,594	66	296	31,626	57,174	7	0	507	9
	14052	14-Aug-18	9.86	29	71,810	13,261	75,269	20,289	6,282	32	101	14,731	20,343	0	0	220	3
Groundwater Samples																	
Homestead	92-AL-50[T]	92-Oct-14	8.03	9.5	422	211	321	15	19	7	41	7	20	0.3	0	0	0.5
	93-AL-59[T]	93-Oct-14	7.74	12.0	390	230	398	17	13	11	42	4	10	0	0	0.1	0.1
	13083	13-Jul-30	6.65	22.0	420	243	433	14	19	6	58	5	19	0.2	0.4	0	0.5
	14063	14-Aug-19	8.30	15.0	0.4	232	408	12	18	6	53	4	19	0.2	0	0	0.4
Wilkinson Piezo Lake 2'	13090	13-Jul-30	9.10	21.8	25,300	15,897	84,533	22,501	7,665	0	143	16,329	19,565	14	0	250	3
	14054	14-Aug-18	9.65	26.3	79,560	15,165	88,746	24,117	6,811	0	93	15,308	26,985	0	0	202	3

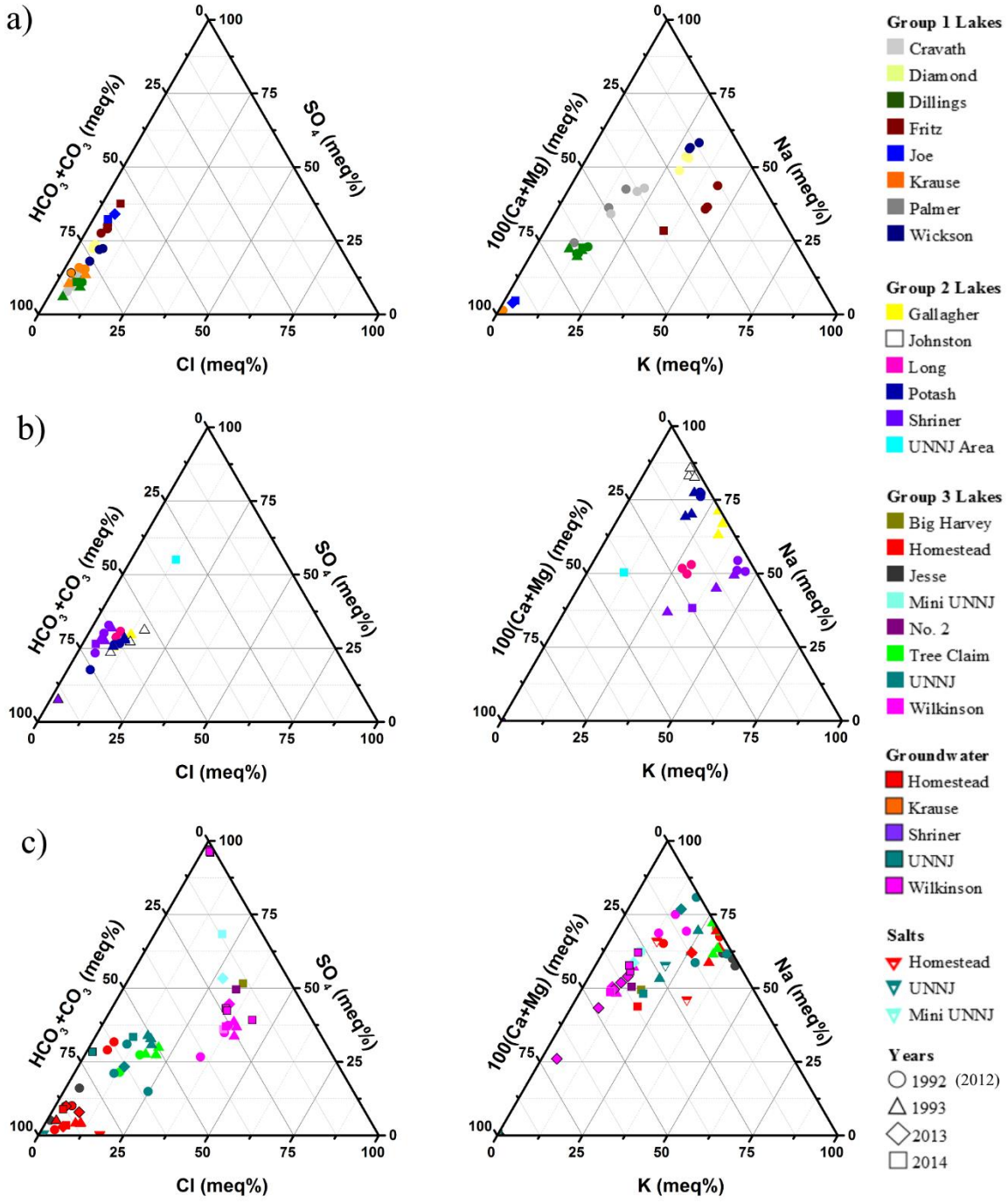

Figure 23. Ternary plots of major anions and cations. Divided into a) Group 1 Lakes anions and cations, b) Group 2 Lakes anions and cations, and c) Group 3 Lakes anions and cations. Groundwater and salt samples are allocated to the ternary plots that contain the associated lake water sample (i.e. the Wilkinson Piezometer samples are found in the Group 3 ternary plot along with the Wilkinson Lake water samples, and the Homestead salt samples are found in the Group 3 ternary plot along with the Homestead Lake water samples).

$\delta^{81}Br$ and $\delta^{37}Cl$

Bromine and chlorine stable isotopes were analyzed from several water, salt, and soil samples from the Sand Hills Region of Nebraska, USA, in an effort to more thoroughly understand the cycling of bromine and chlorine in a naturally evaporitic environment. Isotopic analyses of various saline lakes and salt pans around the world could help in future work to determine the source and quantify the flux of bromine gas to the atmosphere. In addition to the $\delta^{81}Br$ and $\delta^{37}Cl$ isotopic signatures and geochemical analyses, which were discussed in the previous sections, several end-members of the alkaline lakes (Figure 22) were analyzed for $\delta^{81}Br$ and $\delta^{37}Cl$ isotopic signatures.

The results of the $\delta^{81}Br$ and $\delta^{37}Cl$ isotopic analyses for the first end-member, the lake surface water, are shown in Figure 24. The isotopic signatures of the water samples are plotted chronologically. This allows for a better visualization of the potential climatic effects on the subsequent isotopic signatures of the lake waters. The figure is divided according to previous classification method into Groundwater, Group 1, Group 2, and Group 3 lakes. This was done as a means to more easily compare the known hydrogeological and geochemical interpretations of these lakes. A selection of bromine and chlorine stable isotopic signatures for lake, groundwater, and salt samples are provided in Table 6.

An increase in annual precipitation occurred in 2013 and 2014 compared to 2012 (refer to Table 1). Coinciding with this, between 2012 and 2014 in the Group 1 lake waters, there is depletion in the $\delta^{81}Br$ isotopic signatures and enrichment in the $\delta^{37}Cl$ signatures, shown in Figure 24b. Of the group classifications, Group 1 lakes are the most hydraulically connected to the groundwater system and have the lowest concentration of TDS (Gosselin et al., 1994; Gosselin, 1997). Therefore, changes in the isotopic values of these lakes should result from any salt precipitation and dissolution events that may occur on the shorelines and in the lake beds.

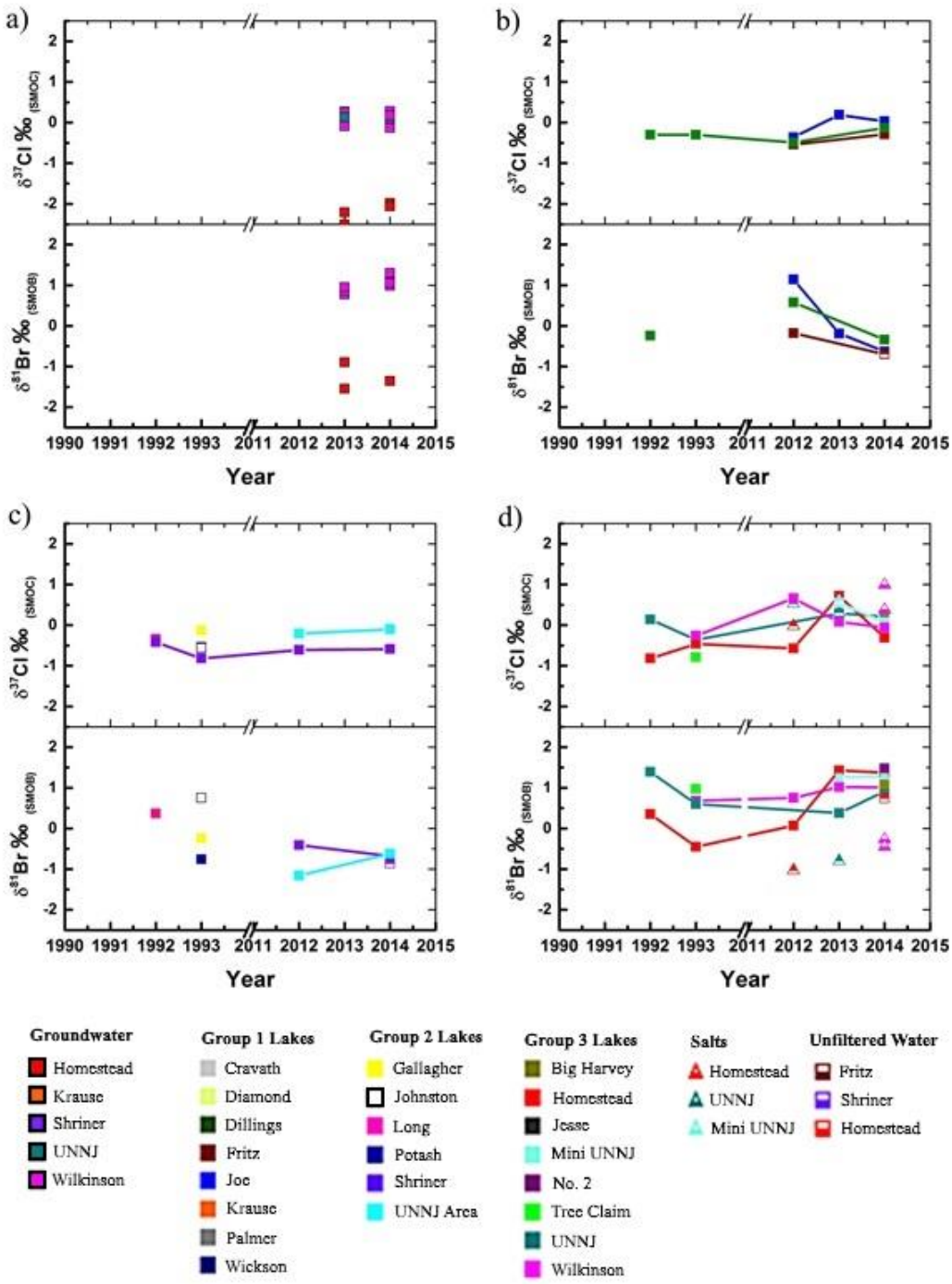

Figure 24. Bromine and chlorine stable isotopic signatures of lakes and salts with time, divided between a) Groundwater, b) Group 1 lakes, c) Group 2 lakes, and d) Group 3 lakes.

Table 6. Bromine and chlorine stable isotope data for selected lakes from the Sand Hills Region of Nebraska, USA. Ppt. notates salt precipitated from water after sampling.

Sample Name	Sample Number	Sample Date	δ^{81}Br ‰ (SMOB)	St. Dev.	δ^{37}Cl ‰ (SMOC)	St. Dev
Lake Samples						
Fritz	291366	12-Aug	-0.18	0.03	--	--
	14068	14-Aug-21	-0.70	0.03	-0.29	0.07
Homestead	92-AL-49[Ŧ]	92-Oct14	0.35	-0.82	--	--
	93-AL-55[Ŧ]	93-Oct-14	-0.45	--	-0.46	--
	291369	12-Aug	0.07	0.08	-0.57	--
	13082	13-Jul-30	1.43	0.17	0.72	0.14
	14059	14-Aug-19	1.37	0.07	-0.31	0.05
Joe	291367	12-Aug	1.14	0.60	--	--
	13085	13-Jul-31	-0.19	0.07	0.19	0.03
	14061	14-Aug-21	-0.63	0.05	0.03	0.08
Mini UNNJ	13087	13-Jul-31	1.26	0.11	0.55	0.15
	14057	14-Aug-20	1.27	0.09	0.07	0.10
Shriner	92-AL-60[Ŧ]	92-Oct-15	--	--	-0.42	--
	93-AL-31[Ŧ]	93-Aug-11	--	--	-0.82	--
	291368	12-Aug	-0.41	0.01	--	--
	14067	14-Aug-21	-0.68	0.08	-0.59	0.09
UNNJ	92-AL-27[Ŧ]	92-Aug-12	1.39	--	0.14	--
	93-AL-9[Ŧ]	93-May-15	0.58	--	-0.36	0.11
	13086	13-Jul-31	0.38	0.16	0.29	0.09
	14056	14-Aug-20	0.91	0.06	0.21	0.05
Wilkinson	93-AL-30[Ŧ]	93-Aug-11	0.68	--	-0.26	--
	291363	12-Aug	0.75	0.06	--	--
	13082	13-Jul-30	-0.39	0.06	--	--
	14052	14-Aug-18	1.01	0.06	-0.06	0.03
Groundwater Samples						
Homestead Spring		13-Jul-30	-1.55	0.01	-2.50	0.11
	14063	14-Aug-19	--	--	-1.98	0.05
UNNJ Windmill		13-Jul-31			0.13	0.11
Wilkinson Piezo Main 2'	13090	13-Jul-30	0.86	0.18	--	--
	14054	14-Aug-18	1.30	0.02	0.28	0.02
Salt Samples						
Wilkinson	A	14-Aug-18	-0.27	0.08	0.38	0.13
	B	14-Aug-18	-0.45	0.08	0.99	0.07
UNNJ	291370	12-Aug	-0.46	0.07	0.49	0.12
	13095 (ppt)	13-Jul-31	-0.80	0.09	0.31	0.15
Homestead	291371	12-Aug	0.08	0.03	0.35	0.07
Mini UNNJ	13094 (ppt)	13-Jul-31	--	--	0.59	0.04

The behaviour of the $\delta^{81}Br$ and $\delta^{37}Cl$ isotopic signatures becomes progressively more complex in Group 2 and Group 3 lakes, presumably due to the increase of TDS, lack of groundwater flow, and ephemeral characteristics of the Group 3 lakes. These qualities result in repeated wetting and drying cycles of the shoreline salts, which complicate the isotopic behaviour. A comparison of the $\delta^{81}Br$ and $\delta^{37}Cl$ isotopic signatures between Group 1 Lakes, Group 2 Lakes, and Group 3 Lakes is shown in Figure 25.

Both the filtered and unfiltered lake water samples which were collected from Fritz Lake, Shriner Lake, and Homestead Lake, were analyzed for the $\delta^{81}Br$ isotopic compositions. The results of this analysis are shown in Figure 26, and reveal that the $\delta^{81}Br$ signatures of the filtered water samples are slightly more enriched than the unfiltered water samples. Upon filtration, particulate sediment, colloidal organics, and salts were potentially removed from the water, which resulted in small enrichment in the $\delta^{81}Br$ isotopic signature of some of the residual water relative to the unfiltered sample. Further studies are needed to identify the exact material which was filtered out of the water samples. It should be noted that the mass of this filtrate in most instances is small compared to the mass of the lake water, and therefore the overall inclusion or removal of filtrate in the lake water isotopic analyses would not significantly change the isotopic signatures for the waters.

The second end-member that is analyzed in this thesis is potential volatile loss from the lake shorelines. In an attempt to verify if brominated gases were in fact being produced in the vicinity of these lakes, bulk gas samples were captured from the shorelines of three different lakes in 2014: Homestead Lake, Mini UNNJ Lake, and Wilkinson Lake. The gas samples were then analyzed for $\delta^{81}Br$ isotopic signatures. The results of this analysis can be found in Table 7.

Although the dataset is small, the $\delta^{81}Br$ signature of all three gas samples are consistently depleted in value. This suggests that a process (photochemical or microbial) on the shorelines of these lakes is causing a selective release of the lighter ^{79}Br in a gaseous form during bromine reduction or oxidation. The gas at Wilkinson Lake provided the best yield, and therefore the isotopic signature of this sample is the most accurate of the three.

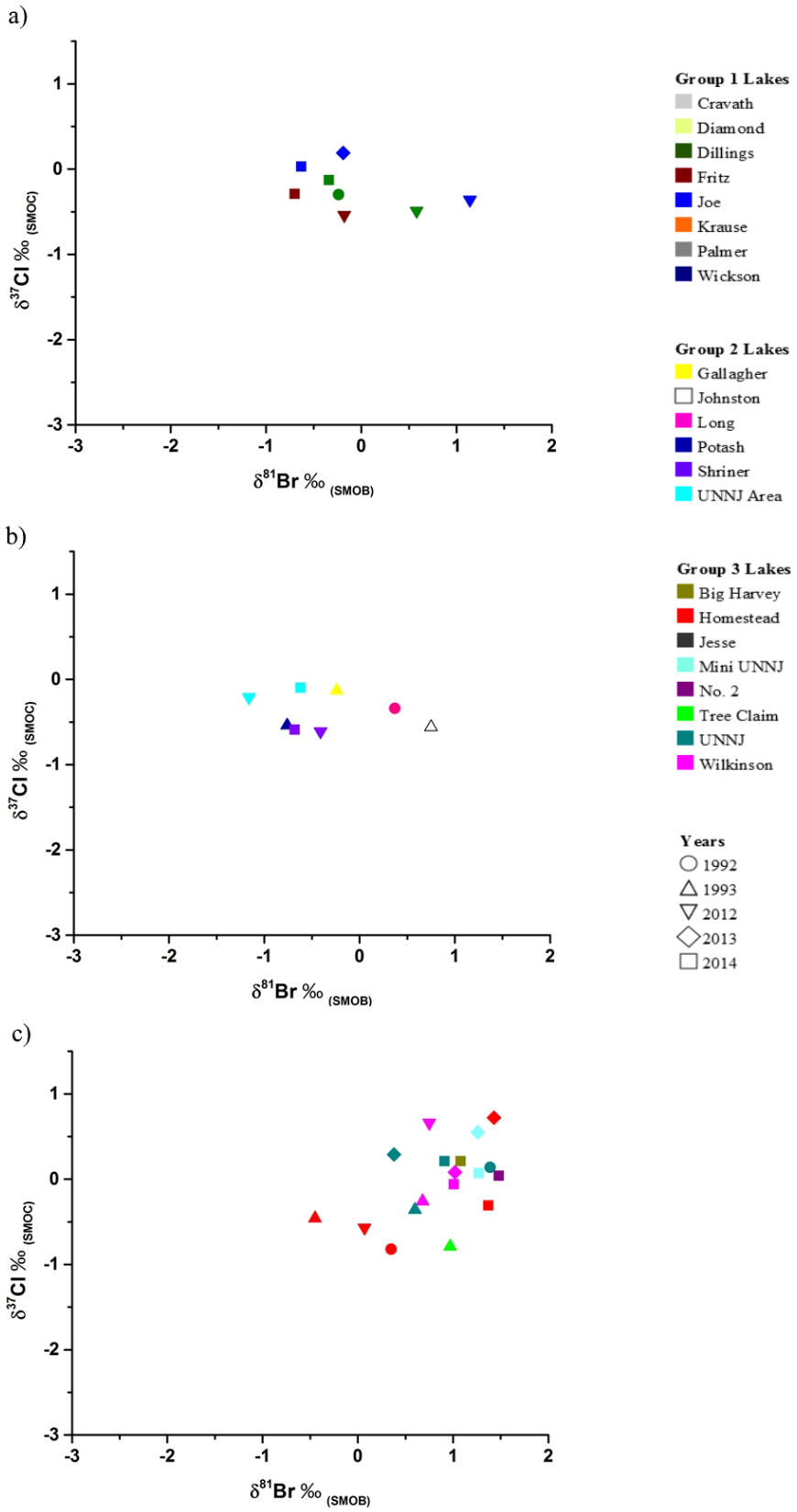

Figure 25. Plot showing $\delta^{81}Br$ and $\delta^{37}Cl$ values of a) Group 1 Lakes, b) Group 2 Lakes, and c) Group 3 Lakes.

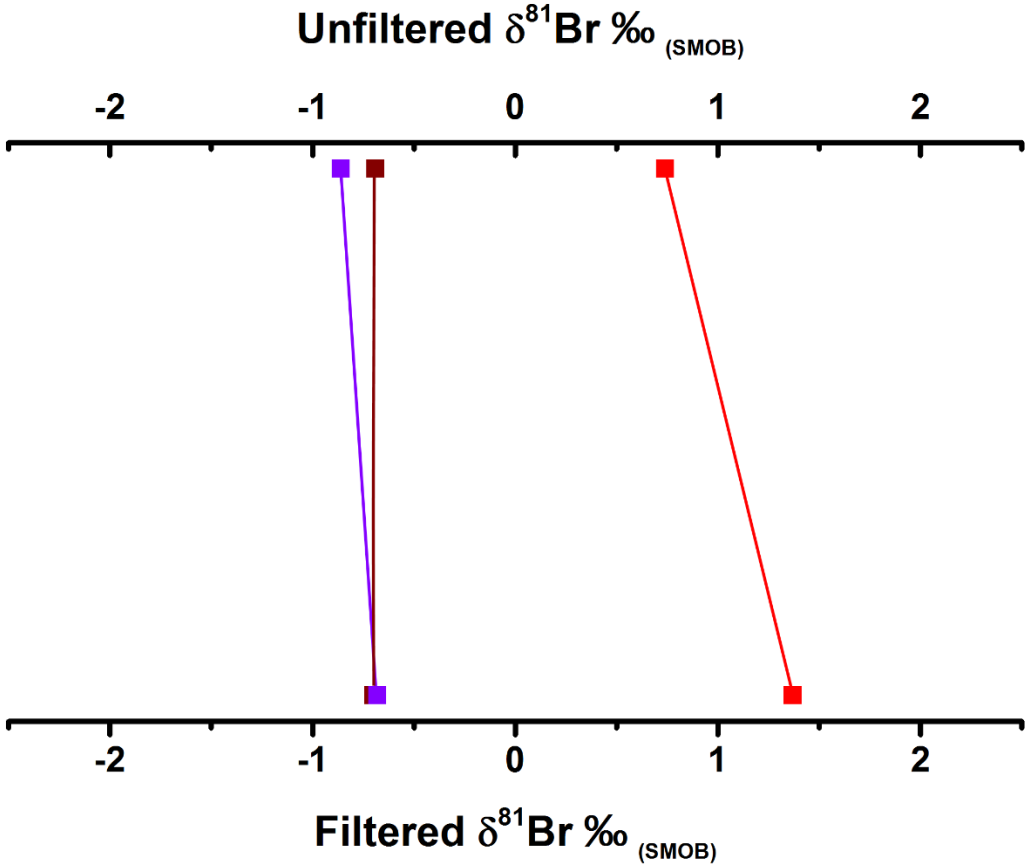

Figure 26. A comparison of δ^{81}Br isotopic signatures from filtered and unfiltered water samples from the same lake. 2014 Homestead Lake is shown by red squares, 2014 Shriner Lake is shown by violet squares, and 2014 Fritz Lake is shown by maroon squares.

Table 7. Stable bromine isotopic signatures of gas captured from three different lakes in 2014.

Lake Name	δ^{81}Br (‰) (SMOB)	Standard Deviation
Homestead	-0.72	0.17
Mini UNNJ	-1.02	0.18
Wilkinson	-0.92	0.10

The isotopic behaviour of the third end-member, the salt precipitates on the lake shorelines, are shown in the relationship between the $\delta^{81}Br$ and $\delta^{37}Cl$ isotopic signatures of the bulk salt samples and lake water samples (Figure 27), as well as the salt layer deposits (Figure 28). The bulk salt samples were analyzed for $\delta^{81}Br$ and $\delta^{37}Cl$ isotopic signatures and compared to the $\delta^{81}Br$ and $\delta^{37}Cl$ isotopic values of the associated lake water samples, shown in Figure 27. Several trends are noted in this figure which suggest that the bulk salt precipitates in this environment preferentially sequester the lighter ^{79}Br and heavier ^{37}Cl isotopes. These observations are as follows: a) aside from a few exceptions associated with Group 1 and Group 2 lakes, all lake water samples are more enriched in $\delta^{81}Br$ than they are in $\delta^{37}Cl$ over their respective seawater standards; b) each salt sample is more enriched in $\delta^{37}Cl$ than it is in $\delta^{81}Br$; and c) each salt that was sampled is depleted in $\delta^{81}Br$ and enriched in $\delta^{37}Cl$ compared to the associated lake isotopic signature from which the salt was formed. These trends suggest two relationships, a) the salt samples in this environment show a reverse isotopic relationship to what is shown in the water samples; and b) salt formation causes the residual lake water to enrich in $\delta^{81}Br$ and deplete in $\delta^{37}Cl$. Figure 29 shows a comparison of the $\delta^{81}Br$ and $\delta^{37}Cl$ isotopic signatures measured from the salts with the lake water (shown earlier in Figure 25). A comparison of these findings to previous studies will be provided in the Discussion.

The layered salt deposits which were collected from UNNJ Lake shorelines in 2012 were analyzed for isotopic values of $\delta^{37}Cl$, as there was insufficient mass in the sample size used to also successfully analyse for $\delta^{81}Br$ isotopic signatures. However, the data acquired from the $\delta^{37}Cl$ isotopic signatures alone is sufficient to draw some preliminary observations. Both UNNJ and UNNJ-1 salts were collected along the southern shoreline of UNNJ Lake, during which time the lake was completely dry and the surface of the lake was covered in a salt crust. The thickness of each analyzed salt layer was in the range of approximately 0.5 mm – 2 mm, however in some samples the layers reached a thickness of ~5 mm. In contrast to these two salt samples, there were no distinguishable layers in the salt that was collected at Homestead Lake during the same sampling period. Results of these analyses are provided in Figure 28.

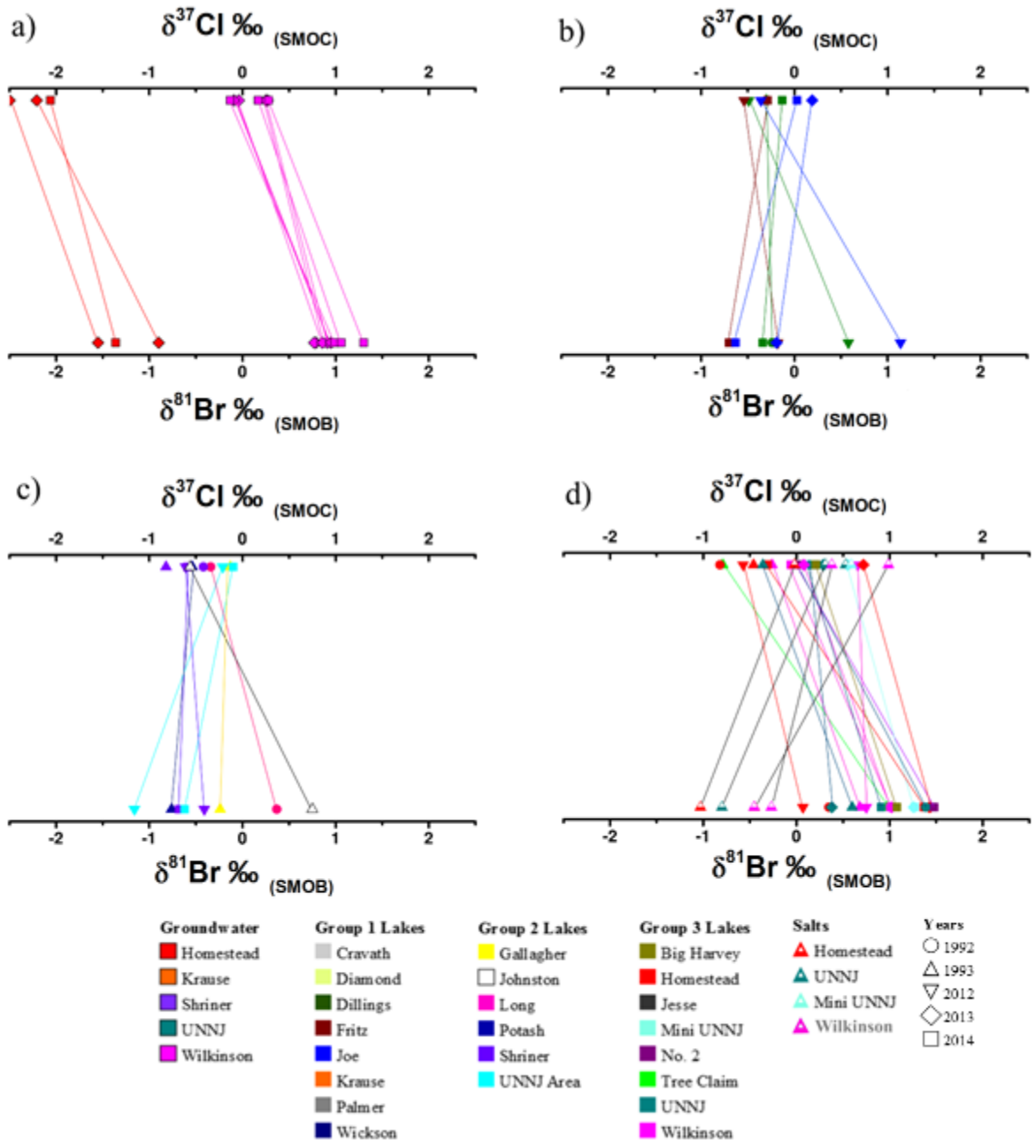

Figure 27. A comparison of bromine and chlorine isotopes from the same water or salt sample, divided into a) Groundwater, b) Group 1 lakes, c) Group 2 lakes, and d) Group 3 lakes and salts.

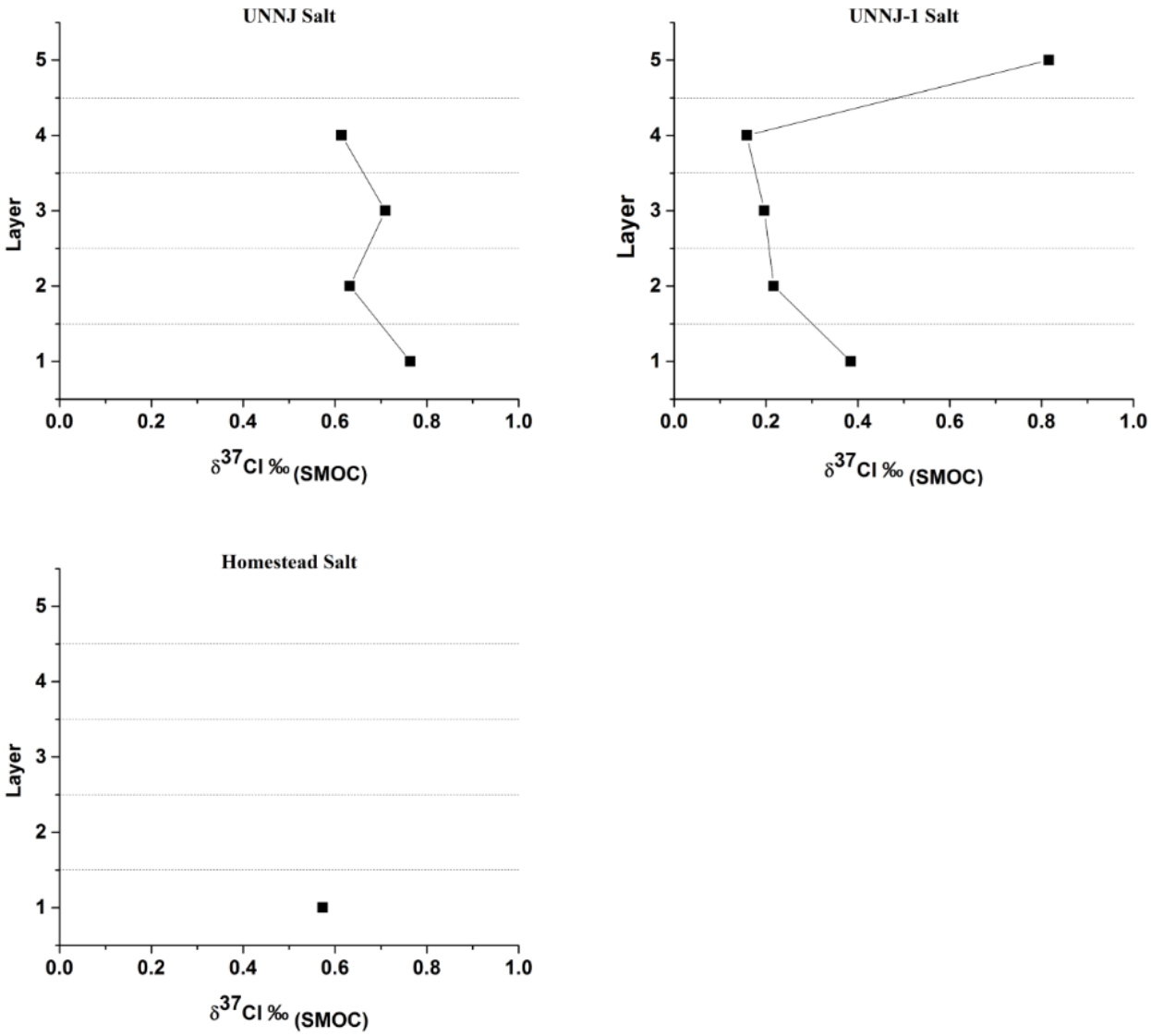

Figure 28. Chlorine stable isotopic signatures of two different layered salt crusts at UNNJ Lake in 2012, and one homogeneous salt sample from Homestead Lake in 2012.

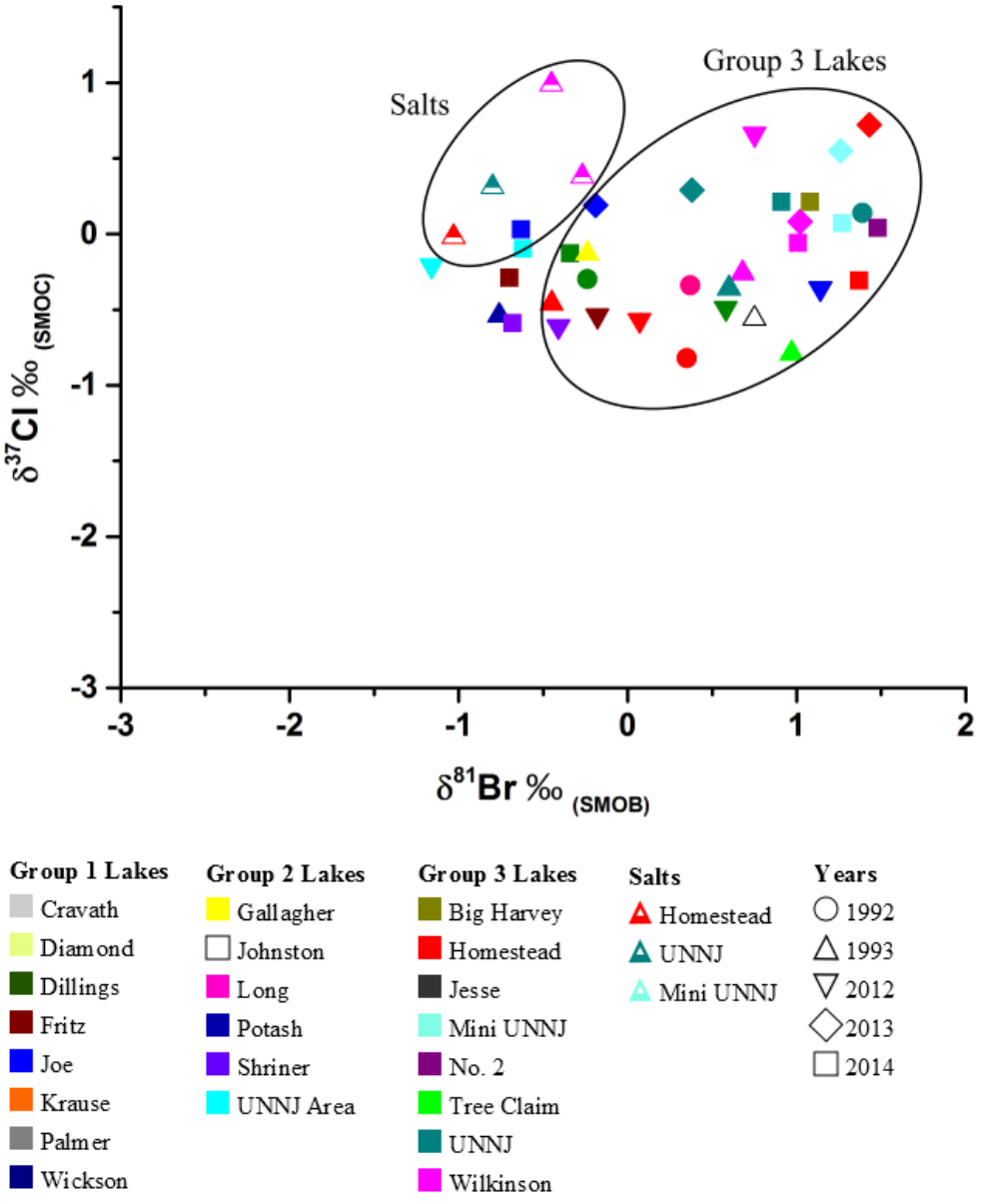

Figure 29. Plot showing $\delta^{81}Br$ and $\delta^{37}Cl$ of precipitated salts in comparison with lake water. Group 3 Lakes are circled because salt precipitates were collected from the shorelines of Group 3 Lakes.

The bulk $\delta^{37}Cl$ isotopic analysis of the UNNJ salt from 2012, shown in Figure 28, measured 0.53‰. This compares well with the $\delta^{37}Cl$ isotopic analysis of the layered salt deposits sampled from UNNJ Lake, as the average $\delta^{37}Cl$ signatures from the UNNJ salt is 0.65‰, and the average $\delta^{37}Cl$ signatures from UNNJ-1 salt is 0.24‰. Overall, there is depletion in both salts towards the top layer; the UNNJ salt is depleted by 0.15‰ ± 0.22‰, whereas the UNNJ-1 salt is depleted by 0.22‰ ± 0.12‰. It is possible that the isotopic values of the salt layers, which have undergone multiple cycles of salt precipitation followed by brief periods of salt dissolution, may resemble a Rayleigh distribution. Meaning, as the lighter bromine isotopes and heavier chlorine isotopes are sequestered during the initial salt precipitation, any further salt precipitation will utilize proportionally more of the heavier bromine and lighter chlorine isotopes. This coincides with the earlier observation that salt precipitation in this environment favours the heavier chlorine stable isotopes and the lighter bromine stable isotopes.

The fourth and fifth end-members which are discussed in this thesis are the regional and local groundwater systems. In a previous study, Gosselin et al. (1997) showed that groundwater samples from the shallow High Plains aquifer are very consistent in many chemical and isotopic parameters, e.g. $\delta^{87}Sr$. As shown in Figure 27a, the groundwater $\delta^{81}Br$ and $\delta^{37}Cl$ isotopic results in this study display uniformly depleted values. Furthermore, the bromine and chlorine isotopic signatures of the groundwater samples clearly show two distinct groundwater systems. One system is artesian, represented by the Homestead Spring groundwater samples in 2013 and 2014, which are depleted in both $\delta^{81}Br$ and $\delta^{37}Cl$ isotopic signatures ($\delta^{81}Br$ = -1.55‰ to -0.90‰; $\delta^{37}Cl$ = -2.50‰ to -1.98‰). The other system is meteoric, represented by the 2013 and 2014 Wilkinson piezometers, which are slightly more enriched in both $\delta^{81}Br$ and $\delta^{37}Cl$ isotopic values than the regional groundwater ($\delta^{81}Br$ = 0.77‰ to 1.30‰; $\delta^{37}Cl$ = -0.13‰ to 0.28‰). Figure 30 shows a comparison of the isotopic values of the regional and local ground water systems with the previously described isotopic signatures of the lake water and salt samples (Figure 29).

In an effort to understand more about the relationship between the saline lake waters and the fresh shallow meteoric groundwater system surrounding most ephemeral Group 3 Lakes, a series of deeper sediment

cores were sampled at three lake sites (Wilkinson Lake, Homestead Lake, and UNNJ Lake). A comparison between the physical and isotopic parameters of these sediment cores with the groundwater samples from the installed mini-piezometers at Wilkinson Lake can provide information regarding the groundwater and lake water exchange processes occurring in the shallow groundwater system adjacent to the alkaline lakes.

In 2014, four longer sediment cores were sampled. These cores ranged in depth from 0.76 m to 1.58 m below the ground surface. Deeper cores could not be collected as the hard clay and sticky nature of the subsurface prevented further extraction. The cores were logged for visual differences in sediment colour and sediment type (Table 8), and tested for water content, electric conductivity, and loss on ignition (Figures 30 and 31). Estimations of the total dissolved solids present in each segment were calculated using the formula outlined in the "Core Sampling Methodology" section of this thesis. Based on these physical measurements, intervals were chosen for an isotopic analysis for $\delta^{81}Br$ and $\delta^{37}Cl$. Results of the $\delta^{81}Br$ and $\delta^{37}Cl$ isotopic data from the analysis is provided in Table 9, and are shown in Figure 31 and Figure 32.

The physical profiles of the lengths of the cores are indicative of a freshwater groundwater component near the bottom of the cores. In general, the concentration of TDS decreases down each core, while the water content increases. It is possible that fresh groundwater from the underlying regional aquifer is slowly diffusing into the overlying layers. Isotopically, this is evident in the bottom of the Wilkinson Core (Figure 31a), where $\delta^{37}Cl$ = -1.79‰. This value compares well with the measured $\delta^{37}Cl$ signatures of the 2013 and 2014 Homestead Island Piezometer water samples ($\delta^{37}Cl$ = -2.21‰, and -2.06‰), and the Homestead Spring water samples ($\delta^{37}Cl$ = -2.50‰, and -1.98‰).

In summary, the presence of several different isotopically and geochemically distinct end-members in the Sand Hills Region may be impactful on the environmental cycling of the stable isotopes of bromine and chlorine in this region. These end-members include lake surface waters, volatile loss, salt precipitation and re-dissolution, and local and regional groundwater systems. An analysis of the interaction between these end-members is provided in the Discussion.

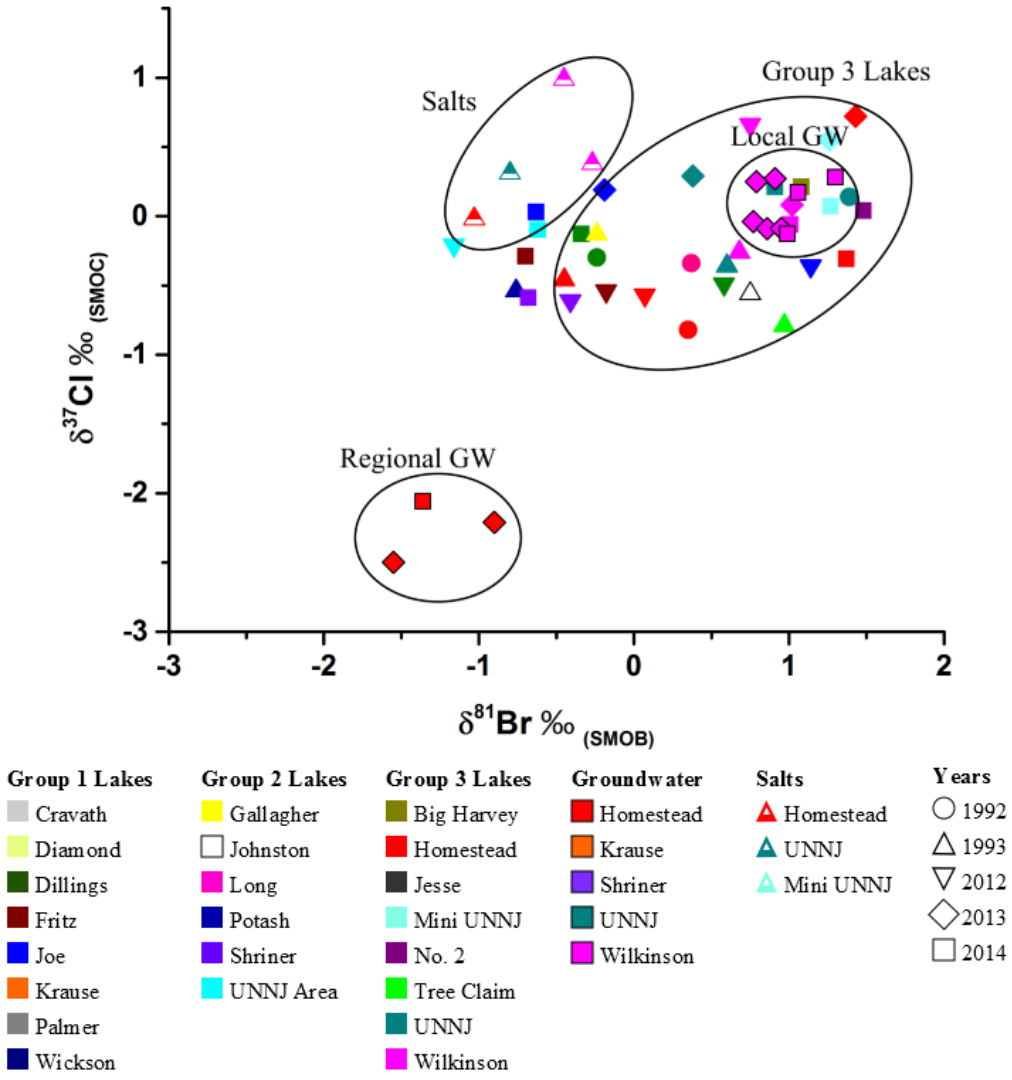

Figure 30. Plot showing δ81Br and δ37Cl of Local Groundwater and Regional Groundwater systems, in comparison to precipitated salts and lake water samples.

Table 8. Bromine and chlorine stable isotope data for selected core samples from the Sand Hills Region of Nebraska, USA.

Sample Name	Sample Date	Depth (cm BGS)	δ^{81}Br ‰ (SMOB)	St. Dev.	δ^{37}Cl ‰ (SMOC)	St. Dev
			Wilkinson Core			
Wilkinson 10-12	14-Aug-18	0	0.77	0.01	-0.29	0.12
Wilkinson 18-20	14-Aug-18	8	0.19	0.06	-0.23	0.14
Wilkinson 40-42	14-Aug-18	30	-0.74	0.07	-0.34	0.09
Wilkinson 66-68	14-Aug-18	56	-0.70	0.04	-0.23	0.04
Wilkinson 90-92	14-Aug-18	80	-0.83	0.02	0.17	0.16
Wilkinson 112-114	14-Aug-18	102	-0.69	0.07	0.25	0.08
Wilkinson 126-128	14-Aug-18	116	-0.59	0.07	0.21	0.10
Wilkinson 158-160	14-Aug-18	148	-0.74	0.25	-1.79	0.04
			UNNJ Core			
UNNJ 0-2	14-Aug-20	0	-0.66	0.07	-0.24	0.20
UNNJ 36-38	14-Aug-20	36	-1.35	0.02	0.18	0.10
UNNJ 66-68	14-Aug-20	66	-0.83	0.17	0.08	0.11
UNNJ 84-86	14-Aug-20	84	-1.38	0.24	0.02	0.09
UNNJ 114-116	14-Aug-20	114	-0.75	0.11	-0.25	0.04
			Homestead 1 Core			
Homestead 1 0-2	14-Aug-19	0	-0.68	0.05	-0.12	0.06
Homestead 1 16-18	14-Aug-19	16	-0.35	0.05	-0.08	0.07
Homestead 1 32-34	14-Aug-19	32	-0.37	0.05	-0.17	0.10
Homestead 1 70-72	14-Aug-19	70	-0.49	0.32	-0.38	0.06
			Homestead 3 Core			
Homestead 3 0-2	14-Aug-19	0	-0.65	0.09	-0.72	0.03
Homestead 3 32-34	14-Aug-19	32	-0.82	0.23	-0.79	0.22
Homestead 3 72-74	14-Aug-19	72	-0.66	0.10	-0.53	0.07

Table 9. Core Sediment Descriptions with Depth of Wilkinson Core, UNNJ Core, Homestead 1 Core, and Homestead 3 Core.

Depth (cm BGS)	Sediment Descriptions			
	Wilkinson Core	**UNNJ Core**	**Homestead 1 Core**	**Homestead 3 Core**
0	Brown silty sand	Brown silty sand	Brown silty sand	Brown silty sand
2				
4				
6				
8		Brown sand	Brown clay with silt	Brown silty clay
10	Brown silty clay with some organics			
12				Brown silty sand
14				
16				
18				
20			Grey clay with silt	
22				
24				Dark brown silty clay
26		Dark brown clay and sand		
28				
30				
32		Grey clay and silt		
34	Light brown silty sand			
36		Grey clay	Dark brown clay	
38				
40				
42				Dark brown clay
44	Brown sand with some silt		Grey clay with silt	
46				
48				
50				
52				Grey clay and silt
54				
56				
58				
60		Light grey clay and silt		
62	Brown sand		Grey clay	Grey clay
64				
66				
68		Light brown sand and clay		
70				
72		Dark brown clay		
74				
76		Grey clay and silt		
78				
80			Light grey clay and silt	
82				
84		Dark grey clay		
86				
88				
90				
92				
94				
96				
98				
100				
102	Grey clay			
104				
106		Dark grey clay and silt		
108				
110	Grey clay and silt			
112				
114				
116				
118				
120				
122	Dark grey clay			
124				
126				
128				
130				
132				
134				
136				
138				
140				
142				
144				
146				
148				
150				
152				
154				
156				
158				

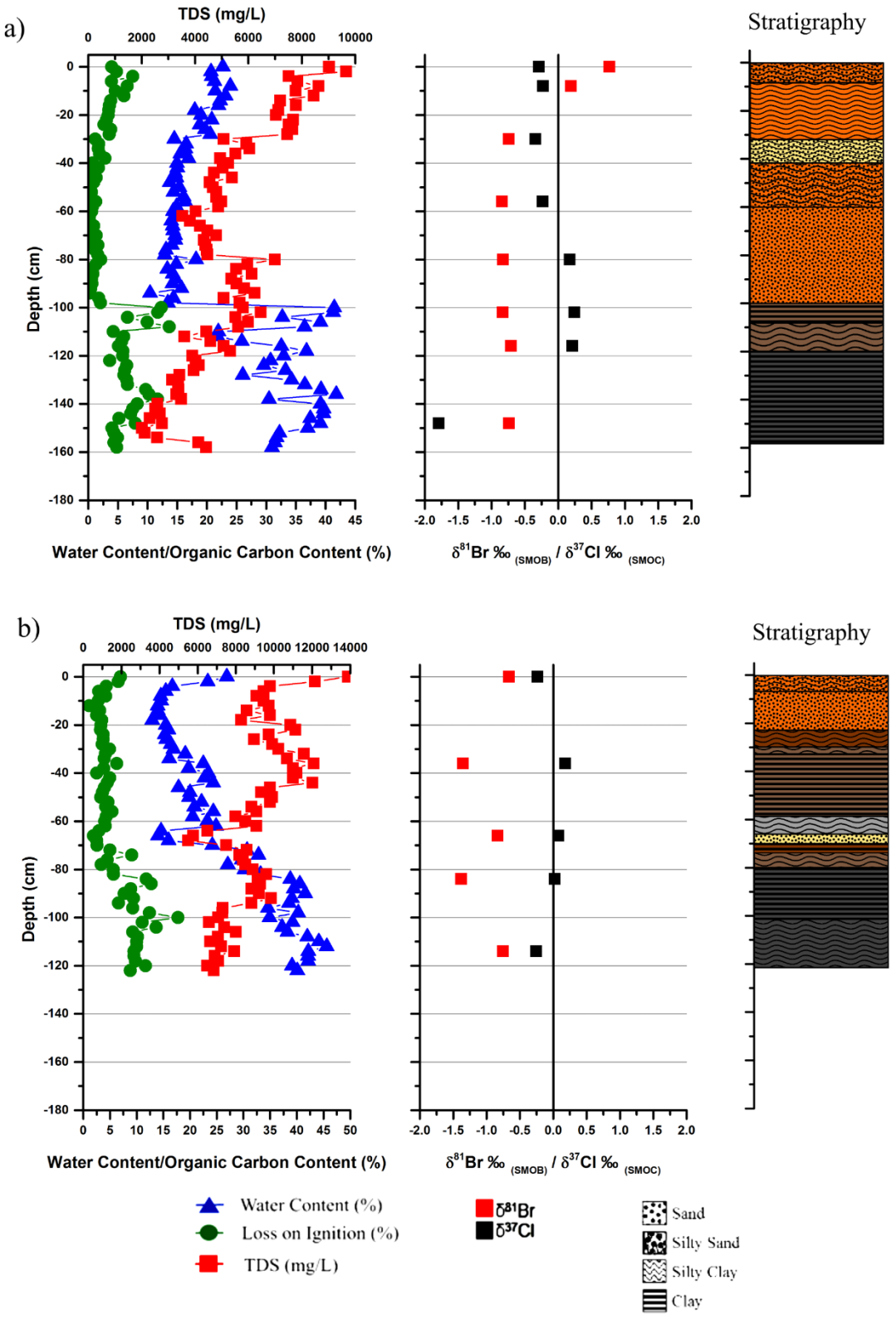

Figure 31. Core profiles of a) Wilkinson Lake, and b) UNNJ Lake, showing changes in water content, loss on ignition, and total dissolved solids, as well as corresponding $\delta^{81}Br$ and $\delta^{37}Cl$ signatures with depth.

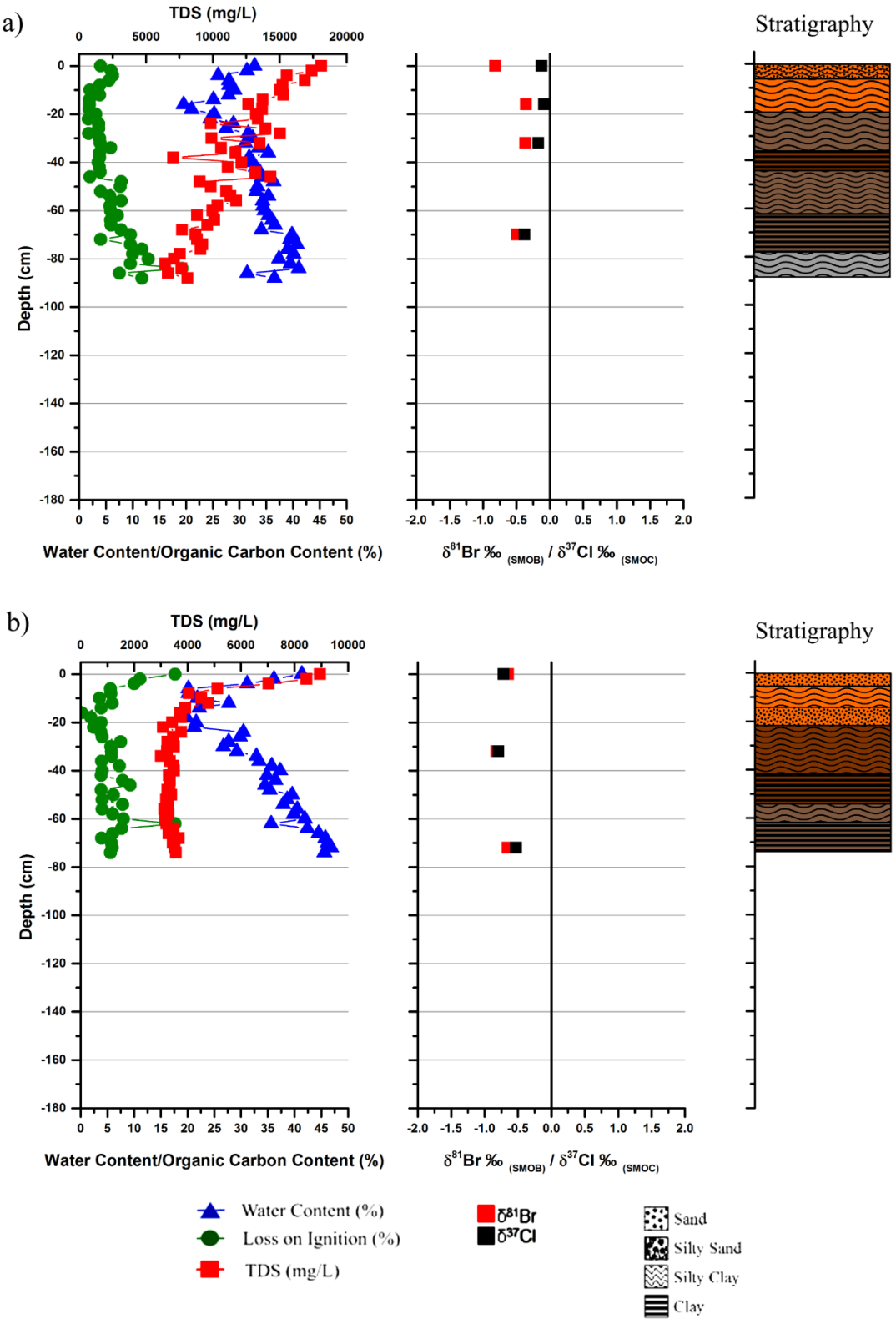

Figure 32. Core profiles from Homestead Lake, a) Homestead 1 Core, and b) Homestead 3 Core, showing changes in water content, loss on ignition, and total dissolved solids, as well as corresponding $\delta^{81}Br$ and $\delta^{37}Cl$ signatures with depth.

Discussion

Geochemistry

Gradual changes in sediment composition, topography, and groundwater configuration within the Sand Hills Region have resulted in lakes with various water balances and geochemical properties. Lakes with lower TDS are likely to be more connected with the groundwater system than lakes with higher TDS (Gosselin, 1997). Furthermore, it was suggested that lakes with higher TDS values are likely to have reduced groundwater inflow due to settling clay particles in the lake beds, therefore restricting porosity and permeability. Coring results from 2014 also suggests increased finer material and clay content at several lakes with increased depth (Figure 28 and Figure 29). Higher TDS concentrations can also be a result of conditions leading to increased evaporation in many basinal settings in the region (Gosselin, 1997).

The anion chemistry of the Group 3 Lakes (Figure 23c) displays a much more variable water chemistry than what is noted in either Group 1 or Group 2 Lakes (Figure 23a and Figure 23b). Group 1 and Group 2 Lakes are dominantly composed of $HCO_3^- + CO_3^{2-}$, whereas Group 3 Lakes vary between dominantly $HCO_3^- + CO_3^{2-}$ to dominantly Cl^- and SO_4^{2-}. Of the Group 3 lakes studied, all contain extremely evaporated brines. The high TDS values and chemically variable compositions suggest that the ephemeral lakes in the area evolve towards different water types. There appears to be three different evolutionary pathways present which result in three separate end member ephemeral lakes: sulphate rich, chloride rich, and carbonate rich. These pathways were shown earlier in Figure 1, and appear in more detail in Figure 33. To further investigate the potential dynamics connecting the geochemically evolving brine pathways to the hydrogeological settings of the lakes, three lakes were chosen as detailed examples for this study: Wilkinson Lake, Homestead Lake, and UNNJ Lake.

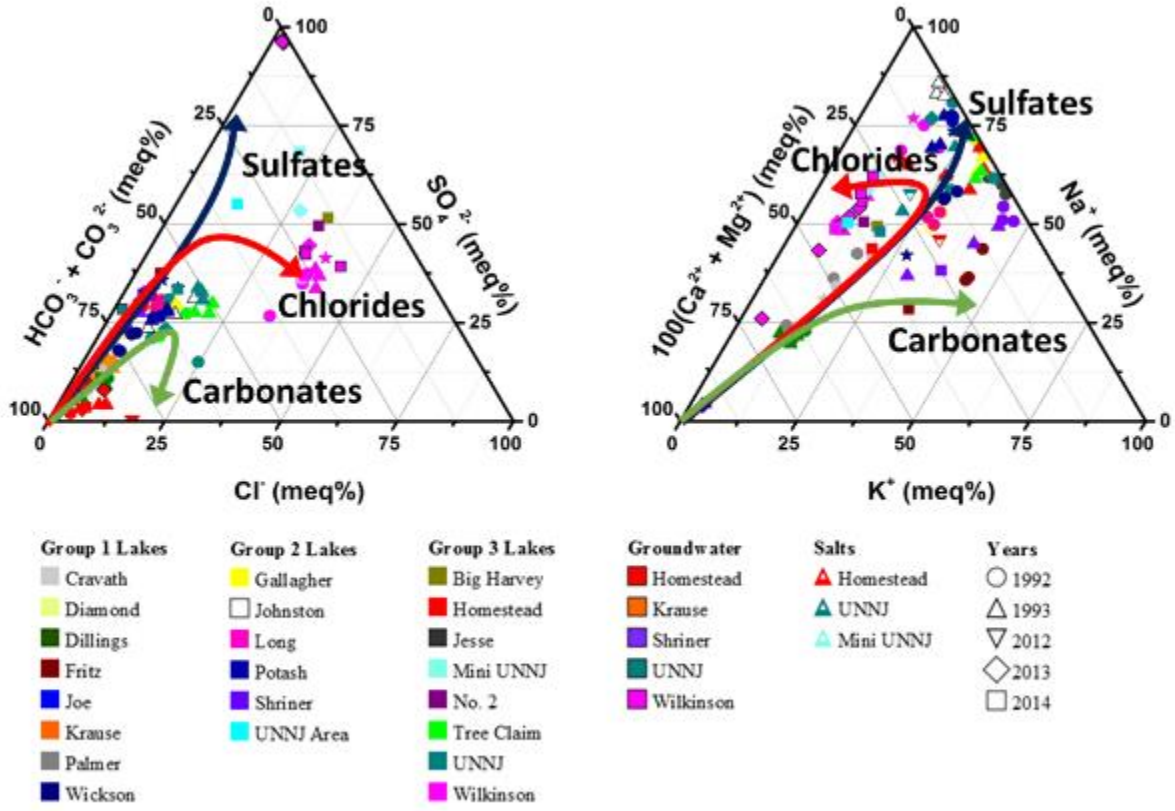

Figure 33. Ternary plots showing three evolutionary pathways of brines: carbonate rich, chloride rich, and sulphate rich.

Field pictures of Wilkinson Lake, Homestead Lake, and UNNJ Lake during the 2012, 2013, and 2014 sampling years are shown in Figure 34. The geochemical analyses of the lake waters, as well as the associated groundwater samples, are provided in the figure as well. The constituent analysis for the water samples from the 2012 sampling year was not precise, however similar climatic conditions occurred between 2012 and 1992, and so the geochemistry from the 1992 samples is substituted for the 2012 dataset.

The responses of the lake systems to the various climatic conditions between sampling years is noticeable in the field images from each year. In the 2012 sampling year, there were very low rates of precipitation. Consequently, during this year the water levels of these lakes were low, and the shorelines of each lake were dry and crusted with various salt precipitates. In 2013 and 2014, the rates of precipitation increased considerably. This resulted in the water level increasing (noted by the gradual enlargement of the distance between the Homestead vegetative island at the groundwater fed spring to the water's edge, shown in Figure 34b), and the subsequent re-dissolution of the shoreline salts from 2012.

It is possible that either a fresh groundwater component, or a large shallow groundwater storage system in the surrounding wet meadows, is present at both Wilkinson Lake and Homestead Lake. This is supported by field observations at these lakes, which showed lush vegetation surrounding the lakes throughout all sampling years (Figure 34a and 34b). Observations by Harvey et al. (2007) noted an evident rise in the water table at the nearby Jumbo Valley in Cherry County, Nebraska, in response to vegetation surrounding the lake being cut down. This indicated a connection between the fresh meteoric groundwater in the surrounding meadows and the saline lake surface waters. Additionally, at Wilkinson Lake, the solute concentrations of the Wilkinson mini-piezometers are more concentrated in the piezometers installed closer to the lake bed (i.e. L2' and L4'), and decrease with increasing distance away from the lake (i.e. M2', M4', and GL), and with depth. The sandy nature of the shallow near shore area around the lake would aid in an active exchange between the lake waters and the shallow groundwater system. This was shown earlier in the $\delta^{18}O$-$\delta^{2}H$ data (Figure 20), and is apparent in the comparison between the 2013 Wilkinson Lake and Piezometer geochemical data, and very obvious in the 2014 dataset (Figure 34a).

a)

Hydrogeological Cross-Sections

2012 (1992)						2013						2014					
Ca	Na	K	HCO_3	SO_4	Cl	Ca	Na	K	HCO_3	SO_4	Cl	Ca	Na	K	HCO_3	SO_4	Cl
5	43,392	14,628	30,396	43,512	31,507	296	57,141	16,594	33,379	57,174	31,626	101	20,289	6,282	13,261	20,343	14,731
WILKINSON PIEZOMETERS																	
					L2'	142	22,501	7,665	15,897	19,565	16,329	93	24,117	6,811	15,165	26,985	15,308
					L4'	72	12,846	4,585	8,930	10,675	10,077	92	18,918	5,553	11,761	20,889	12,343
					M2'	156	15,974	5,059	10,248	15,281	11,089	47	9,120	3,129	4,934	9,428	7,596
					M4'	75	10,389	3,407	7,491	9,226	7,480						
					GL	34	2,012	591	1,108	2,052	1,562						

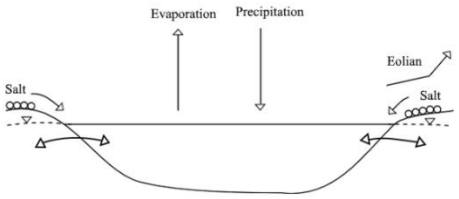

b)

2012 (1992)						2013						2014					
Ca	Na	K	HCO_3	SO_4	Cl	Ca	Na	K	HCO_3	SO_4	Cl	Ca	Na	K	HCO_3	SO_4	Cl
4	47,264	37,659	175,828	12,103	18,179	77	46,311	33,121	136,152	7,505	10,717	190	25,804	19,374	78,934	4,099	5,562
HOMESTEAD SPRING																	
41	15	19	211	20	7	58	14	19	243	19	5	53	12	18	232	19	4

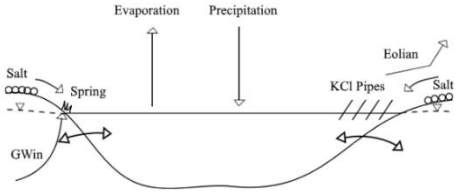

c)

2012 (1992)						2013						2014					
Ca	Na	K	HCO_3	SO_4	Cl	Ca	Na	K	HCO_3	SO_4	Cl	Ca	Na	K	HCO_3	SO_4	Cl
5	131,649	50,050	205,202	86,791	35,085	103	120,213	41,642	224,724	73,970	31,339	187	31,369	20,873	53,436	38,798	9,442
UNNJ WINDMILL																	
												44	36	7	212	69	3

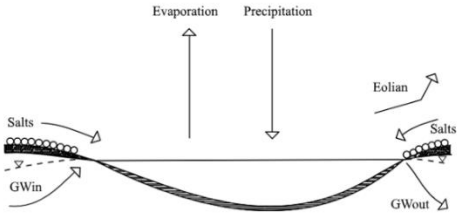

Figure 34. Field images and water sample chemical compositions (mg/L) of 3 lakes (a) Wilkinson Lake, b) Homestead Lake, and c) UNNJ Lake) between 2012 (1992), 2013, and 2014. Diagrams to the right of the figure are the proposed hydrogeological cross-sections of that lake. The Wilkinson Piezometers are notated using L2' (Lake at 2 feet), L4' (Lake at 4 feet), WL2' (Water Line at 2 feet), WL4' (Water Line at 4 feet), and GL (Grass Line at 4 feet).

Unlike both Wilkinson Lake and Homestead Lake, UNNJ Lake is much more concentrated and geochemically evolved. It appears to be a perched system that overlies a very fine grained clay rich lake bed. Coring results in 2014 confirmed that several thick, fine clay, sediment zones underlies the lake shore (Figure 31b and Table 9). This would greatly minimize any groundwater flow into the lake bed. Since the surrounding sediments in the dune regions are composed of sand, groundwater is able to enter the lakes only when the shallow or local water table has risen to an elevation that is greater than the elevation of the clay bed (Figure 31c). PHREEQC 3.0 Mineral Saturation Indices results, described in Appendix B, predict that UNNJ lake waters in 2012 (1992) and 2013 are saturated with respect to several complicated carbonate and sulphate mineral assemblages, including nahcolite, trona, thenardite, burkeite, glaserite, kieserite, arcanite, glauberite, labile salt, and syngenite. These mineral assemblages were not predicted to be present at either Homestead Lake or Wilkinson Lake during the same sampling years. This suggests that the hydrologic setting at UNNJ Lake permits this lake to reach a much higher degree of evaporation and salt precipitation than at the other two lakes discussed in this study.

$\delta^{37}Cl$ and $\delta^{81}Br$ Systematics

Natural Fractionation Mechanisms of $\delta^{37}Cl$ and $\delta^{81}Br$

Specific mechanisms and the extent to which they control the fractionation of stable bromine and chlorine stable isotopes in natural environments are not yet fully understood. Currently, the main contributors to bromine and chlorine isotopic fractionation are considered to be diffusion, mineral precipitation, and microbial activity (Eggenkamp, 2014). A literature review of the fractionation factors of bromine and chlorine stable isotopes as a result of each of these processes is provided in Table 10.

In terms of aqueous diffusion, the fractionation factors for bromine and chlorine have been estimated at 1.0008 ± 0.0002, and 1.0019 ± 0.001 for the lighter isotopes, respectively (Bourg and Sposito, 2007). However, the magnitude of fractionation is dependent on the velocity, time of measurement, and total displacement from the source of release (Eggenkamp, 2014). At the alkaline lakes there are concentration differences between many of the ephemeral lakes and the surrounding shallow groundwater systems. This is best seen in the comparison between Wilkinson Lake chemistry and the shoreline piezometers for the 2013 and 2014 dataset (Figure 34a). The high concentrations in the piezometers that decrease with distance from the lake and depth, the chemical similarities between the lake waters and the shallow groundwater systems, and the nature and permeability of the shallow sandy sediments near the lake shore, all support advective recharge and mixing as processes rather than diffusion. Diffusion may be a dominant process affecting bromine and chlorine fractionation in this environment at a depth under some lakes, but without deep monitoring devices we cannot adequately resolve this issue. For that reason, in this thesis it is not considered to any great degree. Salt precipitation in and around the lakes is a much more probable mechanism controlling bromine and chlorine fractionation and was examined as part of this thesis.

Previous research has demonstrated that bromine and chlorine isotopic fractionation resulting from salt precipitation is dependent on the type of minerals that are precipitated. Laboratory experimentation has verified that upon precipitation, fractionation factors for both bromine and chlorine stable isotopes vary depending on the dominance of NaCl, KCl, or MgCl in the precipitate (Eggenkamp et al., 2011; Eggenkamp et al., 1995; Luo et al., 2014). The information available is presented in Table 10. The majority of this data was developed through the use of a mineralization sequence which reflects evaporating seawater (NaCl, KCl, then MgCl).

Table 10. Literature review of bromine and chlorine stable isotope fractionation factors. [1] Desaulniers et al., 1986; [2] Beekman et al., 1992; [3] Eggenkamp et al., 1994; [4] Groen et al., 2000; [5] Eggenkamp and Coleman, 2009; [6] Richter et al., 2006; [7] Bourg and Sposito, 2007; [8] Eggenkamp et al., 1995; [9] Luo et al., 2014; [10] Eggenkamp et al., 2011; [11] Palau et al., 2014; [12] Abe et al., 2009; [13] Wiegert et al., 2013; [14] Sturchio et al., 2003; [15] Numata et al., 2002; [16] Zakon et al., 2013; [17] Bernstein et al., 2013; [18] Horst et al., 2014, NA = Not available.

Process		**$^{35}Cl/^{37}Cl$ (α)**	**Source**	**$^{79}Br/^{81}Br$ (α)**	**Source**
Aqueous Diffusion		1.0008 – 1.0027	1, 2, 3, 4, 5, 6, 7	1.0006 – 1.0019	5, 7
Salt Precipitation/ Dissolution	NaCl	1.00026 – 1.0005	8, 9	0.99850	10
	KCl	0.99991 – 1.00025	8, 9	1.0001	10
	MgCl	0.99994 – 1.00012	8, 9	1.0000	10
Microbial Activity	Oxidation	0.99621 – 0.99970	11, 12	NA	NA
	Reduction	0.9834 – 0.99850	11, 12, 13, 14, 15	0.99924 – 1.0051	16, 17, 18

The effect of microbial activity on the fractionation of bromine and chlorine isotopic signatures in natural environments is poorly understood. This is primarily due to the large abundance of microbial species in existence, as well as the fact that relatively few studies have been published on the subject. Generally speaking, certain bacteria are able to reduce chlorine to produce energy, during a process known as bioreduction. Previous studies have shown that during this process, microbes preferentially uptake the heavier 37 chlorine isotope, resulting in depletion in chlorine in the residual soils and salts (Numata et al., 2002; Sturchio et al., 2003; Abe et al., 2009; Wiegert et al., 2013; Palau et al., 2014).

Preliminary studies on the effect of microbial bioreduction of bromine have shown both depletion and enrichment following the microbial reduction of brominated phenols or the release of methyl bromides (Bernstein et al., 2013; Horst et al., 2014; Zakon et al., 2013). A generalized formula of the bioreduction of bromine by bacteria is shown in Formula 4, below (Horst et al., 2014). The results of previous studies are summarized in Table 10.

$$H^+ + C + Br \rightarrow HBr \; or \; CH_3Br \qquad (4)$$

It is possible that the release of bromide gas on the surficial soils of the alkaline lakes is a result of photolytic processes, as opposed to microbial activity. Research regarding the mechanisms which produce bromide and chloride gases from continental or coastal salt flats is at a preliminary stage. It has been suggested that a photochemical mechanism is capable of producing Br^-, and this corresponds to the production of BrO (Pratt et al. 2013). The photochemical formation of BrO is shown in Equation 5 and Equation 6, where X represents Br, Cl, or I (Monks, 2005).

$$BrX + hv \rightarrow Br + X \quad (5)$$

$$Br + O_3 \rightarrow BrO + O_2 \quad (6)$$

It is possible that the production of the volatile brominated compounds occurring on the shorelines of the alkaline lakes is through a photolytic or microbial process. Further study is needed to determine which mechanisms are responsible for the emission of bromide gas in this area.

A proper interpretation of the behaviour of the $\delta^{81}Br$ and $\delta^{37}Cl$ isotopic signatures observed throughout the various end-members in the alkaline lakes requires some thought into the processes which may result in salt movement throughout the surface and the subsurface of the Sand Hills Region. A hypothetical schematic displaying the mechanisms which may affect the $\delta^{81}Br$ and $\delta^{37}Cl$ isotopic signatures and balance in the subsurface adjacent to the alkaline lakes is shown in Figure 35. The remainder of this discussion is divided to focus on the interactions occurring between end-members in the surficial region of the alkaline lakes, and the end-members within the subsurface.

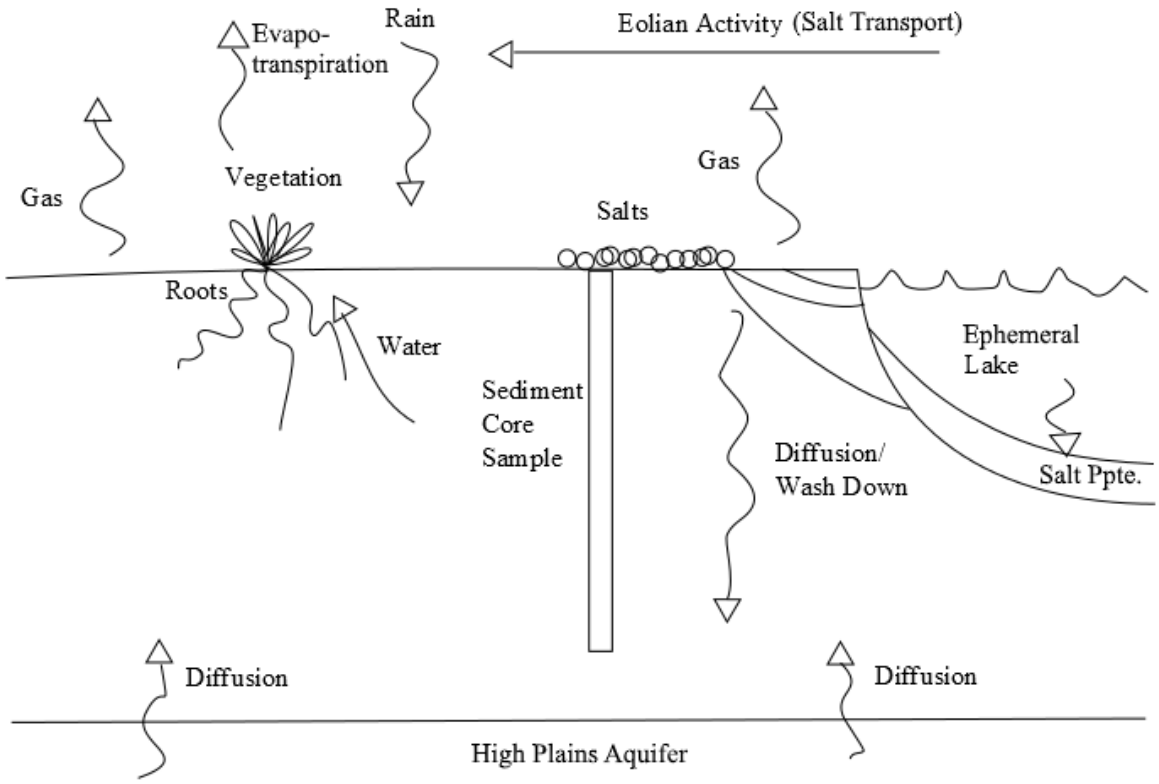

Figure 35. Possible schematic showing mechanisms which may affect the bromine and chlorine isotopic signatures of the subsurface adjacent to an alkaline lake in the Sand Hills Region where the core samples in 2014 were located.

Surficial Effects

Bromine and chlorine isotopically controlled processes around the alkaline lakes is likely to be controlled by the precipitation and dissolution of salt minerals along the lake shorelines, salt deflation through eolian activity, and the release of volatile halogen gases, shown in Figure 35.

The first surficial end-member interaction, the precipitation and dissolution of shoreline salts, was previously described in the "$\delta^{37}Cl$ and $\delta^{81}Br$" section in the Results of this thesis, and is shown in Figure 27 and Figure 29. In summary, the behaviour of the $\delta^{81}Br$ and $\delta^{37}Cl$ isotopic signatures in the lake water samples compared to the salt samples suggests that salt precipitation preferentially sequesters the lighter ^{79}Br and the heavier ^{37}Cl isotopes from solution. This infers that salt precipitation in this region results in the residual lake brine becoming more enriched in $\delta^{81}Br$ and more depleted in $\delta^{37}Cl$.

The second end-member process in the surficial region of the alkaline lakes that may affect the cycling of bromine and chlorine stable isotopes is eolian activity. Following the precipitation of salts depleted in $\delta^{81}Br$ and enriched in $\delta^{37}Cl$ isotopic values, these salts are susceptible to removal by wind. It is possible that certain sulfate minerals are more easily removed through eolian activity than others (Zlotnik et al., 2012). Crystals of mirabilite ($Na_2SO_4 \bullet 10H_2O$) can often turn to thenardite (Na_2SO_4) with persistent evaporation throughout the day. Thenardite is much lighter in density and is easily separated from the substrate by wind. The amount of chlorine or bromine that is bound structurally to sulphate minerals has not been studied in detail. However, there is significant chlorine and bromine concentrations measured in the precipitated salts at Homestead Lake and UNNJ Lake (Br = 2.25 mg/L and 27.1 mg/L, and Cl = 10,451 mg/L and 1,389 mg/L, respectively). Therefore, the impact of eolian activity on the removal of the salt minerals is dependent on the types and densities of minerals which are precipitated, and the concentration of chlorine and bromine contained in the minerals.

The third potential end-member on the shorelines of the alkaline lakes is the release of volatile halide gases, either through microbial or photolytic processes. The effect of microbial or photochemical reduction and oxidation on the fractionation of bromine and chlorine stable isotopes has not been extensively studied in the past. Research on the effect of microbial reduction on chlorine isotopic fractionation is somewhat more understood, as publications are available from the early 2000's, whereas the publications available for bromine isotopic fractionation begin in 2013. Refer to Table 10 for a selection of the currently available publications. The suggested chemical pathway for the release of halide gas was given by Horst et al. (2014), and is shown in Figure 36. In general, carbon macromolecules react with bromide ions and protons to form HBr, and CH_3Br.

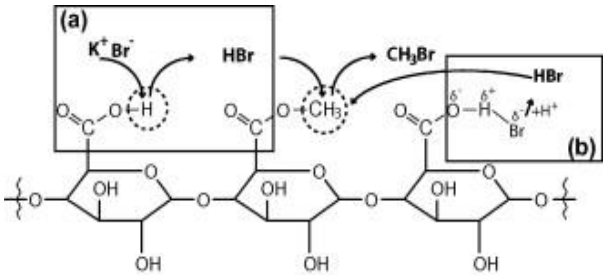

Figure 36. Chemical reaction pathway of the microbial reduction of bromine to HBr and CH_3Br (Horst et al., 2014).

Several field observations that were made at the Alkaline lakes during the sampling years suggest the presence of microbial activity, specifically at Fritz Lake, Wilkinson Lake, UNNJ Area Lake, Mini UNNJ Lake, No. 2 Lake, and Big Harvey Lake. A strong rotten egg smell originating from sulfur reducing bacteria was noted at several lake sites. Furthermore, observations of green or purple colour changes at the lakes and during sediment disturbance were noted, often occurring over very short time frames of minutes to hours. For example, in 2012, a severe thunderstorm at Wilkinson Lake resulted in the beach area transitioning to a deep purple colour. Additionally, later that year, a bottle of the Wilkinson Lake water was left in the sunlight on a laboratory bench, and turned the same shade of purple (Figure 37b). During the same sampling year, Fritz Lake was a distinct green colour (Figure 37a). In addition to the colour of the lakes, freshly dug up soils along the Fritz Lake shoreline revealed damp, dark grey soil directly beneath the salt crust, indicating reducing, anoxic conditions (Figure 37c). Finally, many lake shorelines in 2012 and 2013 were covered in thick, extensive microbial mats (Figure 37d).

Figure 37. Field evidence of microbial activity at the Sand Hills lakes, Nebraska. a) Green colouration to Fritz Lake in 2012, b) Purple colouration of Wilkinson Lake from 2012 after the sample bottle was left in the sun, c) redox conditions just below the surface, d) microbial mats encrusted with salt.

These field observations suggest that the gas samples captured from the shorelines of Homestead Lake, Wilkinson Lake, and UNNJ Lake in 2014 were likely to be microbial in origin, however it is possible that the gases may have been produced through photolytic processes as well. Further study on the speciation of the observed microbial mats is underway in a separate study and would be required to make this distinction. The measured $\delta^{81}Br$ isotopic signatures of the three captured gas samples ranged between $\delta^{81}Br$ = -1.02‰ to -0.72‰, suggesting that the process causing the release of the halide gases (microbial or photolytic) selectively uptakes and releases the lighter ^{79}Br isotope. These results are comparable to the controlled experiments from Horst et al. (2014), who also produced highly depleted CH_3Br gases through a microbial reduction process. Corresponding with these results, the surficial portion of the 2014 Wilkinson Core (Figure 31a) is isotopically enriched in $\delta^{81}Br$ to 0.77‰. This is in agreement that a surficial process, either physical (salt deflation), or chemical (photolysis or microbial) is causing the removal of the lighter ^{79}Br isotope from the sediments at Wilkinson Lake.

Subsurface Effects

Beneath the surface, the interaction between the fresh groundwater systems and the saline lake waters can be affected by several processes, including groundwater diffusion, or a "wash-down" effect from surficial salts into the shallow sediment layer. These processes are shown in Figure 35. In order to determine which processes may be occurring in the subsurface of various alkaline lakes, the $\delta^{81}Br$ and $\delta^{37}Cl$ isotopic signatures measured within four sediment cores are compared with the $\delta^{81}Br$ and $\delta^{37}Cl$ isotopic signatures of various end-members (lake water, salt samples, the regional groundwater, and the local groundwater). The $\delta^{81}Br$ and $\delta^{37}Cl$ isotopic measurements along each sediment core is shown in Figure 38a, 38b, 38c, and 38d. For comparison, an isotopic comparison of the sediment cores with the various end-members is provided in Figure 38e and 38f.

Evidence of long term washing down, or mixing, of precipitated salts into the shallow subsurface along the lake shore is displayed in the $\delta^{81}Br$ and $\delta^{37}Cl$ isotopic relationship throughout the mid-region of the

Wilkinson Core and UNNJ Core, shown in Figure 31a, 31b, and 38e. In the Wilkinson Core, the $\delta^{81}Br$ isotopic values of the sediments are more isotopically depleted than the $\delta^{37}Cl$ isotopic signatures. This behaviour is opposite of the observations for the lake water samples (Figure 27d), and more closely resembles the salt samples (Figure 27d). It is possible that precipitated salts from the shorelines are slowly washing down through the upper sediment layers. In the UNNJ Core, the $\delta^{81}Br$ isotopic signatures throughout the core seem to show depleted values which correspond with core segments containing higher concentrations of TDS. This pattern is in agreement with the earlier conclusion that salt precipitation favours the lighter ^{79}Br isotope. These zones could be indicators of past periods of drought and salt accumulation. In a related study, Hendry and Wassenaar (2004) showed lateral flow through semi-horizontal highly permeable sand layers, similar to other prairie sites. Similarly, the sand layer present in the UNNJ core from 0.66 m to 0.70 m below ground surface corresponds to a decrease in TDS concentration (from 9,088 mg/L to 5,773 mg/L) and an enrichment in $\delta^{81}Br$ (from -1.35‰ to -0.83‰), suggesting that lateral groundwater flow may be present in this sand layer in the core. Additionally, at 0.36 m and 0.84 m below ground surface, there is increased concentrations of TDS that corresponds to depleted $\delta^{81}Br$ isotopic signatures. On Figure 38e, these sections of the core are displaced to the left of the other sections of the other cores. It is possible that an extreme drought occurred in the past 100 – 1,000 years causing depletion in $\delta^{81}Br$ in the salts, and that these old waters and salts have been trapped in the clay layers in the subsurface along the UNNJ lakeshores.

Several regions of the sampled cores suggest that diffusional processes are occurring within the subsurface of the lakeshores. For example, the $\delta^{37}Cl$ isotopic signature measured at the bottom of the Wilkinson Core ($\delta^{37}Cl$ = -1.79‰) (Figure 31a) is very similar to the measured $\delta^{37}Cl$ isotopic signatures of the regional High Plains deeper groundwater system, represented by the Homestead Spring and Homestead Island Piezometer water samples ($\delta^{37}Cl$ = -2.50‰ to -1.98‰). This is also shown in Figure 38e, as the $\delta^{81}Br$ and $\delta^{37}Cl$ isotopic signatures of the bottom of the Wilkinson Core is very close in proximity to the circled region representing the regional groundwater. In addition to this, the concentration of TDS at the bottom of the core is low

(~2,000 mg/L). This suggests there may be a slow upward diffusion component from the fresh regional groundwater system into the subsurface. Additionally, the $\delta^{37}Cl$ isotopic profile down the UNNJ Core also suggests the possible presence of diffusion from a deeper fresh groundwater system (Figure 31b), as the signature gradually becomes more depleted from just beneath the surface sample to the bottom of the core.

Isotopically, both the $\delta^{81}Br$ and $\delta^{37}Cl$ signatures in the Homestead 1 Core and Homestead 3 Core display an almost uniform profile from the surface to the core bottom (Figure 32a and 32b). Unlike the other two lakes, both $\delta^{81}Br$ and $\delta^{37}Cl$ are depleted and virtually the same values. The depletion in both $\delta^{81}Br$ and $\delta^{37}Cl$ in the Homestead Cores is similar to the observed values of $\delta^{81}Br$ and $\delta^{37}Cl$ isotopic values in Group 1 and Group 2 lakes (Figure 27b and 27c) during the 2013 and 2014 sampling years ($\delta^{81}Br$ = -0.82‰ to -0.35‰, $\delta^{37}Cl$ = -0.79‰ to 0.08‰; and $\delta^{81}Br$ = -0.70‰ to -0.19‰, $\delta^{37}Cl$ = -0.59‰ to 0.019‰, respectively), and is shown in Figure 38f. A similar observation can be made using the $\delta^{18}O$ and $\delta^{2}H$ isotopic signatures of the local groundwater, measured from the Wilkinson piezometers, compared with the $\delta^{18}O$ and $\delta^{2}H$ isotopic signatures from Group 1 and Group 2 Lakes sampled in 2014 (Figure 20). The $\delta^{18}O$ and $\delta^{2}H$ isotopic signatures fall along a mixing line, similar to the mixing line that is present between the 2014 Wilkinson piezometers and Wilkinson Lake samples (Figure 21).

In 2013 and 2014, added precipitation resulted in the dilution of many lakes. This was particularly true for Group 1 and Group 2 Lakes which have lower overall TDS concentrations than Group 3 Lakes (refer to Table 5). Two different possibilities can explain the similarities in isotopic signatures between the groups. Firstly, in the past (in the range of 100 – 1,000 years), it is possible that Group 3 Lakes experienced a dilution to a similar concentration of Group 1 and Group 2 Lakes. This would have caused a re-dissolution of the shoreline salts back into the lake waters, and possibly a depletion in both the $\delta^{81}Br$ and $\delta^{37}Cl$ isotopic signatures. Recharge from the higher lake water levels may have occurred into the shallow system. Over time, the signatures may have been solidified into the subsurface sediment layers of silt and clay. It is also possible that the $\delta^{81}Br$ and $\delta^{37}Cl$ isotopic signatures of the Homestead Cores reflect a period in time when the hydrology of Homestead Lake was dominated by flushing of the deeper regional High Plains Aquifer

groundwater system. It is possible that old water was trapped in the subsurface due to the high percentages of clay and silt in the sediment.

Long Term Effects

It is critical to consider the long term impacts of these mechanisms on the $\delta^{81}Br$ and $\delta^{37}Cl$ systematics in this environment. The continual removal of salts, or the release of halide gases, over time may result in a permanent shift in the $\delta^{81}Br$ and $\delta^{37}Cl$ isotopic signatures in the lakes and soil samples in the region.

Earlier in this study, it was determined that salt precipitation preferentially sequesters the lighter ^{79}Br and the heavier ^{37}Cl isotopes from solution. Any subsequent removal of salts, such as eolian activity, will result in a long term enrichment of $\delta^{81}Br$ and depletion of $\delta^{37}Cl$ in the lake waters. This is particularly true in the ephemeral lakes with higher TDS and restricted groundwater flow. In these lakes, their ephemeral qualities mean that salt precipitation along these shorelines is more common than the lower TDS lakes. The higher abundance of mineral precipitates means that larger volumes of salt is available and susceptible to long term removal through eolian activity. Furthermore, the lighter, and lower density mineral precipitates are more likely to be separated from the substrate by wind, as was shown by Zlotnik et al. (2012). As the lighter ^{79}Br and the heavier ^{37}Cl isotopes are removed from the system with salt deflation, lake waters are gradually enriched in $\delta^{81}Br$ and depleted in $\delta^{37}Cl$.

Similarly, over long periods of time, the release of volatile halide gases from the lakeshores can lead to enrichment in $\delta^{81}Br$ isotopic signatures in the lake waters. As was shown earlier in this thesis, gas samples captured from the shorelines of Wilkinson Lake, Homestead Lake, and UNNJ Lake all measured depleted $\delta^{81}Br$ values. This suggests that photochemical or microbial processes occurring on these lakeshores preferentially sequesters and release the lighter ^{79}Br isotope in a gaseous form. It is possible that if these processes, in combination with eolian salt deflation, occur for long enough durations or magnitudes, they can lead to a permanent shift in the regional $\delta^{81}Br$ and $\delta^{37}Cl$ isotopic signatures of the lakes.

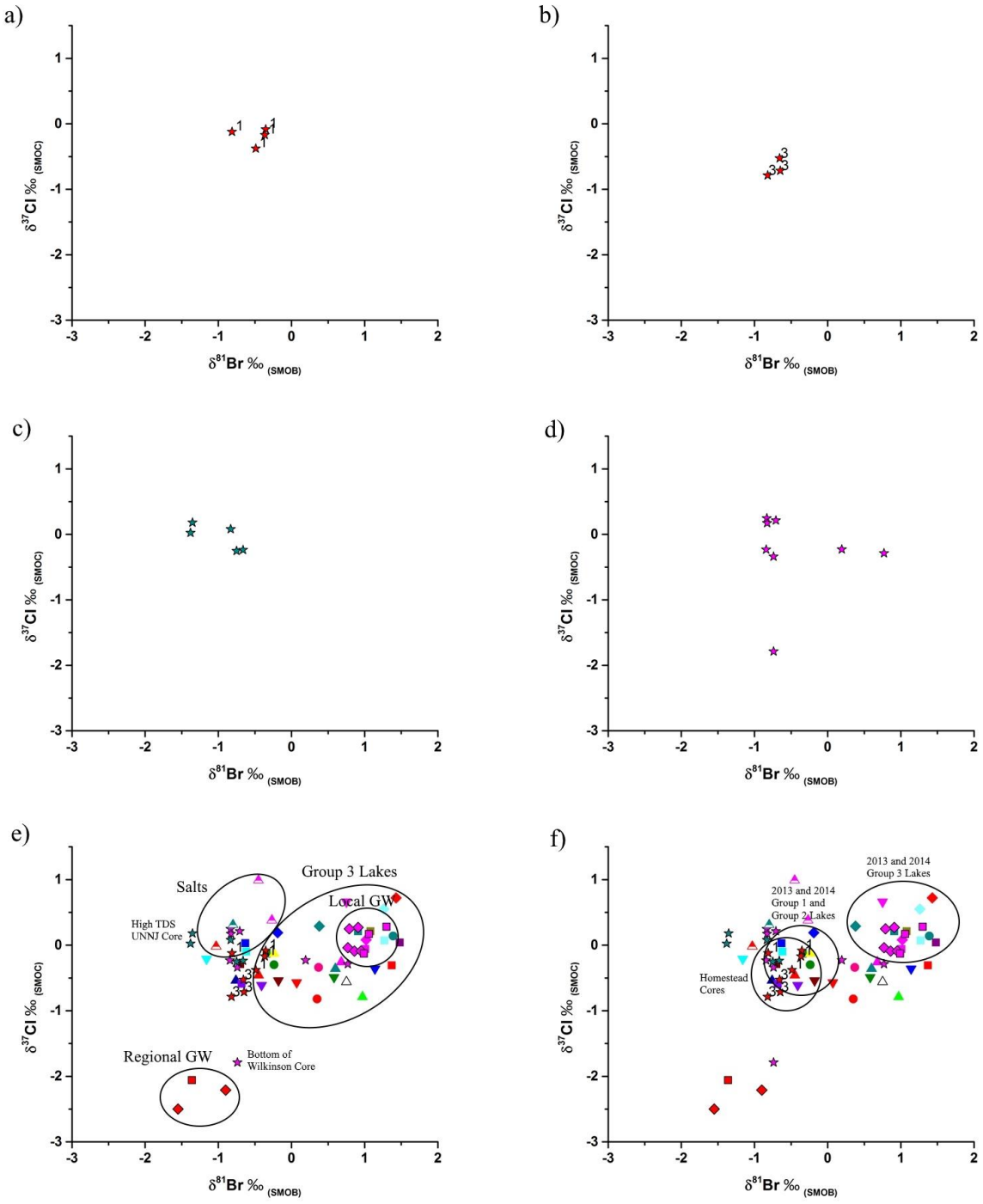

Figure 38. $\delta^{37}Cl$ and $\delta^{81}Br$ of a) Homestead 1 Core, b) Homestead 2 Core, c) UNNJ Core, d) Wilkinson Core, e) all cores and end-members, indicating regions of the UNNJ Core and Wilkinson Core that are points of interest, and e) all cores and end-members, indicating the similarity between the isotopic values of the Homestead Cores to those measured from the 2013 and 2014 Group 1 and Group 2 Lakes.

Conclusion

This thesis provides a basis to discuss the controls on the environmental cycling of bromine and chlorine stable isotopes in a natural evaporitic environment. In future research, this can be used in determining the extent to which salt flats and salt lakes contribute reactive bromine to the atmosphere; a significant finding due to the destructive properties of atmospheric bromine on the ozone layer. It is likely that the Nebraska Sand Hills Region is a significant contributor of bromine gas to the atmosphere as a result of its large surface area. In addition to this, long periods of drought brought on by climate change can increase its contribution even further, as hotter and drier conditions means that chloride and bromide halide salts and gases are more common and more susceptible to removal though eolian and gaseous activity. A full understanding of the behaviour of bromine and chlorine stable isotopes in this environment can help to identify potential regions with higher atmospheric bromine release, and determine if it is a result of microbial processes, photochemical processes, or eolian activity. Furthermore, the findings in the Nebraska Sand Hills Region are applicable to saline lakes worldwide, as similar processes and controls are likely to occur in many other evaporitic environments found.

In the alkaline lakes in the Sand Hills Region of Nebraska, it was determined that the fractionation of $\delta^{81}Br$ and $\delta^{37}Cl$ isotopic signatures are controlled by several different processes. These processes are impacted by the behaviours and the isotopic values of the various end-members throughout the region. These end-members include the lake water, the release of volatile bromide gases, the precipitation of salts along the lake shorelines, and the regional and local groundwater systems.

On the surface sediments of this region, the observed fractionation between the surface salts and lake brines appear to be controlled by two main processes: salt precipitation, and occurrence of photolytic or microbial processes, which cause the reduction or oxidation of halide and its removal as a gas. It was determined in this study that salt precipitation selectively uses the lighter ^{79}Br and heavier ^{37}Cl isotopes, and results in

residual lake waters that are enriched in $\delta^{81}Br$ and depleted in $\delta^{37}Cl$. Salt dissolution has the opposite effect on the isotopic fractionation, as the lighter bromine and heavier chlorine isotopes are reintroduced into the brines as the salts are dissolved. Evidence of this behaviour was presented in the comparison between the $\delta^{81}Br$ and $\delta^{37}Cl$ isotopic signatures of the water and bulk salt samples. Isotopically, reduction processes act to remove the lighter ^{79}Br isotope from the soil around the lakes and convert it to a gaseous state, effectively enriching the residual environment in $\delta^{81}Br$. This was shown by the depleted $\delta^{81}Br$ isotopic signatures of three captured gas samples from disturbed shoreline sediments at Wilkinson Lake, Homestead Lake, and UNNJ Lake. The $\delta^{81}Br$ isotopic signature of the captured gas samples ranged between -1.02‰ to -0.72‰. Indirect evidence of microbial activity was also noted at several lakes. Measurements of gaseous halide production over a lake surface were not made as part of this study. As well, the degree of isotopic impact of gaseous depletion of $\delta^{81}Br$ on either the lake waters or shoreline salt environment could not be measured.

Beneath the surface, the interaction between the fresh groundwater systems and the saline lake waters can have a significant impact on the behaviour of the $\delta^{81}Br$ and $\delta^{37}Cl$ isotopic signatures in the subsurface soils adjacent to the alkaline lakes. This interaction is particularly evident at Wilkinson Lake, as the shallow groundwater mini-piezometers, which were installed next to the lake waters, showed very a similar concentration of TDS to the lake, and the concentrations decrease with distance from the lake and with depth. In some cases, measurements of TDS and water content throughout the core profiles also point towards the presence of a fresh, shallow groundwater component near the lakeshores, as with depth the TDS profile decreases in concentration while the water content increases.

The $\delta^{81}Br$ and $\delta^{37}Cl$ isotopic signatures of the groundwater samples identified two distinct groundwater systems. Both groundwater systems display highly depleted isotopic signatures of $\delta^{81}Br$ and $\delta^{37}Cl$. The first isotopically distinct system is the deeper regional groundwater from the High Plains Aquifer, and is represented by the groundwater samples from the Homestead Spring, and the UNNJ Windmill. The $\delta^{81}Br$ isotopic signatures of this groundwater component range between -1.55‰ to -0.90‰, and the $\delta^{37}Cl$ isotopic signatures range between -2.50‰ to -0.21‰. The second groundwater system is the local, shallow meteoric

groundwater system, and is represented by the groundwater samples from the Wilkinson mini-piezometers. The $\delta^{81}Br$ isotopic signatures of this groundwater component range between 0.77‰ to 1.30‰, and the $\delta^{37}Cl$ isotopic signatures range between -0.13‰ to 0.28‰. The reason behind this distinction between the isotopic values of the groundwater systems is yet to be resolved.

Evidence of the impacts of both groundwater systems are present in the sediment cores sampled from the shorelines of Wilkinson Lake and UNNJ Lake. It is possible that there is a slow, upward migration of fresh groundwater and salts, possibly diffusive, from the underlying High Plains aquifer, or from the mixing and "wash-down" of salts associated with the shallow meteoric groundwater system, which may be responsible for the isotopic signatures of the salts within the sediment cores. This is particularly evident in the bottom of the Wilkinson Lake Core, as the $\delta^{37}Cl$ isotopic signature is -1.79‰, similar to the $\delta^{37}Cl$ isotopic signature of the deep regional groundwater. The isotopic profile of the UNNJ core shows evidence of salts washing down through the shoreline sediments. Over long periods of time, isotopically depleted salts or lake waters from fresher lake periods (such as those that are similar to the waters shown in Figure 27b and Figure 27c) slowly move in a downwards direction.

Over time, the continued removal of salt precipitates through wind activity, and release of halide gaseous compounds to the atmosphere through photolytic or microbial processes, may result in a shift in the regional isotopic signature of the brines and sediments. Based on the isotopic values for the regional High Plains Aquifer ($\delta^{81}Br$ = -1.55‰ to -0.90‰, $\delta^{37}Cl$ = -2.50‰ to 0.13‰), versus the ephemeral Group 3 lakes ($\delta^{81}Br$ = -0.50‰ to 1.48‰, $\delta^{37}Cl$ = -1.1‰ to 0.72‰), this would appear to be true. Both these processes may result in the isotopic values of the lake waters to eventually become enriched in $\delta^{81}Br$ and depleted in $\delta^{37}Cl$. It is possible that Group 3 lakes may be more susceptible to these regional changes, as their ephemeral characteristics and high concentrations of TDS means that salt precipitation and accumulation along their shorelines during periods of drought is more common.

In future research, it is recommended that deeper sediment cores should be sampled, and that they are analysed for $\delta^{81}Br$ and $\delta^{37}Cl$ isotopic values at a higher frequency throughout the core depth. Furthermore,

segments of the cores should be analysed using radiocarbon dating in order to better understand the time and history of deposition. Additionally, XRD analyses should be completed on the salt mineral samples which are collected to obtain more evidence of the degree of salt evolution, as well as the geochemical end-member of the brine type of each lake. In addition to this, bromide gas should be captured at multiple lake sites in order to determine the extent of bromine release to the atmosphere, identification of the type of bromine gas which is released should be determined, as well as a speciation of the microorganisms which are causing its release.

References

Abe, Y., Aravena, R., Zopfi, J., Shouakar-Stash, O., Cox, E., Roberts, J. D., & Hunkeler, D. (2009). Carbon and Chlorine Isotope Fractionation during Aerobic Oxidation and Reductive Dechlorination of Vinyl Chloride and *cis* -1,2-Dichloroethene. *Environmental Science & Technology*, *43*(1), 101–107. http://doi.org/10.1021/es801759k

Anderson, C. (2003). The Great WWI Potash Industry of Southern Sheridan County, Nebraska.

Benson, L. (1984). *Hydrochemical data for the Truckee River drainage system, California and Nevada* (USGS Numbered Series No. 84-440, 1-35).

Bernstein, A., Ronen, Z., Levin, E., Halicz, L., & Gelman, F. (2013). Kinetic bromine isotope effect: example from the microbial debromination of brominated phenols. *Analytical and Bioanalytical Chemistry*, *405*(9), 2923–2929. http://doi.org/10.1007/s00216-012-6446-0

Bleed, A., & Flowerday, C. (1991). The Nebraska Sand Hills. *Rangelands*, *13*(2), 53–55.

Bourg, I. C., & Sposito, G. (2007). Molecular dynamics simulations of kinetic isotope fractionation during the diffusion of ionic species in liquid water. *Geochimica et Cosmochimica Acta*, *71*(23), 5583–5589. http://doi.org/10.1016/j.gca.2007.01.021

Bowen, B. B., & Benison, K. C. (2009). Geochemical characteristics of naturally acid and alkaline saline lakes in southern Western Australia. *Applied Geochemistry*, *24*(2), 268–284. http://doi.org/10.1016/j.apgeochem.2008.11.013

Brauner, C. J., Gonzalez, R. J., & Wilson, J. M. (2013). Extreme Environments: Hypersaline, Alkaline, and Ion-Poor Waters. In *Fish Physiology* (Vol. 32, pp. 435–476). Elsevier Ltd. Retrieved from http://dx.doi.org/10.1016/B978-0-12-396951-4.00009-8

Clark, I., Fritz, P. (1997) *Environmental isotopes in hydrogeology*. Boca Raton, Florida: CRC Press/Lewis Publishers.

Crawford, R. P. (1917). Pumping Potash from Nebraska Lakes. *Engineering and Mining Journal*, *103*(18), 777–778.

Damm, K. L. Von, & Edmond, J. M. (1984). Reverse weathering in the closed-basin lakes of the Ethiopian Rift. *American Journal of Science*, *284*(7), 835–862. http://doi.org/10.2475/ajs.284.7.835

Deocampo, D. M., & Jones, B. F. (2014). Geochemistry of Saline Lakes. In H. D. Holland & K. K. Turekian (Eds.), *Treatise on Geochemistry* (2nd ed., Vol. 7, pp. 437–463). Elsevier Ltd.

Diffendal, R. (1984). Comments on the Geologic History of the Ogallala Formation in the Southern Panhandle of Nebraska. In *Ogallala Aquifer Symposium II*.

Dong, H., Zhang, G., Jiang, H., Yu, B., Chapman, L. R., Lucas, C. R., & Fields, M. W. (2006). Microbial Diversity in Sediments of Saline Qinghai Lake, China: Linking Geochemical Controls to Microbial Ecology. *Microbial Ecology*, *51*(1), 65–82. http://doi.org/10.1007/s00248-005-0228-6

Eggenkamp, H. G. M. (2014). *The Geochemistry of Stable Chlorine and Bromine Isotopes* (1st ed.). Berlin Heidelberg: Springer-Verlag, pp. 1-172.

Eggenkamp, H. G. M., Bonifacie, M., Ader, M., & Agrinier, P. (2011). Fractionation of Cl and Br isotopes during precipitation of salts from their saturated solutions (Vol. 75, p. 798). Presented at the 21th Annual V.M. Goldschmidt Conference, Praque, Czech Republic: Mineral Mag.

Eggenkamp, H. G. M., Kreulen, R., & Koster Van Groos, A. F. (1995). Chlorine Stable Isoptope Fractionation in Evaporites. *Geochimica et Cosmochimica Acta*, *59*(24), 5169–5175.

El-Baz, F. (1984). *The geology of Egypt: an annotated bibliography*. Leiden: E.J. Brill, pp. 1-778.

Enami, S., Vecitis, C. D., Cheng, J., Hoffmann, M. R., & Colussi, A. J. (2007). Global Inorganic Source of Atmospheric Bromine. *Journal of Physical Chemistry*, *111*(1), 8749–8752. http://doi.org/10.1021/jp074903r

Eugster, H. P. (1970). Chemistry and origin of the brines of Lake Magadi, Kenya. *Mineralological Society of America*, *3*, 213–235.

Eugster, H. P., & Hardie, L. A. (1978). Saline Lakes. In A. Lerman (Ed.), *Lakes: Chemistry, Geology, Physics* (pp. 237–289). New York: Springer.

Galat, D. L., Lider, E. L., Vigg, S., & Robertson, S. R. (1981). Limnology of a large, deep, North American terminal lake, Pyramid Lake, Nevada, U.S.A. In W. D. Williams (Ed.), *Salt Lakes* (pp. 281–317). Dordrecht: Springer Netherlands. Retrieved from http://www.springerlink.com/index/10.1007/978-94-009-8665-7_22

Gizaw, B. (1996). The Origin of High Bicarbonate and Fluoride Concentrations in Waters of the Main Ethiopian Rift Valley, East African Rift System. *Journal of African Earth Sciences*, *22*(4), 391–402.

Goble, R. J., Mason, J. A., Loope, D. B., & Swinehart, J. B. (2004). Optical and Radiocarbon Ages of Stacked Paleosols and Dune Sands in the Nebraska Sand Hills, USA. *Quaternary Science Review*, *23*(1), 1173–1182. http://doi.org/10.1016/j.quascirev.2003.09.009

Gosselin, D. C. (1997). Major-Ion Chemistry of Compositionally Diverse Lakes, Western Nebraska, U.S.A.: Implications for Paleoclimatic Interpretations. *Journal of Paleolimnology*, *17*(1), 33–49.

Gosselin, D. C., Nabelek, P. E., Peterman, Z. E., & Sibray, S. (1997). A Reconnaissance Study of Oxygen , Hydrogen, and Strontium Isotopes in Geochemically Diverse Lakes, Western Nebraska, USA. *Journal of Paleolimnology*, *17*(1), 51–65. http://doi.org/10.1023/A:1007913010057

Gosselin, D. C., Sibray, S., & Ayers, J. (1994). Geochemistry of K-rich Alkaline Lakes, Western Sandhills, Nebraska, USA. *Geochimica et Cosmochimica Acta*, *58*(5), 1403–1418.

Gosselin, D. C., Sridar, V., Harvey, F. E., & Goeke, J. W. (2006). Hydrological Effects and Groundwater Fluctuations in Interdunal Environments in the Nebraska Sandhills. *Great Plains Research*, *16*(1), 17–28.

Grant, W. D. (2006). Alkaline Environments and Biodiversity. In C. Gerday & N. Glansdorff (Eds.), *Extremophilies*. Oxford, UK: Eolss Publishers. Retrieved from http://www.eolss.net

Hardie, L. A., & Eugster, H. P. (1970). The evolution of closed-basin brines. *Mineralological Society of America*, *3*, 273–290.

Hardie, L. A., & Eugster, H. P. (1980). Evaporation of Seawater: Calculated Mineral Sequences. *Science, 208*(4443), 498–500. http://doi.org/10.1126/science.208.4443.498

Harvey, E. F., Swinehart, J. B., & Kurtz, T. M. (2007) Groundwater sustenance of Nebraska's unique sand hills peatland fen ecosystems. *Ground Water, 45*(2), 218-234. http://doi.org/10.1111/j.1745-6584.2006.00278.x

Henderson, A.C.G. (2003). A carbon- and oxygen-isotope record of recent environmental change from Qinghai Lake, NE Tibetan Plateau. *Chinese Science Bulletin, 48*(14), 1463. http://doi.org/10.1360/02wd0272

Hendry, M. J., & Wassenaar, L.I. (2004) Transport and geochemical controls on the distribution of solutes and stable isotopes in a thick clay-rich till aquitard, Canada. *Isotopes in Environmental and Health Studies, 40*(1), 3-19. http://doi.org/10.1080/10256010310001644942

Hicks, W. B. (1921). Potash Resources of Nebraska. In *Contributions to Economic Geology Part 1* (pp. 125–140). Washington: Govt Print Office.

Hönninger, G. (2004). Reactive bromine and sulfur emissions at Salar de Uyuni, Bolivia. *Geophysical Research Letters, 31*(4). http://doi.org/10.1029/2003GL018818

Horst, A., Holmstrand, H., Andersson, P., Thornton, B. F., Wishkerman, A., Keppler, F., & Gustafsson, O. (2014). Stable Bromine Isotopic Composition of Methyl Bromide Released from Plant Matter. *Geochimica et Cosmochimica Acta, 125*(1), 186–195. http://doi.org/10.1016/j.gca.2013.10.016

Jellison, R., & Melack, J. M. (1993). Meromixis in hypersaline Mono Lake, California. 1. Stratification and vertical mixing during the onset, persistence, and breakdown of meromixis. *Limnology and Oceanography, 38*(5), 1008–1019. http://doi.org/10.4319/lo.1993.38.5.1008

Joeckel, R. M., & Ang Clement, B. J. (2005). Soils, surficial geology, and geomicrobiology of saline-sodic wetlands, North Platte River Valley, Nebraska, USA. *CATENA, 61*(1), 63–101. http://doi.org/10.1016/j.catena.2004.12.006

Jones, B. F., Naftz, D. L., Spencer, R. J., & Oviatt, C. G. (2009). Geochemical Evolution of Great Salt Lake, Utah, USA. *Aquatic Geochemistry*, *15*(1-2), 95–121. http://doi.org/10.1007/s10498-008-9047-y

Knauth, L. P., & Beeunas, M. A. (1986). Isotope geochemistry of fluid inclusions in Permian halite with implications for the isotopic history of ocean water and the origin of saline formation waters. *Geochimica et Cosmochimica Acta*, *50*(3), 419–433. http://doi.org/10.1016/0016-7037(86)90195-X

Knipping, E. M. (2000). Experiments and Simulations of Ion-Enhanced Interfacial Chemistry on Aqueous NaCl Aerosols. *Science*, *288*(5464), 301–306. http://doi.org/10.1126/science.288.5464.301

Kong, W. G., Zheng, M. P., & Kong, F. J. (2014). Brine evolution in Qaidam Basin, Northern Tibetan Plateau, and the formation of playas as Mars analogue site. Presented at the 45th Lunar and Planetary Science Conference, Beijing.

La Baugh, J. W. (1986). Limnological characteristics of selected lakes in the Nebraska sandhills, U.S.A., and their relation to chemical characteristics of adjacent ground water. *Journal of Hydrology*, *86*(3-4), 279–298. http://doi.org/10.1016/0022-1694(86)90168-X

Laturnus, F. (2001). Marine macroalgae in polar regions as natural sources for volatile organohalogens. *Environmental Science and Pollution Research*, *8*(2), 103–108. http://doi.org/10.1007/BF02987302

Loope, D. B., & Swinehart, J. B. (2000). Thinking Like a Dune Field: Geologic History in the Nebraska Sand Hills. *Great Plains Research*, *10*(1), 5–35.

Loope, D. B., Swinehart, J. B., & Mason, J. P. (1995). Dune-dammed paleovalleys of the Nebraska Sand Hills: Intrinsic versus climatic controls on the accumulation of lake and marsh sediments. *Geological Society of America Bulletin*, *107*(4), 396–0406. http://doi.org/10.1130/0016-7606(1995)107<0396:DDPOTN>2.3.CO;2

Lowenstein, T. K., & Risacher, F. (2009). Closed Basin Brine Evolution and the Influence of Ca–Cl Inflow Waters: Death Valley and Bristol Dry Lake California, Qaidam Basin, China, and Salar de

Atacama, Chile. *Aquatic Geochemistry*, *15*(1-2), 71–94. http://doi.org/10.1007/s10498-008-9046-z

Lower, S. K. (1996). Carbonate equilibria in natural waters. In: *A Chem1 Reference Text* (pp. 1-25). http://www.chem1.com/acad/webtext/virtualtextbook.html

Luo, C., Xiao, Y., Wen, H., Ma, H., Ma, Y., Zhang, Y., … He, M. (2014). Stable isotope fractionation of chlorine during the precipitation of single chloride minerals. *Applied Geochemistry*, *47*, 141–149. http://doi.org/10.1016/j.apgeochem.2014.06.005

Mangan, J. M., Overpeck, J. T., Webb, R. S., Wessman, C., & Goetz, A. F. H. (2004). Response of Nebraska Sand Hills Natural Vegetation to Drought, Fire, Grazing, and Plant Functional Type Shifts as Simulated by the Century Model. *Climatic Change*, *63*(1/2), 49–90. http://doi.org/10.1023/B:CLIM.0000018516.53419.90

McLeod, R. A. (1980). *Development and application of a new method for collecting soil moisture samples for chemical analysis* (Masters of Science). Queen's University, Kingston, Ontario.

Monks, P. S. (2005) Gas-phase radical chemistry in the troposphere. *Chemical Society Reviews, 34*(5), 376. http://doi.org/10.1039/b307982c

Mono Basin Research Group. (1977). *An Ecological Study of Mono Lake, California*. (D. W. Winkler, Ed.). Universty of California: Institute of Ecology, pp 6-37.

Newton, A. (2015). Archaean Earth: Alkaline lakes of old. *Nature Geoscience*, *8*(2), 90–90. http://doi.org/10.1038/ngeo2361

Numata, M., Nakamura, N., Koshikawa, H., & Terashima, Y. (2002). Chlorine Isotope Fractionation during Reductive Dechlorination of Chlorinated Ethenes by Anaerobic Bacteria. *Environmental Science & Technology*, *36*(20), 4389–4394. http://doi.org/10.1021/es025547n

Palau, J., Cretnik, S., Shouakar-Stash, O., Höche, M., Elsner, M., & Hunkeler, D. (2014). C and Cl Isotope Fractionation of 1,2-Dichloroethane Displays Unique δ13C/δ37Cl Patterns for Pathway

Identification and Reveals Surprising C–Cl Bond Involvement in Microbial Oxidation. *Environmental Science & Technology*, *48*(16), 9430–9437. http://doi.org/10.1021/es5031917

Parkhurst, D. L., & Appelo, C. A. J. (2013). Description of input and examples for PHREEQC Version 3 - A computer program for speciation, batch-reaction, one-dimensional transport, and inverse geochemical calculations. U.S. Geological Survey Techniques and Methods, book 6, chap A43, 497. http://pubs.usgs.gov/tm/06/a43.

Parrella, J. P., Jacob, D. J., Liang, Q., Zhang, Y., Mickley, L. J., Miller, B., … Van Roosendael, M. (2012). Tropospheric Bromine Chemistry: Implications for Present and Pre-Industrial Ozone and Mercury. *Atmospheric Chemistry and Physics*, *12*(1), 6723–6740. http://doi.org/10.5194/acp-12-6723-2012

Plummer, L. N., Parkhurst, D. L., Flemming, G. W., & Dunkle, S. A. (1988). A computer program incorperating Pitzer's equations for calculation of geochemical reactions in brines. U.S. Geological Survey Water-Resources Investigations Report 88-4153, 310.

Plummer, L. N., Prestemon, E. C., & Parkhurst, D. L. (1991). An interactive code (NETPATH) for modelling NET geochemical reactions along a flow PATH. U.S. Geological Survey Water-Resources Investigations Report 91-4078, 227.

Prather, M. J., & Watson, R. T. (1990). Stratospheric Ozone Depletion and Future Levels of Atmospheric Chlorine and Bromine. *Nature*, *344*(1), 729–734.

Pratt, K. A., Custard, K. D., Shepson, P. B., Douglas, T. A., Pohler, D., General, S., … Stirm, B. H. (2013). Photochemical production of molecular bromine in Arctic surface snowpacks. *Nature Geoscience*, *6*(5), 351-356. http://doi.org/10.1038ngeo1779

Reddy, M. M. (1995). Carbonate Precipitation in Pyramid Lake, Nevada: Probably Control by Magnesium. *Mineral Scale Formation and Inhibition*, 21–33.

Risacher, F., Fritz, B., & Alonso, H. (2006). Non-conservative Behaviour of Bromide in Surface Waters and Brines of Central Andes: A Release into the Atmosphere? *Geochimica et Cosmochimica Acta*, *70*(1), 2143–2152. http://doi.org/10.1016.j.quagca.2006.01.019

Rundquist, D. C. (1983). *Wetland inventories of Nebraska's Sandhills* (Resource Report No. 9). University of Nebraska-Lincoln, pp. 1-46.

Salama, R. B., Otto, C. J., & Fitzpatrick, R. W. (1999). Contributions of groundwater conditions to soil and water salinization. *Hydrogeology Journal*, *7*(1), 46–64. http://doi.org/10.1007/s100400050179

Santos, G. S., & Rast, S. (2013). A Global Model Study of Natural Bromine Sources and the Effects on Tropospheric Chemistry using MOZART4. *Journal of Atmospheric Chemistry*, *70*(1), 69–89. http://doi.org/10.1007/s10874-013-9252-y

Shouakar-Stash, O., Drimmie, R. J., & Frape, S. K. (2005). Determination of inorganic chlorine stable isotopes by continuous flow isotope ratio mass spectrometry. *Rapid Communications in Mass Spectrometry*, *19*(2), 121–127. http://doi.org/10.1002/rcm.1762

Shouakar-Stash, O., Frape, S. K., & Drimmie, R. J. (2005). Determination of Bromine Stable Isotopes Using Continuous-Flow Isotope Ratio Mass Spectrometry. *Analytical Chemistry*, *77*(13), 4027–4033. http://doi.org/10.1021/ac048318n

Sinnhuber, B. M., Sheode, N., Sinnhuber, M., Chipperfield, M. P., & Feng, W. (2009). The contribution of anthropogenic bromine emissions to past stratospheric ozone trends: a modelling study. *Atmospheric Chemistry and Physics*, *9*, 2863–2871.

Spencer, R. J., Eugster, H. P., & Jones, B. F. (1985). Geochemistry of Great Salt Lake, Utah II: Pleistocene-Holocene Evolution. *Geochimica et Cosmochimica Acta*, *49*, 739–747.

Spencer, R. J., Eugster, H. P., Jones, B. F., & Rettig, S. L. (1985). Geochemistry of Great Salt Lake, Utah I: Hydrochemistry since 1850. *Geochimica et Cosmochimica Acta*, *49*, 727–737.

Sridhar, V., & Hubbard, K. G. (2010). Estimation of the Water Balance Using Observed Soil Water in the Nebraska Sandhills. *Journal of Hydrologic Engineering*, *15*(1). http://doi.org/10.1061/(ASCE)HE.1943-5584.0000157

Stumm, W., & Morgan, J. (1996). Aquatic Chemistry: chemical equilibria and rates in natural waters. In *Environmental science and technology.* New York, USA: Wiley.

Sturchio, N. C., Hatzinger, P. B., Arkins, M. D., Suh, C., & Heraty, L. J. (2003). Chlorine Isotope Fractionation during Microbial Reduction of Perchlorate. *Environmental Science & Technology*, *37*(17), 3859–3863. http://doi.org/10.1021/es034066g

Sturges, W. T., & Barrie, L. A. (1988). Chlorine, Bromine and Iodine in Arctic Aerosols. *Atmospheric Environment*, *22*(6), 1179–1194.

Sturges, W. T., & Harrison, R. M. (1986). Bromine: Lead Ratios in Airborne Particles from Urban and Rural Sites. *Atmospheric Environment*, *20*(3), 577–588.

Szilagyi, J., Zlotnik, V. A., Gates, J. B., & Jozsa, J. (2011). Mapping mean annual groundwater recharge in the Nebraska Sand Hills, USA. *Hydrogeology Journal*, *19*(8), 1503–1513. http://doi.org/10.1007/s10040-011-0769-3

Taher, A. G. (1999). Inland saline lakes of Wadi El Natrun depression, Egypt. *International Journal of Salt Lake Research*, *8*(2), 149–169. http://doi.org/10.1007/BF02442128

U.S. Bureau of the Census. (1990). Nebraska Outline Map. U.S. Department of Commerce.

Wang, T., Zlotnik, V. A., Wedin, D., & Wally, K. D. (2008). Spatial Trends in Saturated Hydraulic Conductivity of Vegetated Dunes in the Nebraska Sand Hills: Effects of Depth and Topography. *Journal of Hydrology*, *349*(1-2), 88–97. http://doi.org/10.1016/j.jhydrol.2007.10.027

Weeks, J. B., & Gutentag, E. D. (1988). Region 17, High Plains. In W. Back, J. S. Rosenshein, & P. R. Seaber (Eds.), *Hydrogeology* (Vol. 0–2, pp. 157–164). Boulder, CO: Geological Society of America.

Whitcomb, R. F. (1989). Nebraska Sand Hills: The Last Prairie (pp. 57–69). Presented at the Eleventh North American Prairie Conference. Beltsville, Maryland.

Wiegert, C., Mandalakis, M., Knowles, T., Polymenakou, P. N., Aeppli, C., Macháčková, J., … Gustafsson, Ö. (2013). Carbon and Chlorine Isotope Fractionation During Microbial Degradation of Tetra- and Trichloroethene. *Environmental Science & Technology*, 130604132217008. http://doi.org/10.1021/es305236y

Williams, W. D. (1986). Conductivity and Salinity of Australian Salt Lakes. *Australian Journal of Marine and Freshwater Research*, *37*, 177–182.

Winter, T. C. (1986). Effect of ground-water recharge on configuration of the water table beneath sand dunes and on seepage in lakes in the sandhills of Nebraska, U.S.A. *Journal of Hydrology*, *86*(3-4), 221–237. http://doi.org/10.1016/0022-1694(86)90166-6

Wofsy, S. C., McElroy, M. B., & Yung, Y. L. (1975). The Chemistry of Atmospheric Bromine. *Geophysical Research Letters*, *2*(6), 215–218.

Yizhaq, H., Ashkenazy, Y., & Tsoar, H. (2009). Sand dune dynamics and climate change: A modeling approach. *Journal of Geophysical Research*, *114*(F1). http://doi.org/10.1029/2008JF001138

Yung, Y. L., Pinto, J. P., Watson, R. T., & Sander, S. P. (1980). Atmospheric Bromine and Ozone Perturbations in the Lower Stratosphere. *Journal of the Atmospheric Sciences*, *37*(1), 339–353.

Zakon, Y., Halicz, L., & Gelman, F. (2013). Bromine and Carbon Isotope Effects during Photolysis of Brominated Phenols. *Environmental Science & Technology*, *47*(24), 14147–14153. http://doi.org/10.1021/es403545r

Ziegler, V. (1915). The potash deposites of the sand hills region of northwestern Nebraska. In *Quarterly of the Colorado School of Mines* (Vol. 10, pp. 6–26).

Zlotnik, V. A., Olaguera, F., & Ong, J. B. (2009). An approach to assessment of flow regimes of groundwater-dominated lakes in arid environments. *Journal of Hydrology*, *371*(1-4), 22–30. http://doi.org/10.1016/j.jhydrol.2009.03.012

Zlotnik, V. A., Ong, J. B., Lenters, J. D., Schmeider, J., & Fritz, S. C. (2012) Quantification of salt dust pathways from a groundwater fed lake: Implications for solute budgets and dust emission rates. *Journal of Geophysical Research, 117*, 1-12. http://doi.org/10.1029/2011/JF002107

Zlotnik, V. A. (2012) Kansas Geological Survey Talk, Lawrence Kansas, USA.

Appendix A

Details of Chlorine Stable Isotope Analysis

The following is a summary of the Chlorine Stable Isotope Methodology outlined in Shouakar-Stash et al., 2005a. Water samples were adjusted to the appropriate concentration of chlorine. This was completed using ultrapure water to dilute the sample, or by allowing the sample to evaporate on a heating element to the desired concentration (200 mg/L) and desired volume (100 mL). The minimum concentration required, however, is 10 mg/L. Following this, the samples were acidified to pH ~ 2 using roughly 2 mL of 10% nitric acid. The sample was checked for its acidity using litmus paper, then placed on a heating element at 280^{o}C. A mixture of 6.000 g 0.4M potassium nitrate, 2.060 g anhydrous sodium phosphate diabasic, and 0.070 g citric acid monohydrate was then added to the warmed solution. This acted to increase the ionic strength while buffering the pH at 2. Lastly, 2 mL of 0.2M silver nitrate was added, resulting in precipitation of silver chloride. The solution was stored overnight in a dark location to allow complete precipitation to occur. Once the precipitate had settled, the residual solvent was decanted and the solute was transferred to an amber vial then rinsed with 5% HNO_3. The vials were placed in an oven to dry overnight.

After the samples had dried, approximately 0.2 mg of each sample was weighed and placed into 20 mL amber vials. The vials were then positioned in an inflatable glove bag connected to an ultrapure helium tank. Helium was used to seal the bag and gently flush out each amber vial. Then, 0.1 mL of CH_3I was added to each sample. The vials were then placed in an oven at 80^{0}C for 48 hours.

Three protocols were followed during the sample analysis: sample injection, GC set up, and use of the CF-IRMS. The GC was prepared in such a way that CH_3Cl and CH_3I gases were separated. It was also connected to the CF-IRMS so that the CH_3Cl gas could be sent directly into the mass spectrometer.

Details of Bromine Stable Isotope Analysis

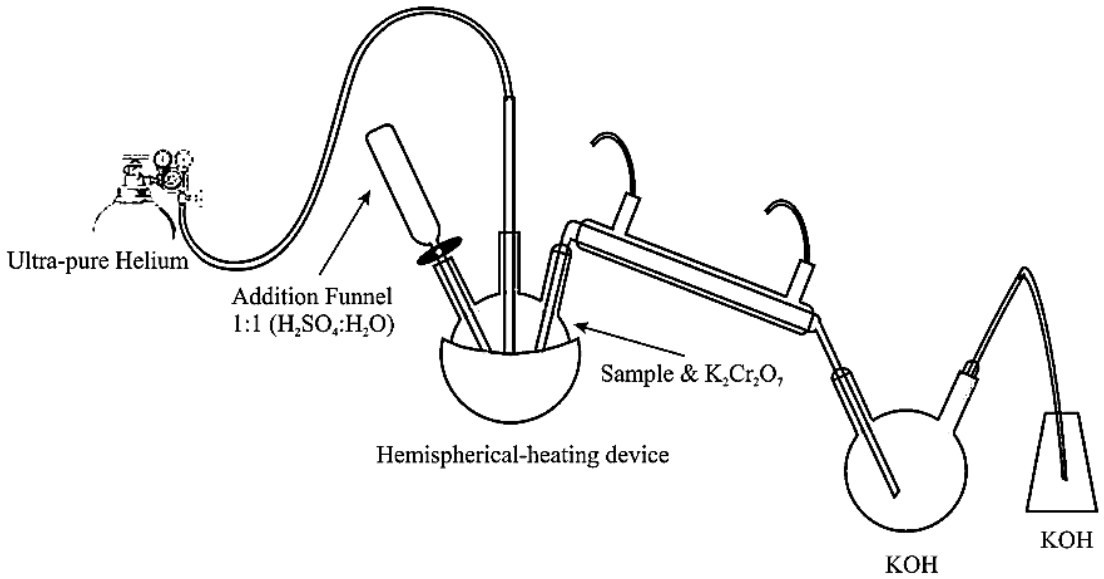

Figure 39. Bromine Separation Apparatus, from (Shouakar-Stash et al., 2005b).

The following is a summary of the Bromine Stable Isotope Methodology outlined in Shouakar-Stash et al., 2005b. For a successful analysis, each sample must contain 1-10 mg of bromine. To attain this, water samples were evaporated on a heating element at 80°C, or diluted to 100 mL using ultrapure water. Ideally, samples will be 100 mL in volume and contain bromine at a concentration of 200 mg/L. The bromine separation was completed using the apparatus outlined in Figure 39. The water sample was added to the three-hole round-bottom flask along with 10 g of $K_2Cr_2O_7$ and some glass beads to aid the mixing process. The flask was placed on a heating pad to facilitate boiling. The two-hole round-bottom flask was filled with a solution of 200 mL ultrapure water and 2 g of KOH. This flask was placed in a cooling bath of crushed ice. The Erlenmeyer flask was filled with 100 mL of ultrapure water and 1 g of KOH. The addition funnel was filled with 20 mL of 1:1 H_2SO_4:H_2O. The apparatus was assembled using a fritted gas dispersion tube connected to a water supply, and attached to a source of ultrapure helium gas. Once all connections were secured, the helium was allowed to flow through the system at roughly 200 mL/min. The addition funnel was opened to release the 1:1 H_2SO_4:H_2O solution into the three-hole round-bottom flask, resulting in the

formation of Br_2 gas. This gas was forced through the distillation tube and captured in the two-hole round-bottom flask as KBr and KBrO due to its reaction with KOH. Any bromine gas that escapes was captured in the Erlenmeyer flask containing KOH. The device was allowed to run for a 20 minutes to ensure full bromine separation. The final solutions in the two-hole round-bottom and Erlenmeyer flasks were combined in a beaker with 3 g zinc powder, then boiled for 10 minutes to reduce the bromine species to Br^-. Then the resulting solution was filtered on a 22µm Millipore Express Plus filter.

Following these steps, the protocol for the formation of CH_3Br and subsequent isotopic analysis is comparable to that of chlorine isotopes. The precipitation of AgBr was facilitated by the acidification of the solution to pH ~ 2 using 2 mL 10% HNO_3, followed by the addition of 18 g KNO_3 to increase the ionic strength, and 2 mL 0.2M $AgNO_3$. The beakers were stored in a dark location overnight to ensure all AgBr was precipitated. After this, the solvent was decanted, and the precipitate was rinsed using 5% HNO_3 and transferred to amber vials. These vials were then situated in an oven at 80°C to dry overnight.

In order to form CH_3Br, 0.5 g of each sample was weighed into 20 mL amber vials. Then the addition of 0.1 mg CH_3I is performed inside an inflatable glove bag that is connected to a source of ultrapure helium. Once complete, samples are placed in an oven at 80°C for 56 ± 5 hours.

Both a GC and a CF-IRMS was used for sample analysis. The GC was used to separate CH_3Br and CH_3I gases. The gas was then sent directly from the GC into the CF-IRMS to complete the analysis.

Appendix B

PHREEQC 3.0 Saturation Indices Results

The wide variation in the geochemistry of the lakes suggests that different mineral assemblages, resulting from different degrees of evaporation, and incongruent dissolution, may be present at each lake. Therefore, the subsequent precipitation and dissolution of these minerals can potentially impact the resulting chemical composition of the lake waters. To explore this possibility, saturation indices for 40 different salt minerals were modelled using PHREEQC 3.0 software (Parkhurst and Appelo, 2013), using the Pitzer database for waters with high ionic strengths, and utilizing field measurements for temperature, pH, and pe. 1992 data from Gosselin et al. (1994) is used as a proxy for the 2012 data. This is felt to be an acceptable substitution due to the similar climatic conditions prior to these years and similarities between the 1992 and 2012 sampling years (shown in Table 1) and discussed with Gosselin.

The results of the PHREEQC 3.0 model are shown in Table 12. The calculated saturated mineral results primarily include carbonate minerals, consisting of aragonite and calcite ($CaCO_3$), dolomite, ($(Ca+Mg)CO_3$), magnesite ($MgCO_3$), gaylussite ($Na_2Ca(CO_3)_2 \cdot 5H_2O$), and pirssonite ($Na_2Ca(CO_3)_2 \cdot 2H_2O$). All lake samples are saturated with respect to aragonite, calcite, and dolomite. Almost all lakes are saturated with respect to magnesite, and approximately one third of lakes (mainly from the ephemeral Group 3 lakes) are saturated with respect to gaylussite and pirssonite. These results are comparable to the XRD results from Gosselin et al. (1994), which revealed mineral assemblages of aphthitalite (also referred to as glaserite), mirabilite, thenardite, trona, and thermonatrite present at UNNJ Lake, Homestead Lake, and Jesse Lake in 1992. The PHREEQC 3.0 model calculated the UNNJ brines to be in saturation with respect to aphthitalite, thenardite, and trona, however the model did not calculate for thermonatrite.

The recharge groundwater systems have very low Ca-Mg concentrations. Saturation for Ca-Mg minerals appears to occur very rapidly and once removed further evaporation tends to precipitate sodium carbonate minerals (Deocampo & Jones, 2014). In the Sand Hills Region, the lakes which are calculated to be at saturation with respect to gaylussite and pirssonite are likely to have undergone a higher degree of evaporation. For example, between 2012 (1992), and 2014, all sampled Group 3 lakes are saturated with these minerals, half of Group 2 lakes are saturated, and all Group 1 lakes are undersaturated with respect to gaylussite and pirssonite. Increased groundwater or freshwater input into Group 1 or Group 2 lakes would reduce saturation and thus lead to the precipitation of sodium carbonate minerals. This is because the groundwater lowers the overall TDS of the lakes and adds calcium and magnesium ions to the lake water, which permits the continued precipitation of calcium and magnesium carbonates (Gosselin, 1997). Restricted groundwater flow, or excessive periods of evaporation in the Group 3 lakes would favour the precipitation of more evolved salt minerals at these lakes, following the right side pathway in Figure 1 (Deocampo and Jones, 2014).

Fluctuating temperatures and pH measurements in the water samples may affect the PHREEQC mineral saturation results. It was noted that certain lakes experienced a significant shift in surface water temperature and pH values between sampling periods, shown in Table 11. Wilkinson Lake, for example, showed the greatest difference in measured temperature and pH values of all the lakes sampled. Comparing physical data from 2012 and 2014, the difference between the measured temperatures of Wilkinson Lake waters varied by 11.3^0C, and the pH varied by 0.8. The 1992 Wilkinson Lake temperature measurement for August of that year is at odds with other nearby lakes such as UNNJ Lake (33.8^0C) and Homestead Lake (27.4^0C) and may not be correct and was not used in calculations. In order to monitor the effects of changing temperature, pH, or pe, multiple models of the Wilkinson Lake samples were conducted using PHREEQC 3.0, varying one parameter while keeping the other factors constant. The results of these model runs are shown Table 13. The subsequent effect of the modified parameters on the value of the saturation indices is

minor, and although the values do change, altering the temperature, pH, or pe did very little to influence the final predicted saturation or undersaturation of mineral phases.

Table 11. Variation in field measurements of temperature, pH, and pe in Wilkinson Lake in the 1992, 2013, and 2014 sampling years.

Lake Name	Year	Temperature (^{0}C)	pH	pe (V)
Wilkinson	1992	17.7	9.74	-0.1
	2013	26.3	8.94	-0.098
	2014	29.0	9.66	-0.1094

Table 12. Calculated Saturation Indices of select minerals for lakes sampled in 1992 (2012), 2013, and 2014. 1992 field measurements from Gosselin et al. (1994) are substituted for the current study's 2012 lake chemistry.

Lake	Year	Anhydrite	Aragonite	Arcanite	Burkeite	Calcite	Dolomite	Gaylussite	Glaserite	Glauberite	Gypsum	Keiserite	Labile	Magnesite	Nahcolite	Pirssonite	Syngenite	Thenardite	Trona
Big Harvey	2014	-0.49	2.38	-0.86	-4.86	2.56	4.79	0.77	-0.77	-1.09	-0.29	-5.4	-2.24	1.29	-0.51	0.68	0.06	-1.17	-2.52
Dillings	2012	-3.06	1.52	-4.07	-15.22	1.71	4.01	-2.22	-7.76	-7.54	-2.68	-6.79	-12.63	1.49	-2.61	-2.4	-5.68	-5.17	-6.92
	2014	-2.65	1.63	-4.36	-15.87	1.81	3.96	-2.55	-8.13	-7.35	-2.36	-6.8	-12.57	1.24	-2.56	-2.74	-5.56	-5.3	-7.26
Fritz	2012	-2.71	1.42	-2.96	-14.13	1.61	2.7	-2.25	-5.94	-6.59	-2.26	-7.42	-11.17	0.35	-4.1	-2.44	-4.22	-4.65	-7.09
	2014	-2.41	-0.04	-3.43	-17.28	0.15	-0.19	-5.93	-6.86	-6.77	-1.97	-7.1	-11.8	-1.08	-2.74	-6.12	-4.39	-5.11	-9.23
Homestead	2012	-3.97	1.29	-0.82	-4.42	1.48	2.49	1.37	-1.12	-5.14	-3.74	-8.91	-6.96	0.14	-0.55	1.33	-3.39	-1.81	-0.87
	2013	-2.79	2.51	-1.26	-4.93	2.69	--	2.47	-1.76	-4.26	-2.63	--	-6.26	--	-0.66	2.39	-2.65	-2.01	-1.08
	2014	-2.3	2.98	-1.83	-7.03	3.17	--	2.36	-3.18	-4.27	-1.95	--	-6.91	--	-0.89	2.23	-2.71	-2.68	-2.04
Joe	2013	-2.03	0.4	-4.36	-18.01	0.59	2.37	-5.72	-8.17	-6.83	-1.74	-5.34	-12.16	0.87	-2.79	-5.9	-4.94	-5.4	-9.43
Mini UNNJ	2013	-0.46	2.44	-1	-3.29	2.62	4.93	1.33	-0.72	-0.56	-0.29	-5.37	-1.22	1.36	-0.32	1.26	-0.06	-0.66	-1.81
No. 2	2014	-0.99	2.21	-1.74	-6.82	2.39	4.25	0.27	-2.5	-2.33	-0.73	-6.06	-4.2	0.93	-1.37	0.12	-1.3	-1.93	-3.79
Shriner	2012	-2.93	1.19	-1.95	-10.35	1.38	2.25	-1.21	-3.81	-5.5	-2.47	-7.59	-8.79	0.16	-2.04	-1.38	-3.44	-3.35	-5.03
	2014	-2.07	0.61	-2.79	-14.16	0.79	--	-4.06	-5.33	-5.58	-1.71	--	-9.69	--	-1.93	-4.24	-3.42	-4.19	-7.15
UNNJ	2012	-2.67	2.36	0.48	2.32	2.54	5.08	3.7	2.09	-1.61	-2.84	7.46	-1.45	1.58	0.56	4.14	-0.96	0.05	2.03
	2013	-0.63	4.21	-0.04	1.21	4.39	--	5.24	1.18	0.09	-0.75	--	0.02	--	1.12	5.56	0.59	0.19	2.18
	2014	-1.36	2.83	-0.97	-4.95	3.02	--	2.16	-1.31	-2.31	-1.04	--	-3.9	--	-1.78	2.03	-0.91	-1.62	-2.96
UNNJ Area	2014	-0.84	2.76	-1.51	-5.11	2.94	4.96	1.63	-1.95	-1.73	-0.58	-6.27	-3.17	1.11	-0.92	1.5	-0.92	-1.49	-2.52
Wilkinson	2012	-2.59	1.25	-1.26	-4.31	1.44	3.87	0.51	-1.7	-3.11	-2.2	-5.82	-4.37	1.69	-0.91	0.41	-2.43	-1.28	-2.16
	2013	-0.49	2.99	-1.2	-3.58	3.17	6.01	2.2	-1.28	-0.77	-0.23	-5.27	-1.7	1.97	-0.24	2.12	-0.28	-0.93	-1.46
	2014	-1.13	2.5	-2.13	-6.52	2.68	5.2	0.94	-3.13	-2.47	-0.84	-5.76	-4.39	1.63	-1.32	0.79	-1.82	-1.97	-3.37

Table 13. Effect of temperature, pH, and pe variation on calculated mineral saturation indices.

Variation	Temp (^{0}C)	pH	Pe (V)	Aragonite	Calcite	Dolomite	Gaylussite	Magnesite	Pirssonite
Temp	17.7	9.66	-0.098	2.97	3.16	5.96	2.43	2.06	2.35
	26.3	9.66	-0.098	3.05	3.23	6.16	2.51	2.06	2.44
	29	9.66	-0.098	3.07	3.25	6.21	2.53	2.06	2.46
pH	26.3	9.74	-0.098	3.05	3.23	6.16	2.52	2.07	2.45
	26.3	8.94	-0.098	2.99	3.17	6.01	2.2	1.97	2.12
	26.3	9.66	-0.098	3.05	3.23	6.16	2.51	2.06	2.44
pe	26.3	9.66	-0.1	3.05	3.23	6.16	2.51	2.06	2.44
	26.3	9.66	-0.098	3.05	3.23	6.16	2.51	2.06	2.44
	26.3	9.66	-0.1094	3.05	3.23	6.16	2.51	2.06	2.44